

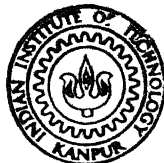
VORTEX SHEDDING IN CONFINED FLOWS

By
RAJESH AGARWAL

C/

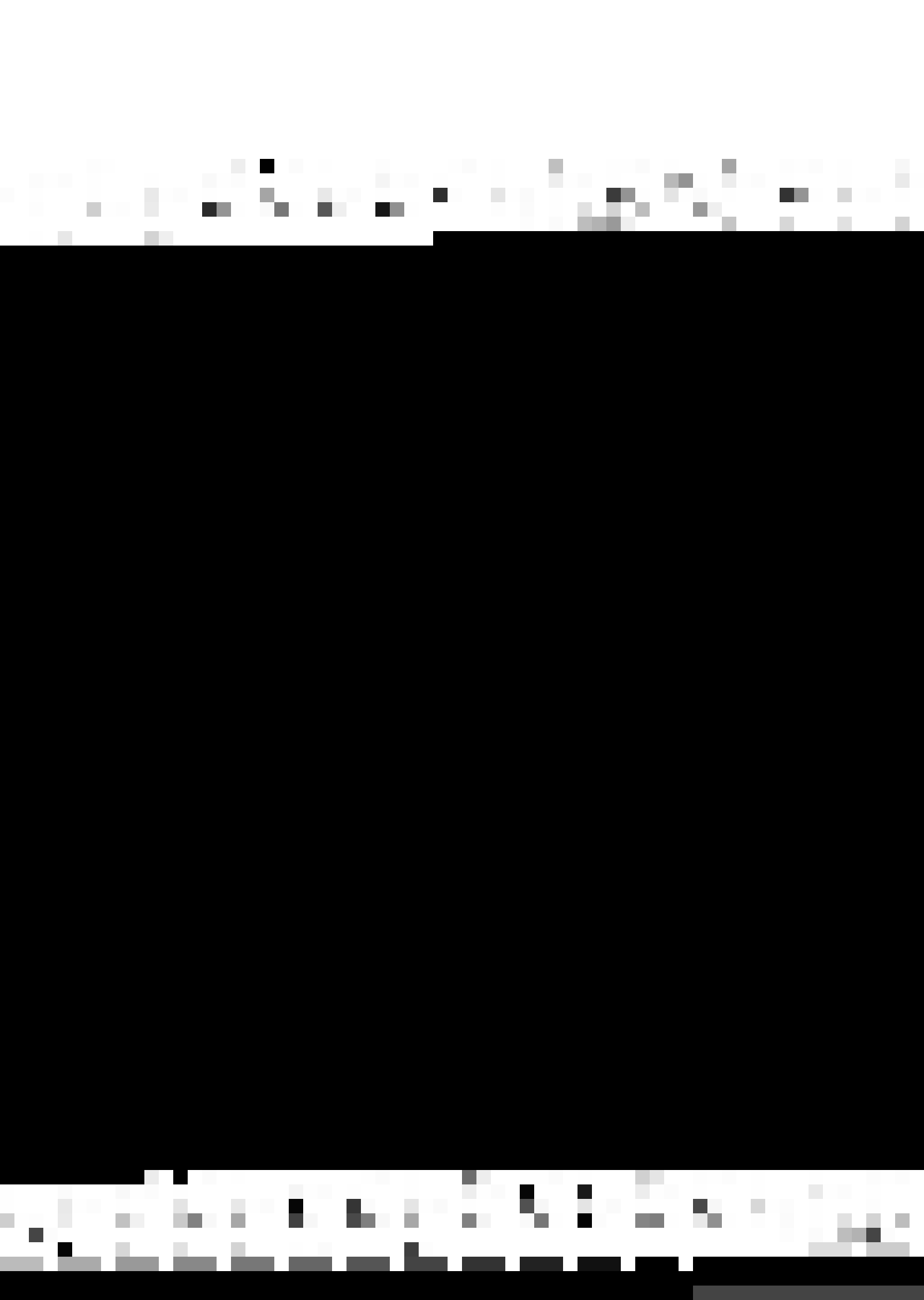
ME
1974
M
AGA
VOR

Tn
me/ 1979/m
Ag 595V



DEPARTMENT OF MECHANICAL ENGINEERING
INDIAN INSTITUTE OF TECHNOLOGY KANPUR
JUNE 1974

M. Tech
A. 29980



VORTEX SHEDDING IN CONFINED FLOWS

A Thesis Submitted
In Partial Fulfilment of the Requirements
for the Degree of
MASTER OF TECHNOLOGY

By
RAJESH AGARWAL

to the

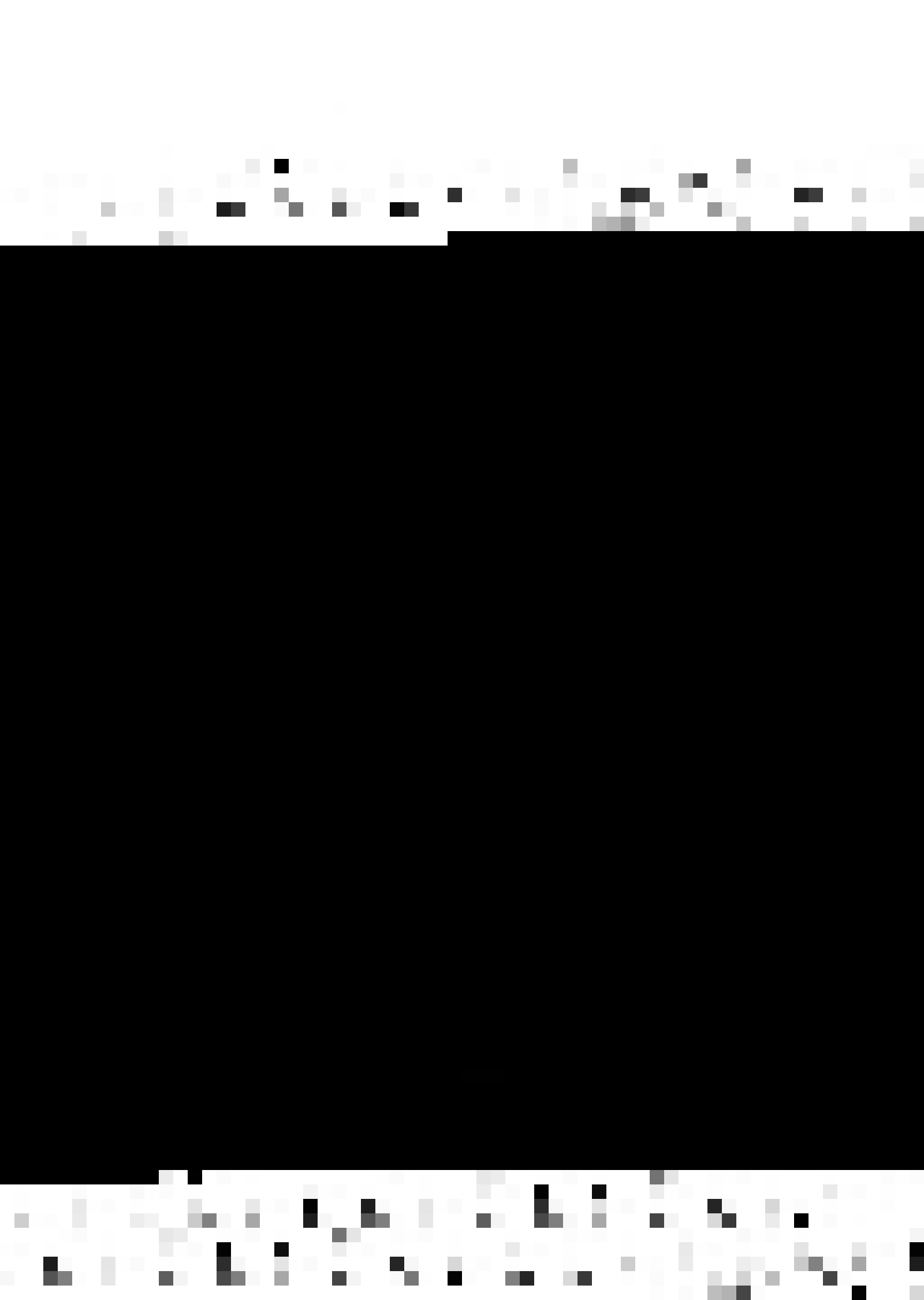
DEPARTMENT OF MECHANICAL ENGINEERING
INDIAN INSTITUTE OF TECHNOLOGY KANPUR
JUNE 1974

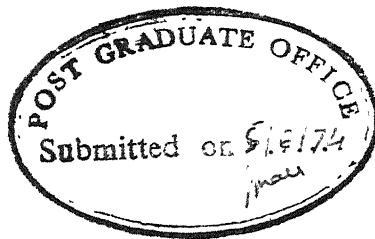


Acc. No. **A** 299.80

V
JUNE '76

ME-1974-m-AGA-VOR






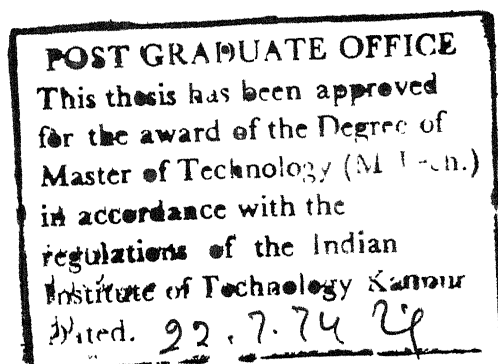
(ii)

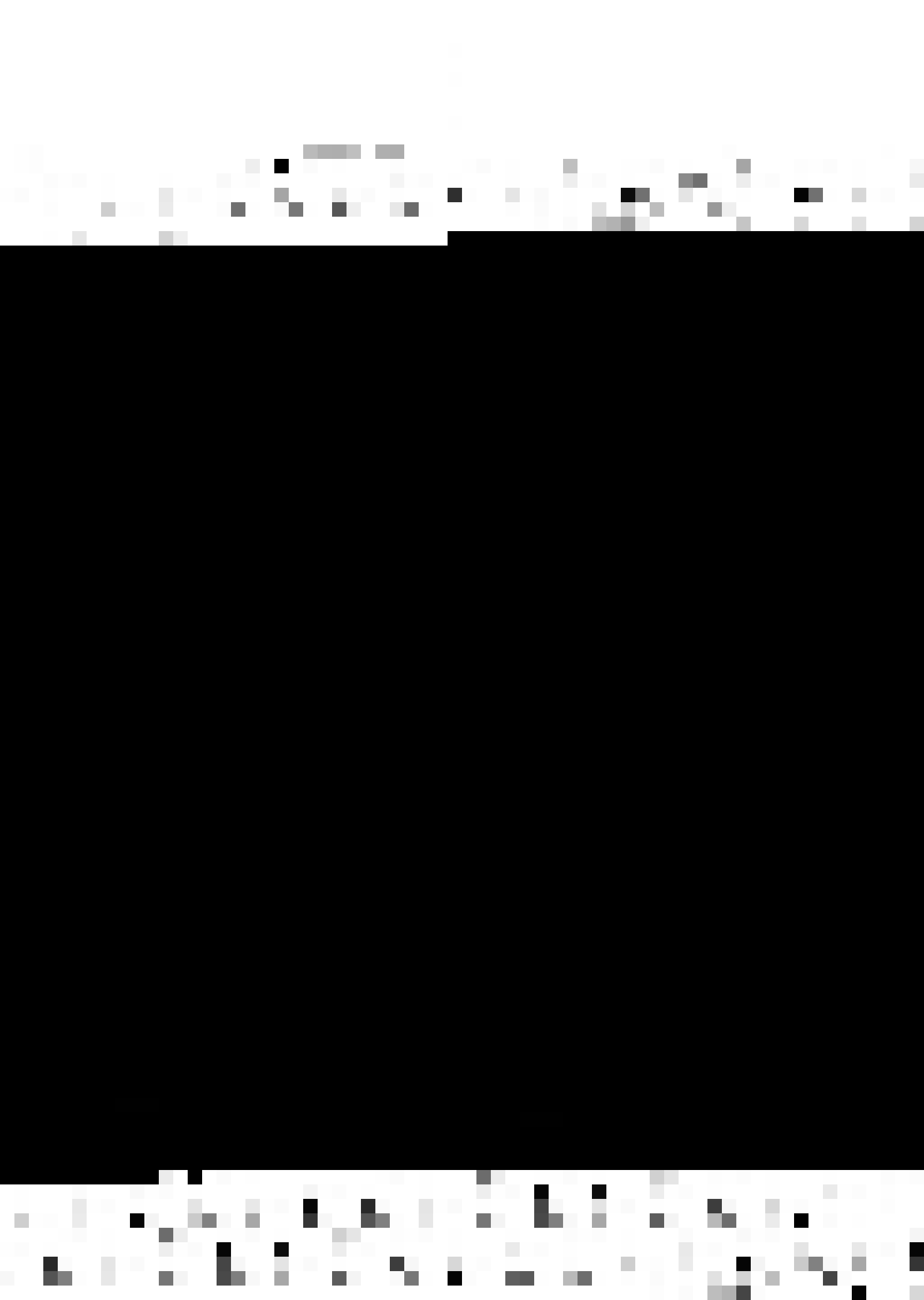
CERTIFICATE

This is to certify that the thesis entitled "Vortex Shedding in Confined Flows" by Rajesh Agarwal is a record of work carried out under my supervision and has not been submitted elsewhere for a degree.

4th June 1974


V. Sundararajan
Associate Professor
Department of Mechanical Engineering
Indian Institute of Technology, Kanpur.





ACKNOWLEDGEMENT

I am deeply indebted to Dr. V. Sundararajan for his guidance, encouragement and inspiration and to Dr. R. Singh for his critical comments and fruitful discussions while conducting the experiments.

My thanks are also due to
Mr. B.S. Rohewal for making the Wind-Tunnel
and the hot-wire probe.

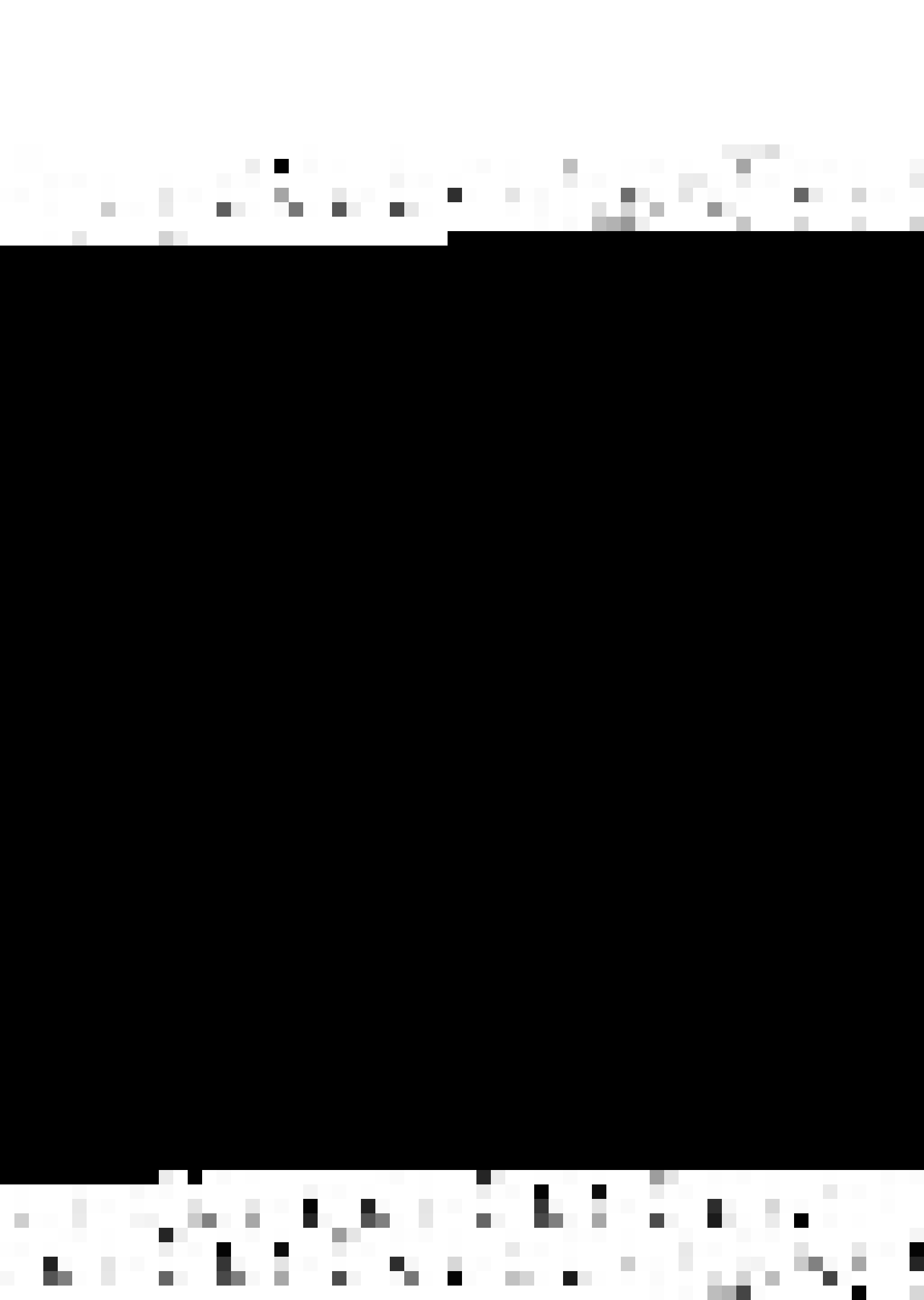
Mr. M.M. Singh for his continuous and sincere
help in conducting the experiments.

Mr. K.S. Raghavan for photography.

Mr. D.P. Saini for his excellent typing of
the manuscript.

Messors A. Rajamani, Singhasan Yadav, B.L.Sharma
Muddappa, S.N.M. Mallik and all others whose timely help
and presence made my task easier.

RAJESH AGARWAL

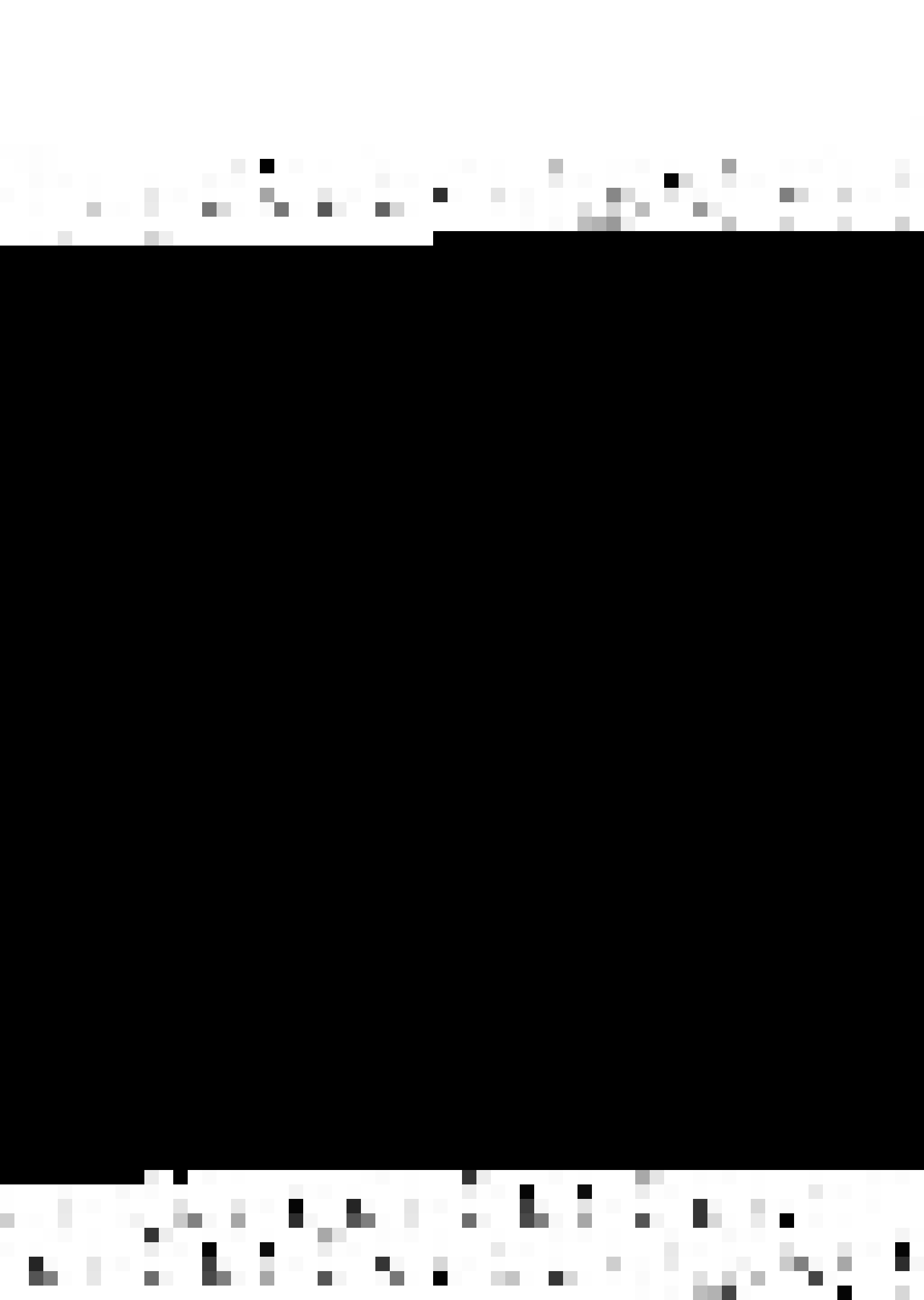


CONTENTS

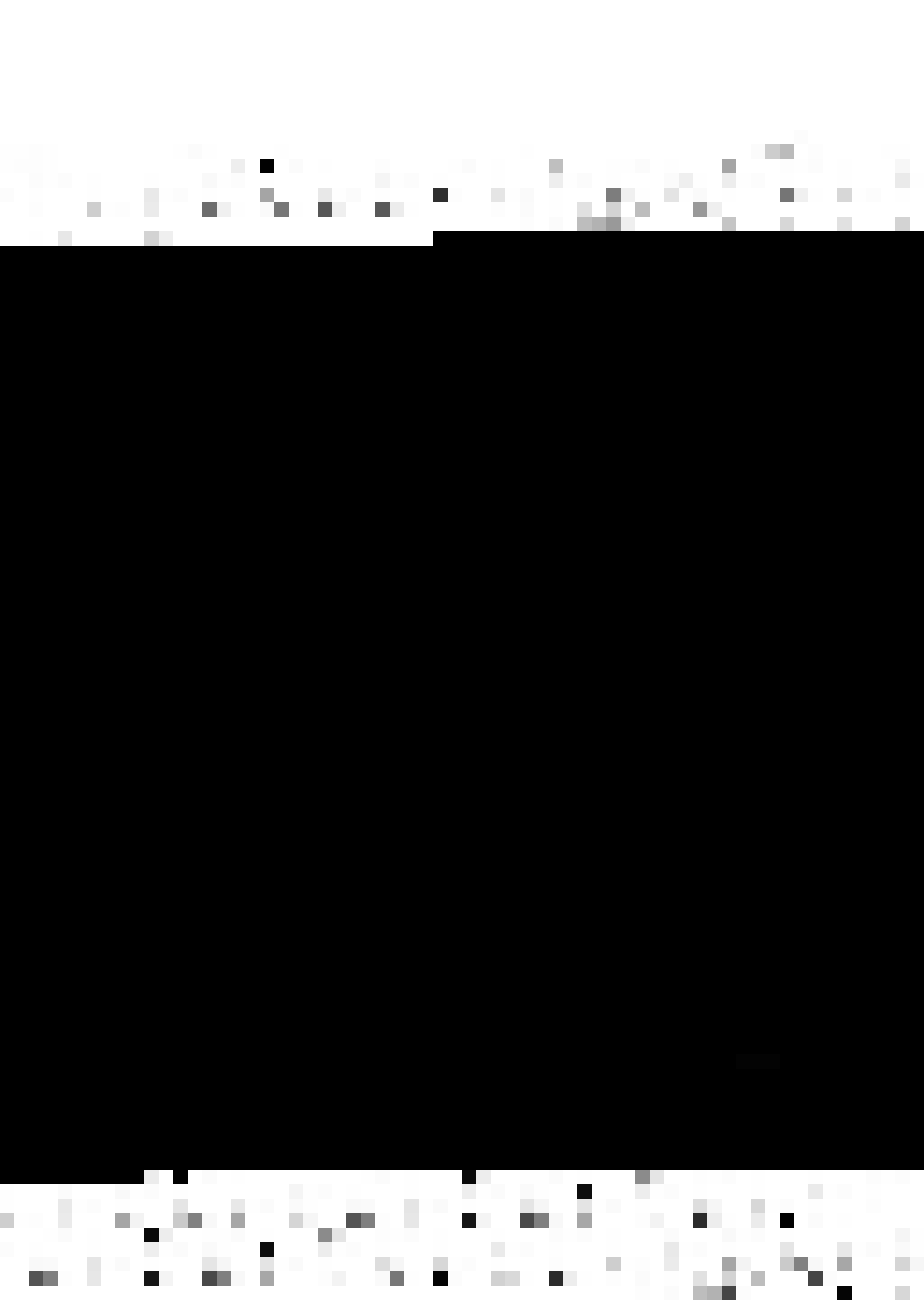
	<u>Page</u>
LIST OF FIGURES	(vii)
LIST OF PLATES	(viii)
NOMENCLATURE	(ix)
SYNOPSIS	(xi)
CHAPTER-I : INTRODUCTION	
1.1: General	1
1.2: Previous Work	
1.2.1: Experimental	2
1.2.2: Theoretical	5
1.3: Present Work	7
CHAPTER-II : MECHANISM AND FACTORS AFFECTING VORTEX SHEDDING	
2.1: Mechanism of Vortex Shedding	8
2.2: Effect of Various Parameters on Shedding Frequency	
2.2.1: Effect of Reynolds number	12
2.2.2: Effect of Cylinder Roughness and Turbulence Level	13
2.2.3: Effect of Shape of the Body	14
2.2.4: Effect of Orientation of the Cylinder	15



	<u>Page</u>
2.2.5: Effect of Cylinder Flexibility	15
2.2.6: Effect of Cylinder and Conditions	16
 CHAPTER-III : EXPERIMENTAL SET-UP AND TEST PROCEDURE	
3.1: Subsonic Wind Tunnel	17
3.2: Models	17
3.3: Measurement of Velocity	
3.3.1: Defining the Velocity	18
3.3.2: Micromanometer and Pressure Probes	19
3.3.3: Measurement	19
3.4: Vortex Sensing Transducer and Amplifier	
3.4.1: Hot-Wire Probe	19
3.4.2: Hot-Wire Anemometer Amplifier	20
3.4.3: Low-Pass Filter	20
3.5: Measurement of Turbulence	21
3.6: Measurement of Shedding Frequency	
3.6.1: Positioning the Hot-Wire Probe	21
3.6.2: Filtering the Input Signal-Wave Analyzer	22
3.6.3: Measurement of Shedding Frequency-Frequency Counter	22

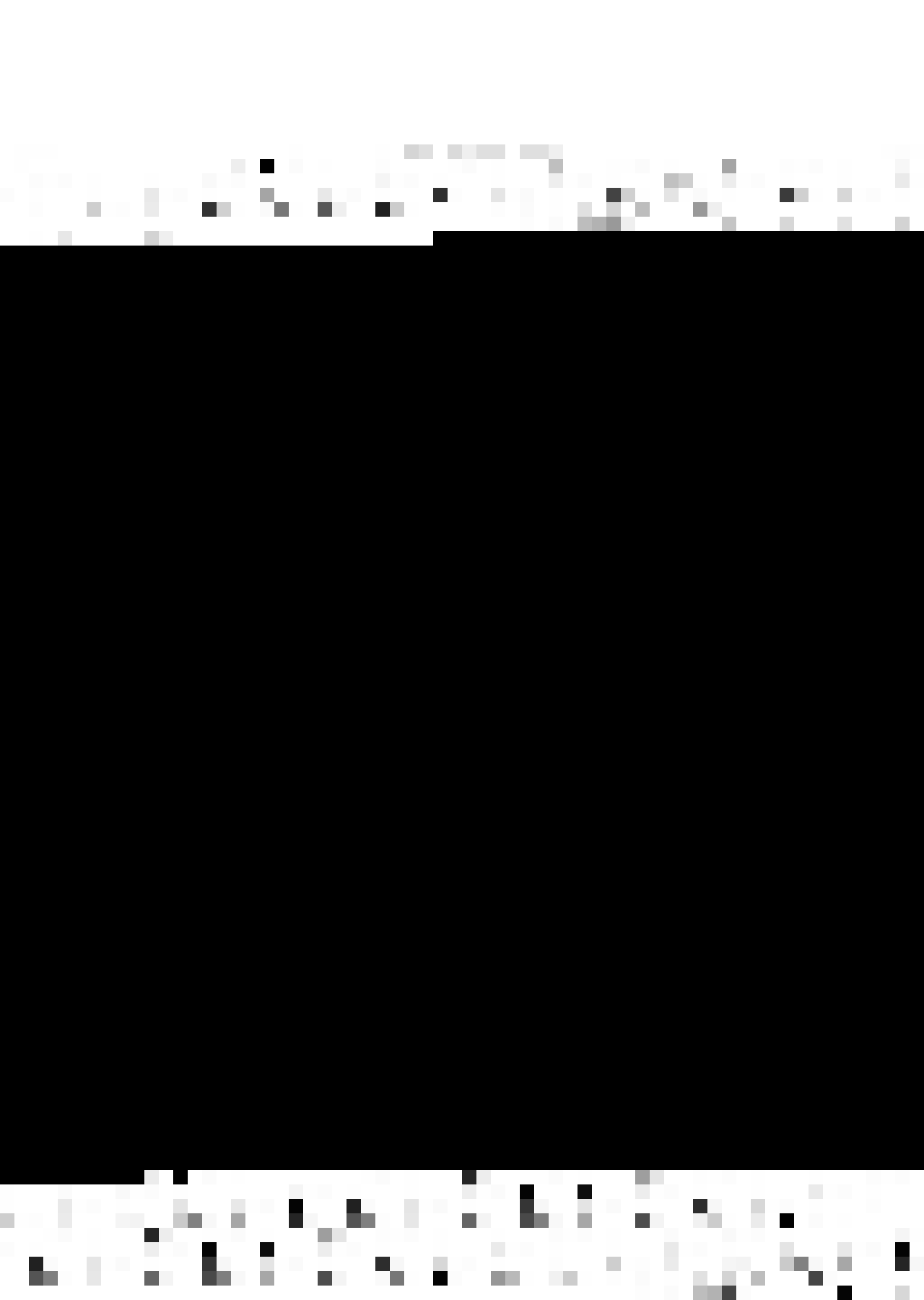


	<u>Page</u>
3.7: Leading Specifications of the Instrument Used	23
CHAPTER-IV : . . RESULTS AND DISCUSSIONS	
4.1: General	26
4.2: Parallel Wall Effect	
4.2.1: Graphical Plots	27
4.2.2: Discussion	27
4.3: One Wall Effect	
4.3.1: Graphical Plot	29
4.3.2: Discussion	30
4.4: Effect of Converging Walls	
4.4.1: Graphical Plots	30
4.4.2: Discussion	31
4.5: Effect of Diverging Walls	
4.5.1: Graphical Plots	32
4.5.2: Discussion	32
CHAPTER-V : CONCLUSION AND SCOPE FOR FUTURE WORK	
5.1: Conclusions	48
5.2: Scope for Future Work	50
REFERENCES :	51
BIBLIOGRAPHY:	56
APPENDIX-A : Wall Correction Theories	58



LIST OF FIGURES

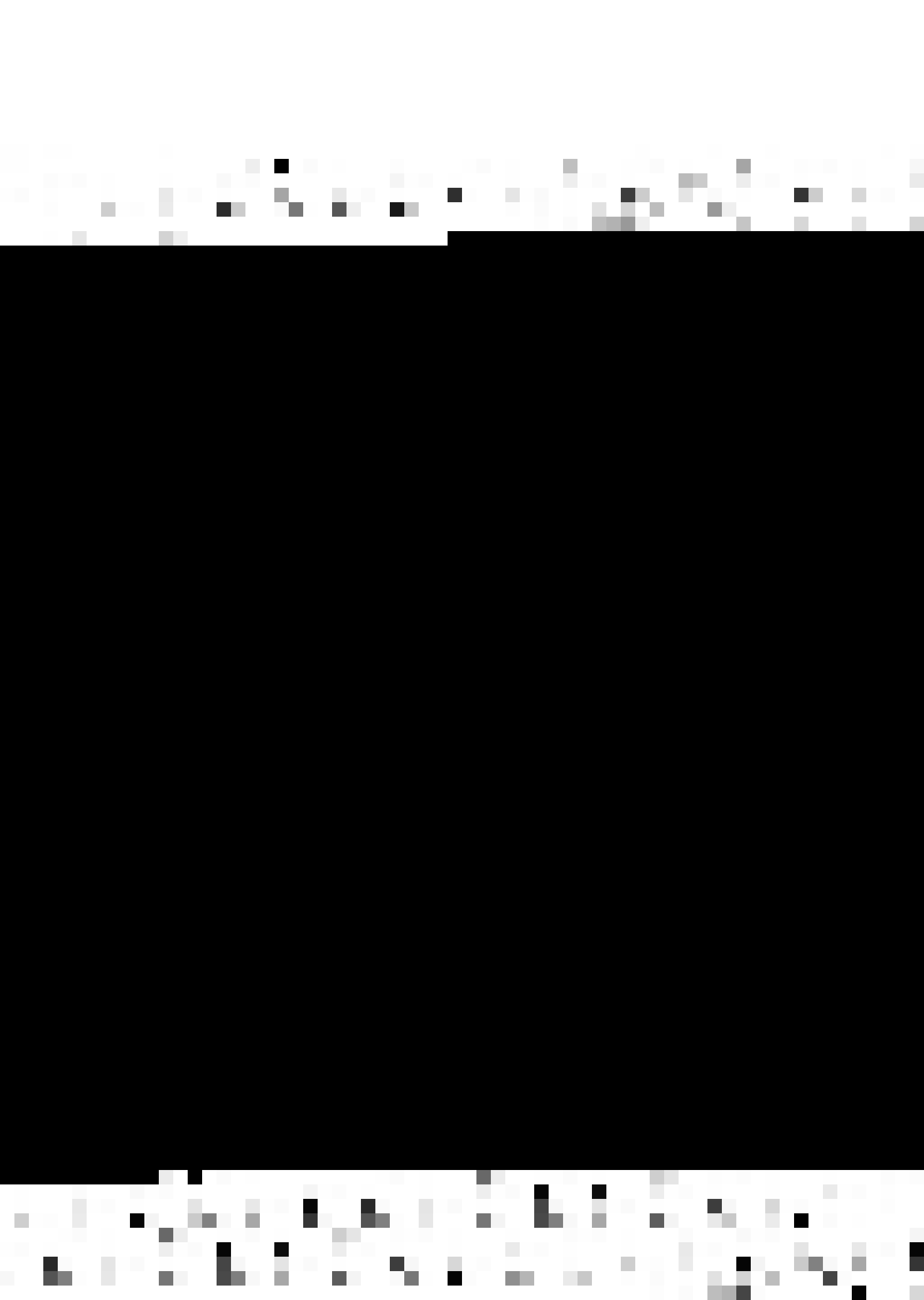
	<u>Page</u>
Fig. 1 : Line Sketch of Experimental Set-Up	26
Fig. 2 : Effect of Parallel and Walls for $R = 144, 161, 258$ and 436 Strouhal Number Vs. H/d .	36
Fig. 3 : Effect of Parallel and Walls for $R = 902, 1230$ and 1530 Strouhal Number Vs. H/d	37
Fig. 4 : Application of Blockage Correction Theories - % Error Vs. H/d	38
Fig. 5 : Effect of Only One Wall for $R = 902, 1230, 1530$ Strouhal Number Vs. H/d	39
Following Figures show the effect of Converging Walls Strouhal Number Vs. H/d	
Fig. 6 : For $R = 311$	40
Fig. 7 : For $R = 902$	41
Fig. 8 : For $R = 1230$	42
Fig. 9 : For $R = 1530$	43
Following Figures show the effect of Diverging Walls Strouhal Number Vs. H/d	
Fig. 10 : For $R = 311$	44
Fig. 11 : For $R = 902$	45
Fig. 12 : For $R = 1230$	46
Fig. 13 : For $R = 1530$	47



LIST OF PLATES

PLATE 1 : Instrumentation

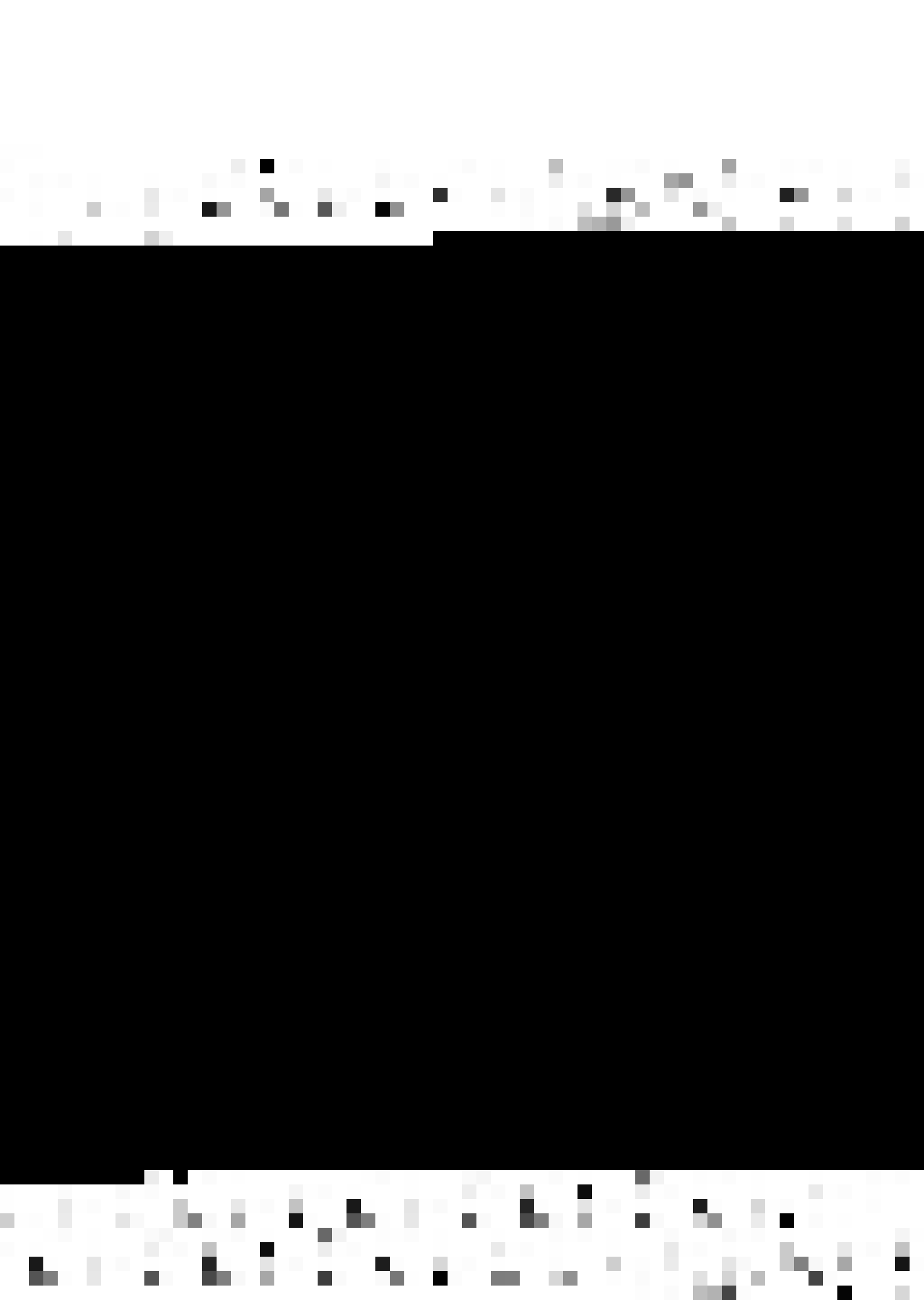
PLATE 2 : Wind - Tunnel



(ix)

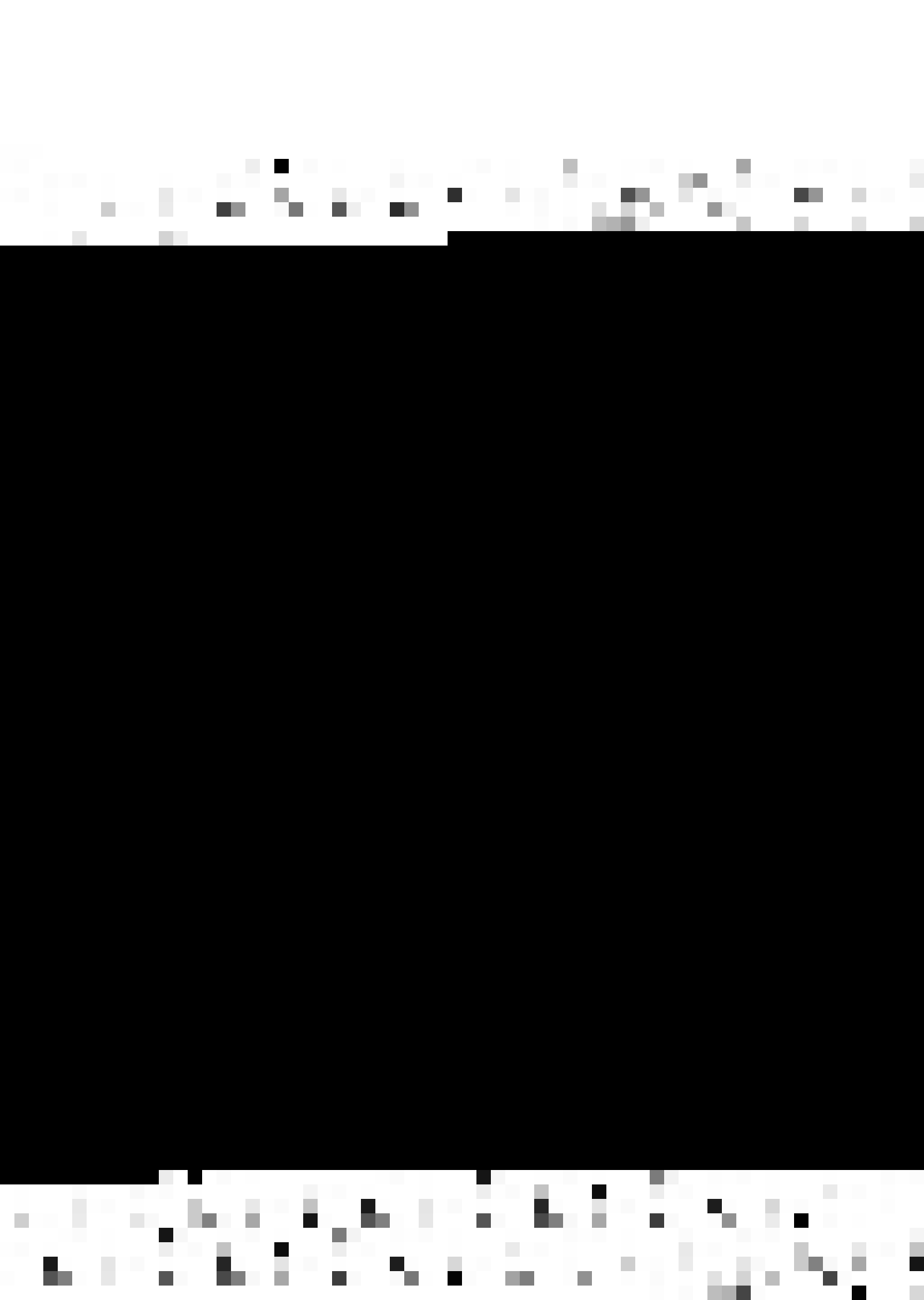
NOMENCLATURE

d	Diameter of the Cylinder
l	Length of the Cylinder
A_m	Reference area of the Model
A_t	Reference area of the Tunnel
H	Separation between Tunnel Walls
A_m/A_t	Blockage Ratio (d/H)
f	Frequency of Shedding of the Vortices
h	: Transverse Spacing between Two Row of Vortices
h^*	Maximum h
a	Longitudinal Spacing between Two Vortices in a Row
S	: Strouhal Number (fd/V)
S^*	Roshko's Universal Strouhal Number ($\frac{fh^*}{V_s}$)
V_s	: Separation Velocity = $V (1 - C_{ps})^{1/2}$
C_{pb}	: Base Pressure Coefficient, Average Pressure Coefficient over the Portion of a Body Extending into the Wake
B_p	Base Pressure Parameter $(1 - C_{pb})^{1/2}$
C_{ps}	Pressure Coefficient at the point of Separation
k	Vortex Strength



NOMENCLATURE

d	Diameter of the Cylinder
l	Length of the Cylinder
A_m	Reference area of the Model
A_t	Reference area of the Tunnel
H	Separation between Tunnel Walls
A_m/A_t	Blockage Ratio (d/H)
f	Frequency of Shedding of the Vortices
h	Transverse Spacing between Two Row of Vortices
h^*	Maximum h
a	Longitudinal Spacing between Two Vortices in a Row
S	• Strouhal Number (fd/V)
S^*	Roshko's Universal Strouhal Number ($\frac{fh^*}{Vs}$)
V_s	• Separation Velocity = $V (1 - c_{ps})^{1/2}$
C_{pb}	Base Pressure Coefficient, Average Pressure Coefficient over the Portion of a Body Extending into the Wake
B_p	Base Pressure Parameter $(1 - c_{pb})^{1/2}$
C_{ps}	Pressure Coefficient at the point of Separation
k	• Vortex Strength

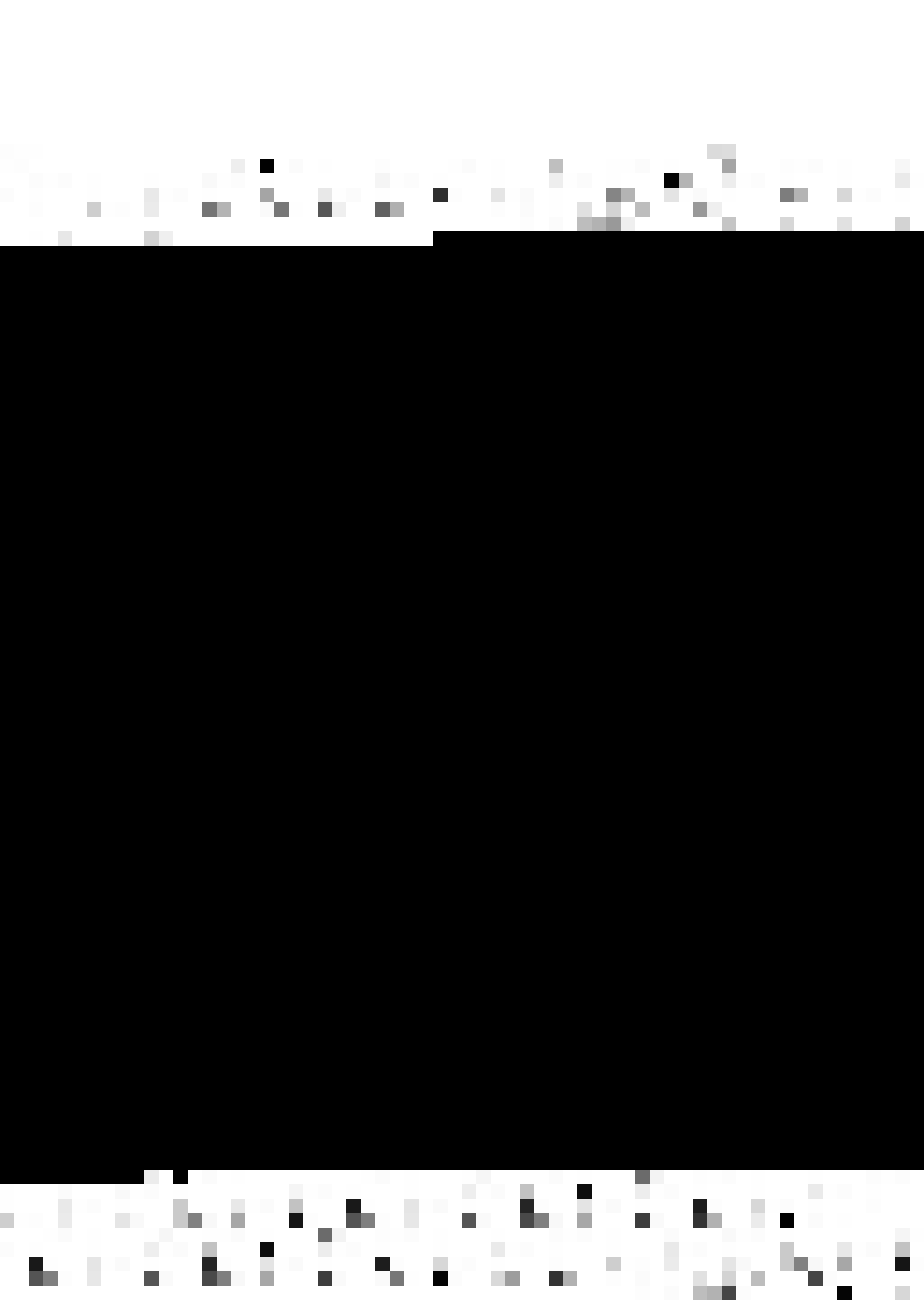


(x)

u	Translational Velocity of the Vortex Street
ν	. Kinematic Viscosity of Air
R	Reynolds Number (Vd/ν)
C_d	Drag Coefficient
F	Dimensionless frequency parameter (fd^2/ν)
C_L	Average Amplitude of Sectional Fluctuating Lift Coefficient at the Fundamental Frequency
R_c	Critical Reynolds Number at which the First Vortex Shedding takes place
α	. Half the Angle made by Vertical Tunnel Walls in Converging or Diverging Position.

Subscripts

c	Refers to the Corrected Value.
---	--------------------------------



SYNOPSIS

The vortex shedding frequency of rigid circular cylinders in confined flow is measured experimentally. Four kinds of confinement are studied in a wind-tunnel-parallel vertical walls, effect of only one wall, convergent and divergent vertical walls. Experiments are carried out in the Transition and lower Subcritical Reynolds number range ($R=144$ to 1530) with blockages upto 36%.

Plots are given in terms of Strouhal number or the shedding frequency versus H/d ratio. Available blockage correction theories are applied to the measured data to assess their validity. ✓

(The effect of confinement is to increase the shedding frequency. The increase being very steep for blockages greater than 10-15%. For convergent sections the rise is constant while for divergent sections there is decrease in shedding frequency for moderate blockages (upto 10%). Both for convergent and divergent sections shedding frequency again rises for higher blockage (greater than 10 to 15%).)



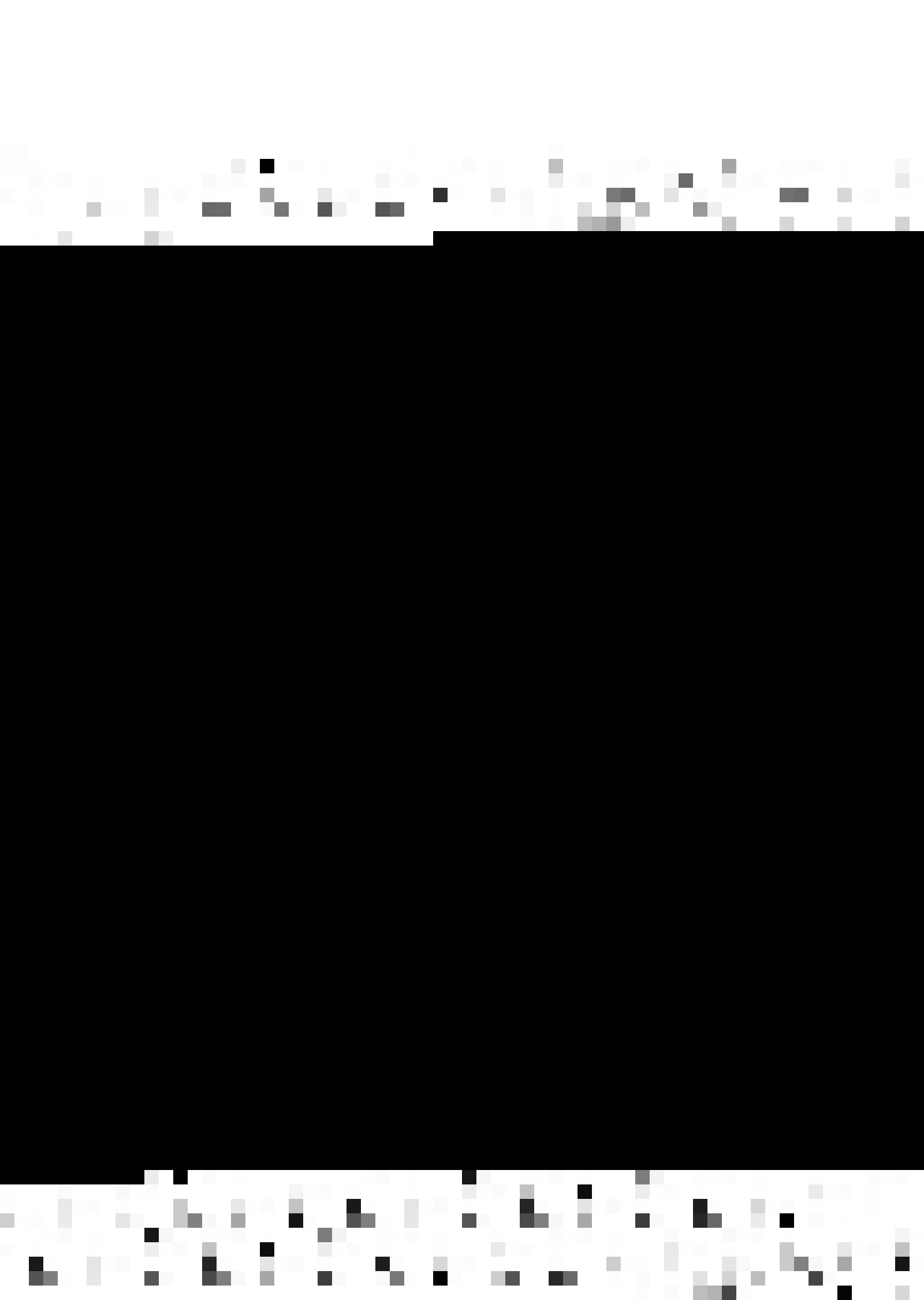
CHAPTER-I

INTRODUCTION

1.1 General

The phenomena of transverse flow induced vibration due to Von Karman Vortex Street has been catching the attention of the investigators right from the beginning of this century. The immediate problem being the vibration due to fluid flow of transmission line conductors, smoke stacks, suspension bridges, marine structures, T.V. antennas, sky-scraper buildings, launch vehicles, condenser tubes in heat exchangers, jetty piles, submarine periscopes, under-sea cables, sluice gates etc.

From a practical view point, much of the model testing is done in flows bound by walls, while the actual applications are generally in unlimited flow. Hence it becomes imperative to know the effect of walls on Karman Vortex Street. The result of blockage study on single bodies will often provide some quantitative leads related to interference effects caused by adjacent members in grouped bodies such as in heat exchanger tubes, ocean piles, bridge piers, a row of chimneys, grouped buildings and the like.



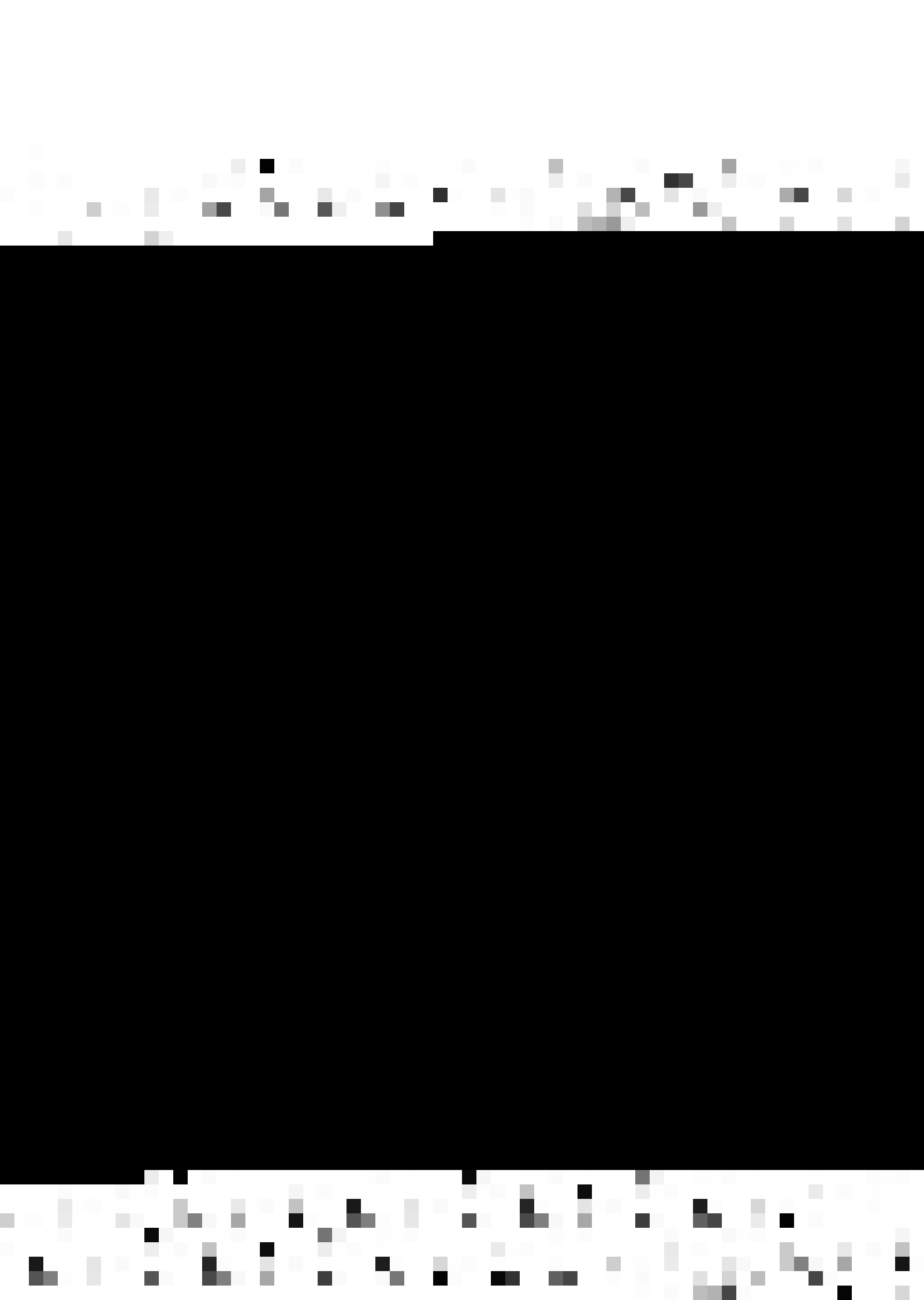
The possible interaction of walls with Karman Street geometry has been appreciated by researchers. But curiously enough until a few years back very little had been done to know the effect of walls on vortex shedding frequency - a factor of prime interest to the design engineers, as the matching of shedding frequency with systems natural frequency would result in catastrophic vibrations. Still no theoretical model is available to account for steep increase in vortex frequencies at higher blockages, some empirical attempts however have been made.

1.2 Previous Work

1.2.1 Experimental

Far back from the thirties it has been known that confining walls increase the stability of wake behind a cylinder that is the Critical Reynolds number (R_c) at which the vortex starts shedding increases as walls are brought closer. Thom (1) 1933, found that R_c increased from 30 to 62 as blockage was increased from 2.5% to 10%. Similar observations were made by Shair et. al (2) 1963, working in an oil tunnel, Fage (3) and Tomochika (4). -

Rosenhead and Schawabe (5) 1930, working in a water tank found experimentally that the ratio of the dimensions of the vortex street (h, a) to diameter (d) decreases with increasing Reynolds number and obtained asymptotic



values. At a fixed Reynolds number, the ratios of the dimensions of the street to 'd' decrease as the diameter of the cylinders become larger in comparison to the width of channel. The ratio of vortex velocity to cylinder velocity increases with Reynolds number and attain asymptotic value. At a fixed Reynolds number the velocity ratio increases with the width of the cylinder.

During recent years the interest in the effect of walls on shedding frequency has revived. Wilson and Caldwell (6) 1971, during a model study to simulate the transatlantic ocean pipe laying found that due to ocean floor, the frequency of shedding of a flexible cylinder increased as much as five times in comparison to if there was no floor (or wall). They also studied the effect of proximity of another pipe.

To use the remarkable dependence of the shedding frequency on the velocity, specially at lower velocities (< 400 cm/sec.), researchers have tried to use the shedding frequency as a measure of velocity. To use as a commercial flow meter Tsuchiya, et. al (7) 1970, studied the effect of walls (cylindrical pipe). In this particular study they found that if the strouhal number was based on velocity near the cylinder (gap velocity) and not on free stream velocity, then there was no effect of cylinder size.



They found that Strouhal number based on this modified velocity has a constant value of 0.184 for blockages less than 30%, independent of the geometrical sizes. A flow meter based on Vortex shedding frequency has now been marketed by Westinghouse Electric Company, U S A (8). An accuracy of $\pm 5\%$ and max. velocity of 30 ft/sec. is claimed.

A number of studies (listed below), done on various shapes of cylinders and plates show that the effect of blockage is to increase the Strouhal number, first gradually but in pronounced fashion at the higher value.

Ramamurthy (9) 1973, did his experiments on circular cylinders ($R = 1.3 \times 10^4$ to 23×10^4 , blockages 7 to 70%) and triangular cylinders at various orientation. Twigg - Molecey (10) 1973 used triangular cylinders ($R = 10^3$ to 5×10^4 but low blockages - max. 8%) also in low-speed wind tunnel. Chen (11) 1967, experimenting on flow past 90° wedge, concluded that dominant frequency of vortex shedding becomes weaker when the blockage increases. Toebe and Ramamurthy (12) 1970, presented experimental data related to the Strouhal frequency and lift forces for circular cylinders and triangular prism upto a blockage of 44.5%. They demonstrated that the contracted jet velocity and the gap velocity were useful scales to formulate



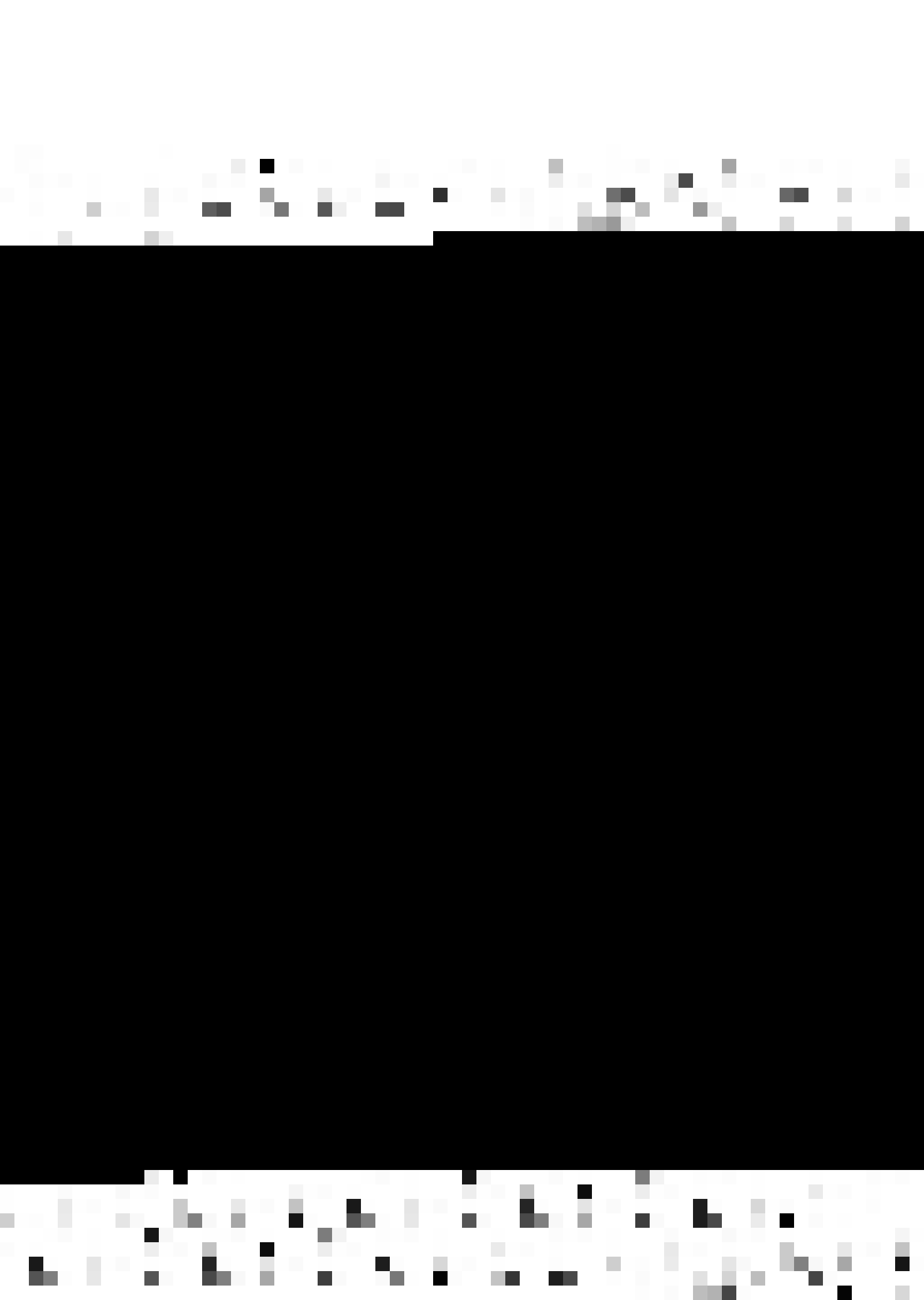
the Strouhal number. Tozkas (13) 1965, examined the effect of flow confinement on the 2-dimensional cylinder and sharp edge plates on the Strouhal number. Abernathy (14) 1958, and Champagne (15) 1971, studied the confined flow effect on flat plates at various angles of attack. Shaw (16, 17) 1971, did experiments on circular and square cylinders and on flat plate in water tunnel for blockages upto 35%. Toebe's (18) 1971, gave experimental results for circular and triangular cylinders in water tunnel for blockages upto 45%. Modi and El-Sherbiny (19, 20, 21) 1971-73, did investigation on a set of stationary circular cylinders and flat plates, representing the blockage ratio range of 3-35 % at the subcritical Reynolds number of $10-12 \times 10^4$.

However no study has been made at low Reynolds number (stable, transition and lower subcritical range of vortex shedding, that is, 50 to 10,000), nor much of theoretical explanation is available.

1.2.2 Theoretical

Glauret (22) in 1928 and Rosenhead (23) in 1929 obtained some estimates for various parameters of the vortex street in a channel of finite width. (given in Appendix-A) Later experimental results however do not verify them.

Researchers have also tried to obtain formulas to correct the measured values analytically. As pointed



out by Roshko (24) 1961, any correction method must include the effects of -

- (i) interference between wall and cylinder
- (ii) interference between wall and wake
- (iii) possible interference effects on the separation mechanism and the structure of the wake.

No correction method is available which takes in account the third effect. Allen and Vincenti (25) 1944, have used the method of images to obtain corrected velocity and drag (given in detail in Appendix A) Maskell (26) 1965, used momentum model to achieve the same. But these methods are absolutely inadequate particularly at higher blockages (Modi, 19). Modi also has tried to modify these methods through inclusion of the higher order terms to improve their applicability (greater blockages).

1.3 Present Work

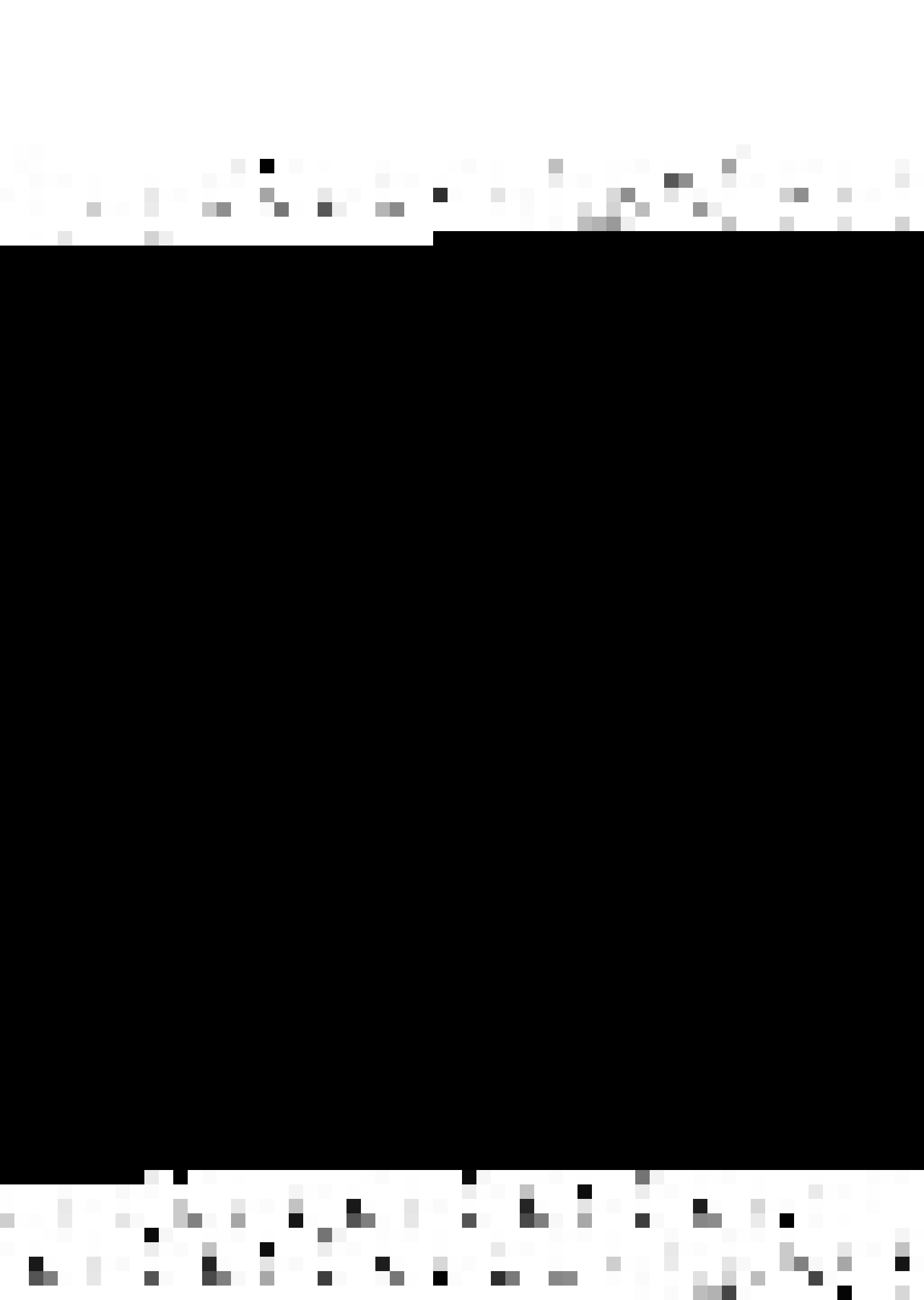
As there is no study of blockage effects at low Reynolds number ranges, experiments are carried out here in an open type, low speed, variable cross-section wind tunnel in the range $R = 144$ to 1530 , with blockages upto 36% to measure the shedding frequency. In a particular set velocity and cylinder diameter and hence Reynolds number was kept constant, while the vertical walls separation was changed.



Effect of only 'One-Wall' is further studied. This was done to see the difference with the 'Two-Wall' effect and the reported large (5 times) increase in vortex shedding of the pipes anchored above the ocean floor (6).

At small wall separation we can never be sure that the tunnel walls are exactly parallel. A slight deviation from parallelism may affect the shedding frequency. Hence the effect of convergence and divergence of the tunnel walls (vertical ones only) with various blockage ratios is also studied. This study was made also to see the effect of increase or decrease of adverse pressure gradient on the vortex shedding frequency.

The available blockage correction theories are applied to the measured data on the two parallel wall effect, to assess their validity.



CHAPTER-II

MECHANISM AND FACTORS AFFECTING VORTEX SHEDDING

In this chapter, the Vortex shedding mechanism and the effect of other parameters on the shedding frequency are discussed as found in literature. This may help in isolating the effect of walls from any other parameter if any.

2.1 Mechanism of Vortex Shedding

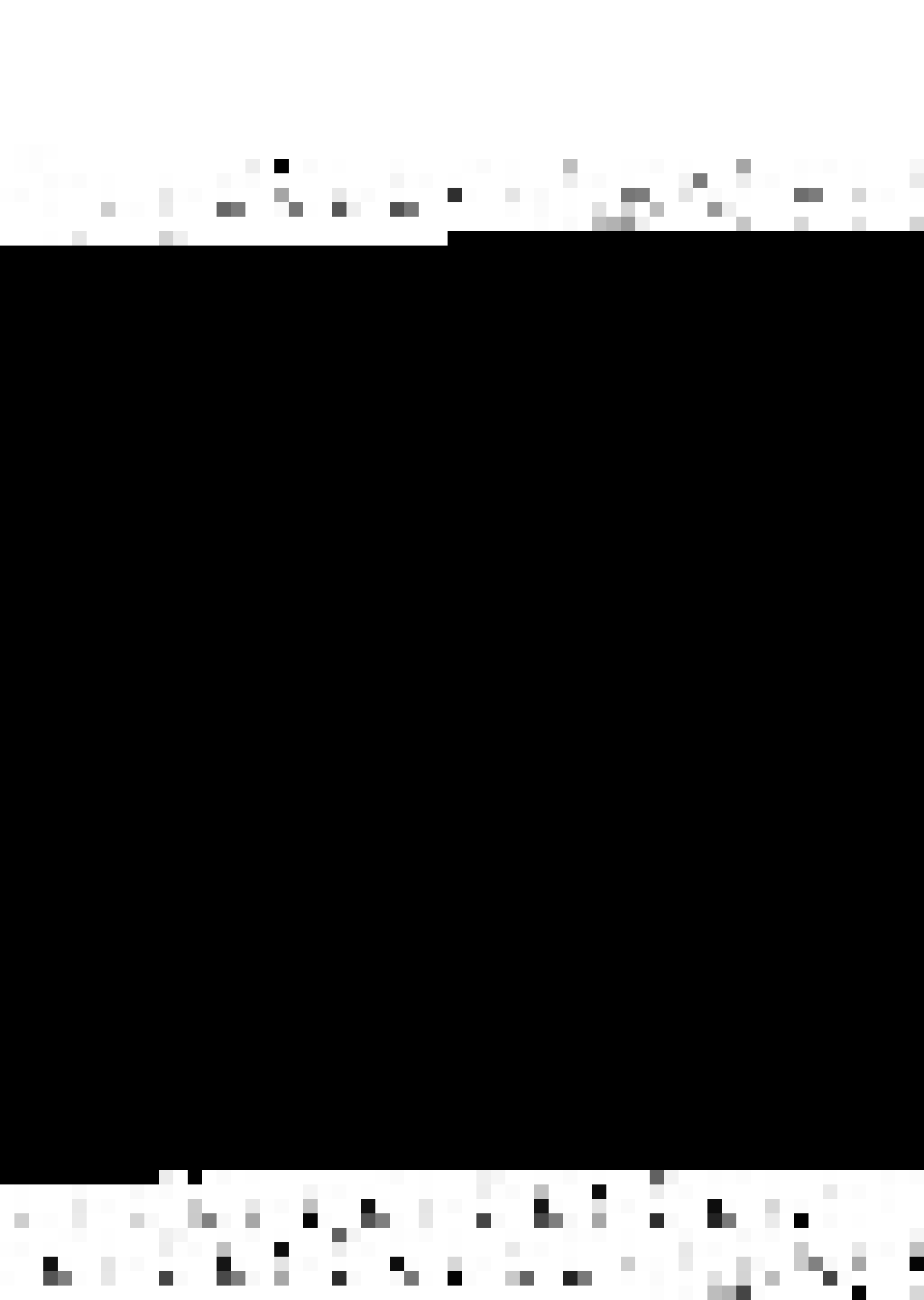
The manner in which Vortices are shed, depends upon the Reynolds number $R = Vd/\nu$. The mechanism of Vortex shedding in various Reynolds number regimes are given below

(A) Regime of unseparated flow ($R \ll 5$)

At extremely low Reynolds numbers ($\ll 5$) the flow in the immediate vicinity of the cylinder is very much like an ideal flow and no Vortices are formed.

(B) Twin Vortex stage (5 to $15 \ll R \ll 40$)

Due to the presence of boundary layer around the cylinder and the adverse pressure gradient, flow separation



takes place. The vortex layer, leaving the surface at positions of separation, on the two sides of the body, come together further downstream. Vorticity diffuses from the layers into the main body of the fluid, but is also generated in the boundary layer and added to the vortex pair. At small Reynolds number (≤ 40) a state of equilibrium is set up between the rates of generation and diffusion of vortices and two symmetrical stationary Vortices are formed (foppl vortices).

(C) Stable range of vortex shedding

(1) $40 \leq Re \leq 90$ (Trittons(27) low speed mode)

As the velocity is increased the vortices continue to grow and elongate, being fed by circulation from shear layer. Above some critical Reynolds number (R_c), depending upon (i) shape of the obstacle (ii) the degree of turbulence in the mainstream and (iii) proximity of the channel walls to cylinder, the vortex become strong enough to draw the other shear layer across the wake. The approach of oppositely signed vorticity in sufficient concentration cuts off further supply of circulation to the vortex, which then ceases to increase in strength. The first vortex shedding takes place at this stage. The second vortex continues to grow in size until it reaches the same stage as of the first one and is then shed, Hence now a



regular alternating shedding of vortices begins and the shed vortices arrange themselves asymmetrically and move down the flow called Von Karman Vortex Street. each vortex being opposite the mid-point of the interval between 2 vortices in the opposite row. It is experimentally found that the vortices actually do not arrange themselves exactly in two parallel rows with definite spacing ratio (h/a), but they change along the direction of flow (28).

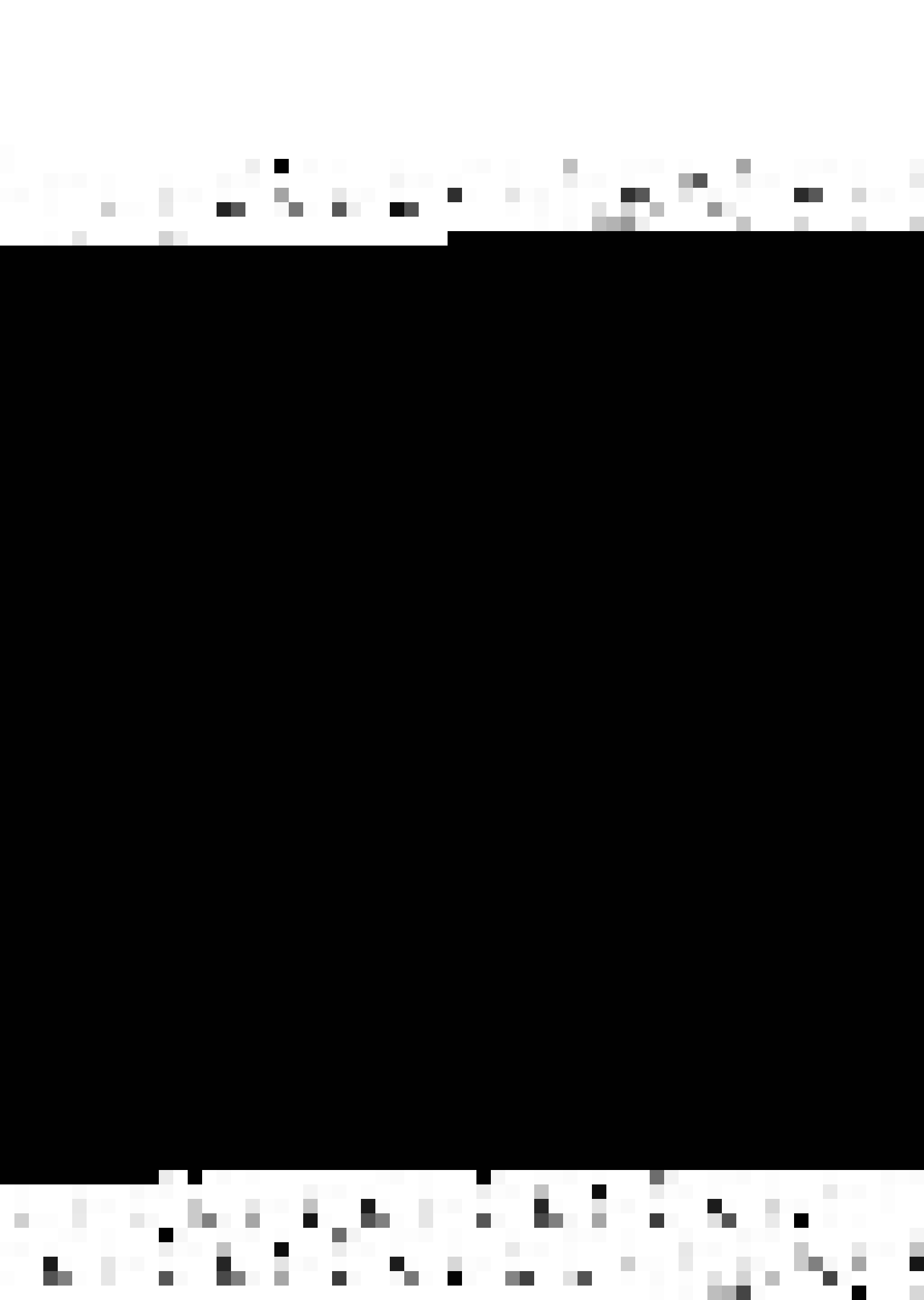
In this Trittons low speed mode the periodicity is governed by wake instability.

$$(11) \quad 90 \leq R \leq 150 \quad (\text{Trittons high speed mode})$$

In this range according to Tritton the periodicity is governed by vortex shedding. The flow is still laminar and the street extend far behind the cylinder. The vortices decay by viscous diffusion.

$$(D) \quad \underline{\text{Transition range}} \quad 150 \leq R \leq 300$$

As the Reynolds number is increased, a laminar to turbulent transition begins in the free vortex layer leaving the cylinder. The resulting vortices in the wake are composed of turbulent fluid and by the time the Reynolds number becomes equal to 300, the vortex periodicity completely vanishes at a distance approximately 48 dia downstream from the cylinder.



(E) Irregular Range(i) Subcritical range $300 \leq R \leq 3 \times 10^5$

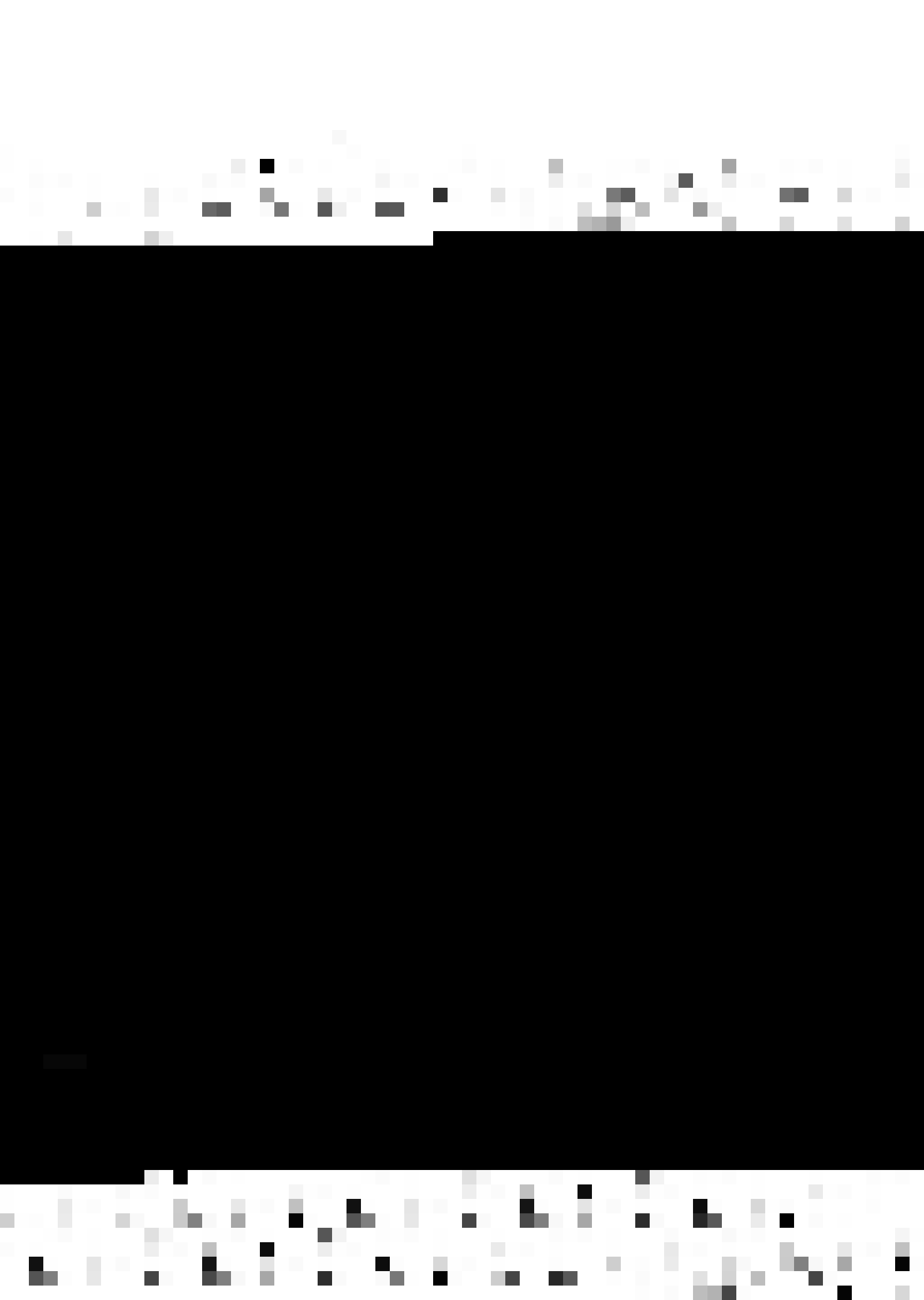
Above $R = 300$ the flow becomes turbulent at the separation point. Vortex shedding is periodic and fairly constant throughout this range, but the velocity in the immediate vicinity of the cylinder fluctuates in an irregular manner because of flow turbulence. The flow becomes fully turbulent 40 to 50 dia. downstream.

(ii) Transition Range $3 \times 10^5 \leq R < 3.5 \times 10^6$

The next important transition occurs somewhere in the range $10^5 \leq R \leq 5 \times 10^5$, depending upon cylinder roughness and the free stream turbulence level. The laminar boundary layer becomes turbulent, the wake becomes 3 dimensional and the vortex action is diffused, we can no longer speak of vortex shedding frequencies, but can only mention the dominant frequency in a spectrum of component frequencies.

(iii) Transcritical Range. $3.5 \times 10^6 \leq R < ?$

The turbulent vortex shedding is reestablished at $R \approx 3.5 \times 10^6$, Strouhal number becomes higher and wake narrower. This region persists out to the upper limit of the experiment, a Reynolds number of almost 10^7 .



2.2 Effect of Various Parameters on Shedding Frequency (Strouhal Number)

2.2.1 Effect of Reynolds number

The shedding frequency is dependent on the Reynolds number. (All the values given below apply for cylindrical model with low turbulence level $\approx 0.05\%$)

(1) The Strouhal number rises steeply with velocity in the stable range.

According to Roshko (29)

$$S = 0.212 \left(1 - \frac{21.2}{R} \right)$$

$$\text{or } \left. \begin{array}{l} F \text{ (Dimensionless) } \\ \text{Frequency} \end{array} \right\} = \frac{fd^2}{V} = .212 R - 4.5 \left. \vphantom{\begin{array}{l} F \text{ (Dimensionless) } \\ \text{Frequency} \end{array}} \right\} \text{ for } 50 < R < 150$$

but according to Tritton (27) a small transition occurs at $R \approx 90$ and he gives

$$S = .144 - 2.1/R + .00041 R \text{ for } R < 105 \text{ low speed mode}$$

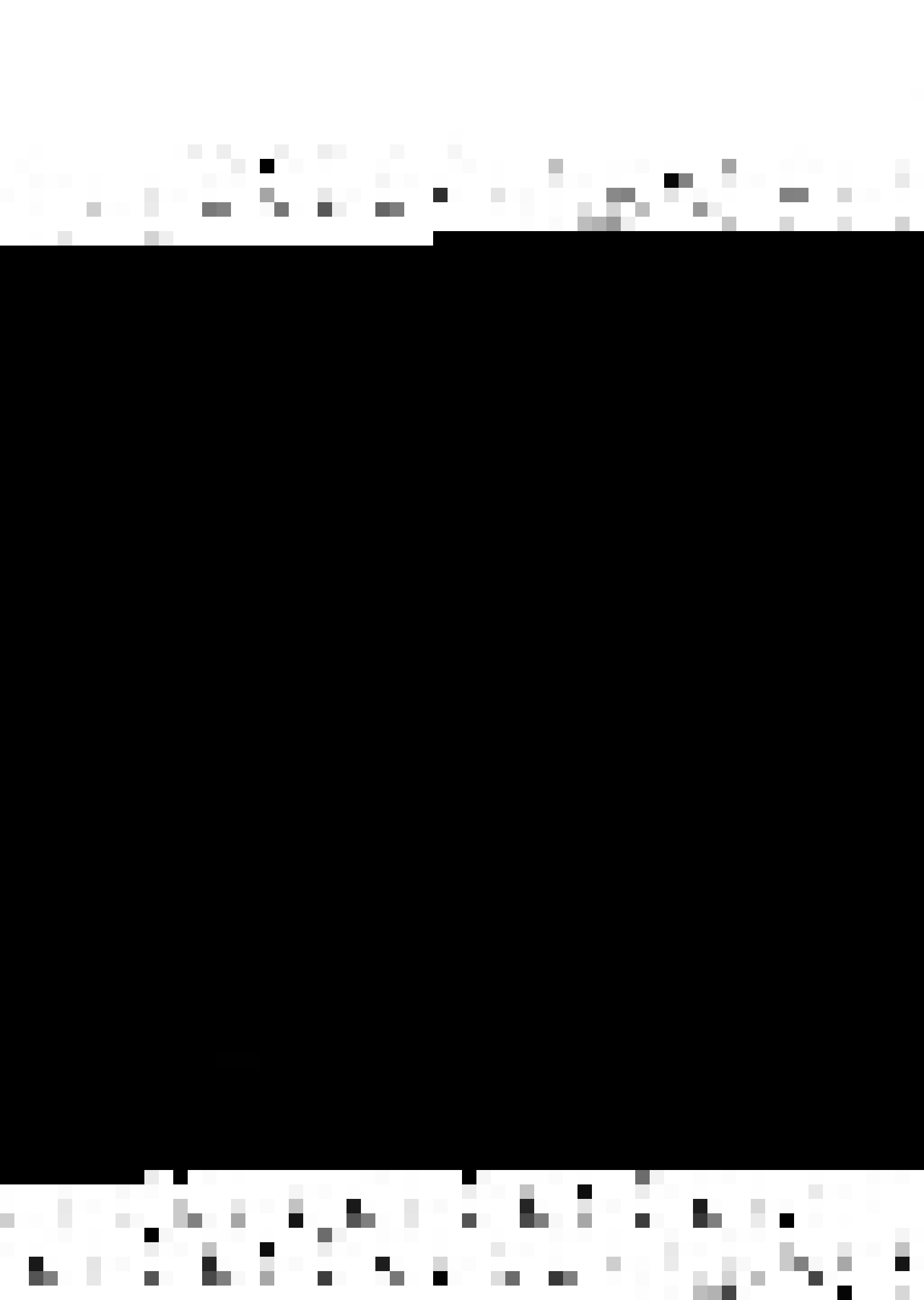
$$\text{and } S = .224 - 6.7/R \text{ for } 80 < R < 160 \text{ high speed mode}$$

(11) In transition range $150 < R < 300$ no $S - R$ law holds, but frequency of shedding increases with Reynolds number.

(111) In irregular range, according to Roshko

$$S = .212 \left(1 - \frac{12.7}{R} \right) \quad \text{for } 300 < R < 2,000$$

$$\text{or } F = .212 R - 2.7$$

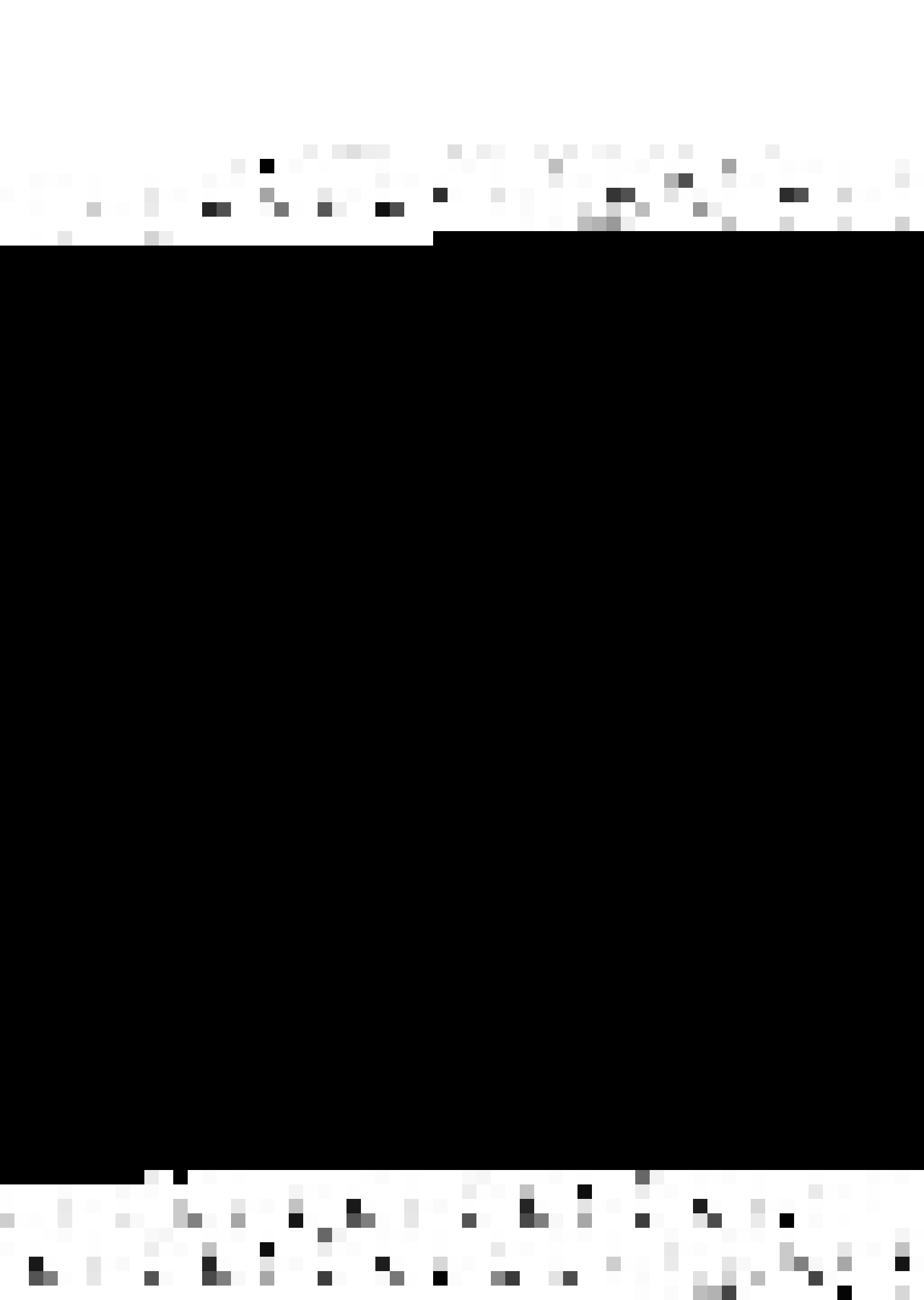


For Reynolds number greater than 2,000 no law has been given in literature but following observations have been made. The Strouhal number increases with increasing Reynolds number to a maximum at 2×10^3 and then decreases to a minimum, finally rising again in the critical Reynolds number range to a high value of 0.47 at about $R = 4.5 \times 10^5$. The vortex street is very narrow and this high Strouhal number is maintained upto $R = 5.5 \times 10^5$. The narrow vortex street is very unstable and it becomes fully turbulent when the value $R = 5.5 \times 10^5$ is exceeded.

In the transcritical range (24) however turbulent vortex street is reestablished and the Strouhal number is about .267, higher than the lower turbulent vortex shedding range $300 \leq R < 2 \times 10^3$.

2.2.2 Effect of Cylinder Roughness and Turbulence Level

The vortex shedding frequency is effected by both the surface roughness of the vortex generating body and the free stream turbulence level. Not much quantitative study has been made. However it is found that a smooth, polished cylinder in a low level turbulence flow has a greater shedding frequency than a rough cylinder in a high turbulence flow for Reynolds number below 10^5 (Chen (30)).



Surry (31) and Petty (32) have also shown that for low intensity turbulence of small scale the effect of turbulence was additive to the vortex shedding effects but for scales of turbulence of the same order or greater than cylinder diameter, the shear layers and the vortex shedding were effected even to the extent of suppressing vortex shedding.

2.2.3 Effect of Shape of the Body

Besides circular cylinders, vortex shedding can take place from flat plates, wedges, ogival and elliptical cylindrical models etc.

According to Roshko (29) distance between vortex row increases as the body becomes more bluff, while the shedding frequency decreases. He, however, found that if Strouhal number (S^*) is defined on the basis of 'h' (transverse spacing between vortices) instead of cylinder diameter, then a universal value of $S^* \approx .28$ is obtained for a variety of 'bluff' shapes.

Fage and Johnson (1928) found a mean value of $S = .148$ for flat plates (for angle of incidence 30°) Tyler (1931) $S = .158$ and Blanks, et. al. (1935) $S = .18$.

Tyler gives an average value of .150 for his aerofoils (less than for plates) and Blank .21 (greater than plates).



2.2.4 Effect of Orientation of the Cylinder to the Flow Direction

A slight tilt of the cylinder - that is, its axis not being perpendicular to the flow direction changes shedding frequency.

Chiu (33) found that Strouhal number decreases as cosine law as angle of tilt increases.

$$(S)_{\text{yawed cylinder}} = (S)_{\text{unyawed cylinder}} \times \cos \beta$$

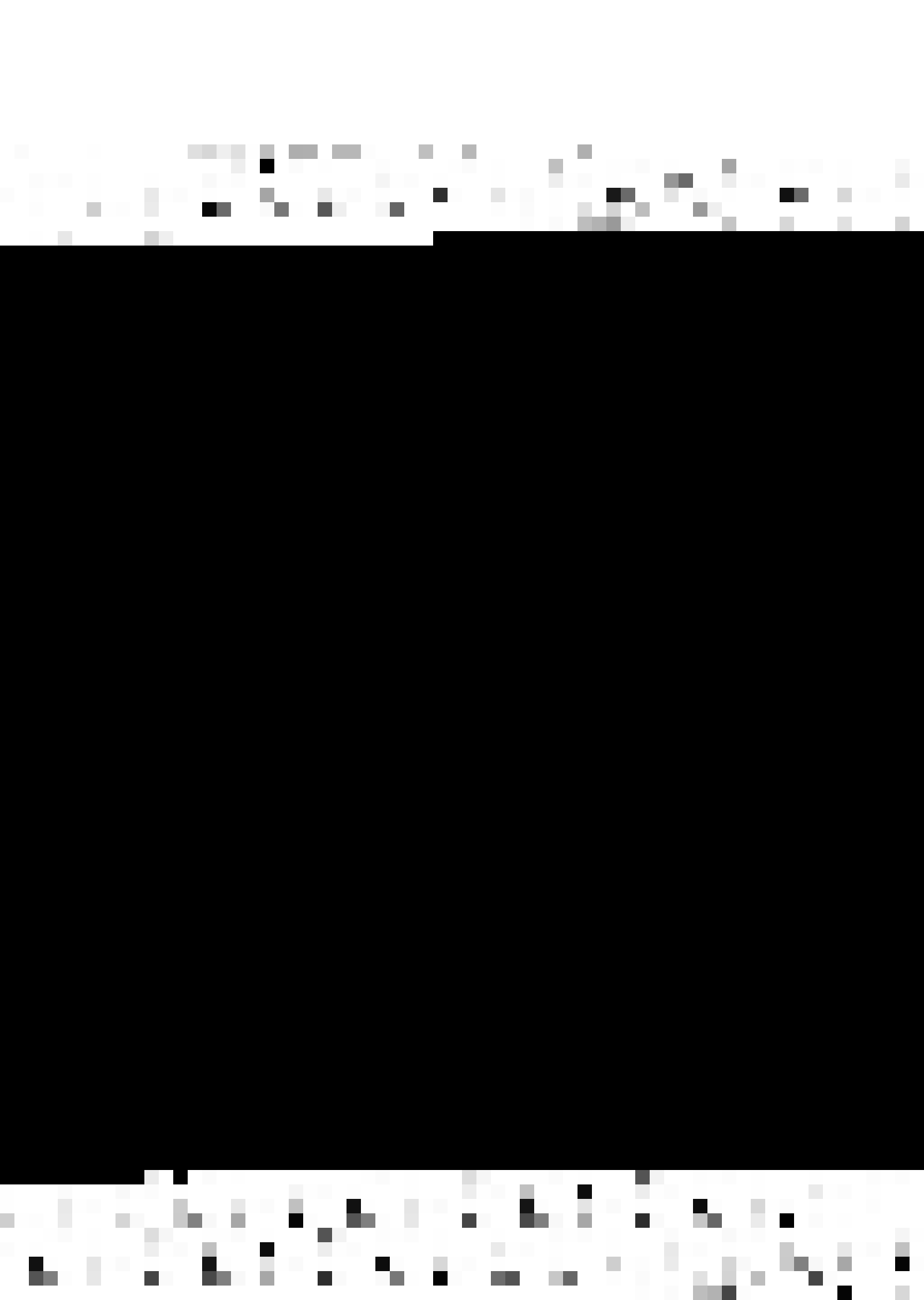
where β = angle between normal to cylinder axis and flow direction.

The drag and lift forces exerted on the yawed cylinder however followed a $\cos^2 \beta$ law.

2.2.5 Effect of Cylinder Flexibility

It is not possible to find a absolutely rigid body. A vibrating (flexible) structure changes the vortex street geometry.

Steinman (34) and others have found that the model vibration causes increase in the magnitude of forces on the model. The additional aerodynamic force is probably associated with periodic shifting of the separation points of the flow from the surface of the structure, thereby causing increased circulation, that is, to say that

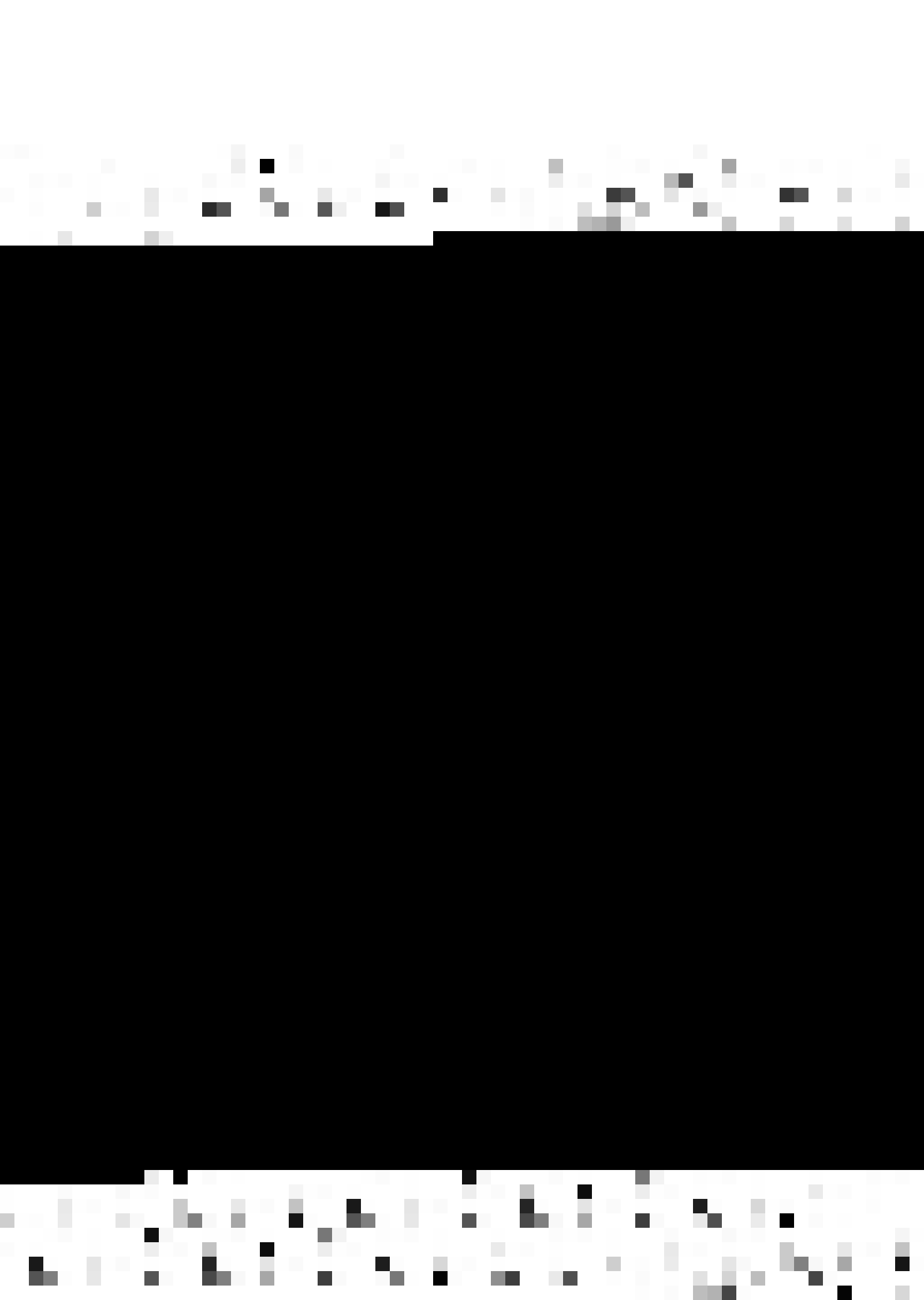


vortices in the wake are larger and stronger (than stationary cylinder). For the vortices to be stable, the distance between the vortices in each row must also increase in the same ratio and hence the shedding frequency and Strouhal number are decreased.

It is also noted by Den Hertog (35) and Griffen, et. al. (36) etc. that if cylinder vibrations reach a critical threshold, then the cylinder motion forces the vortex shedding to take place at the cylinder vibration frequency and not at the Strouhal frequency (called locking or synchronization of cylinder vibration and eddy shedding frequency). It is accompanied by large correlation in the phase of the vortex shedding along the cylinder axis.

2.2.6 Cylinder End Conditions

Both Gerrard (37) and Humphreys (38) have demonstrated the considerable effect that the end disturbance can have on the vortex shedding mechanism and the forces acting on the cylinder. Humphreys found that the lift force was reduced if the hole where the test cylinder passed through the tunnel was unsealed. However R.T. Keefe (39) found no difference in Strouhal number whether the clearance holes were open or sealed.



CHAPTER-III

EXPERIMENTAL SET-UP AND TEST PROCEDURE

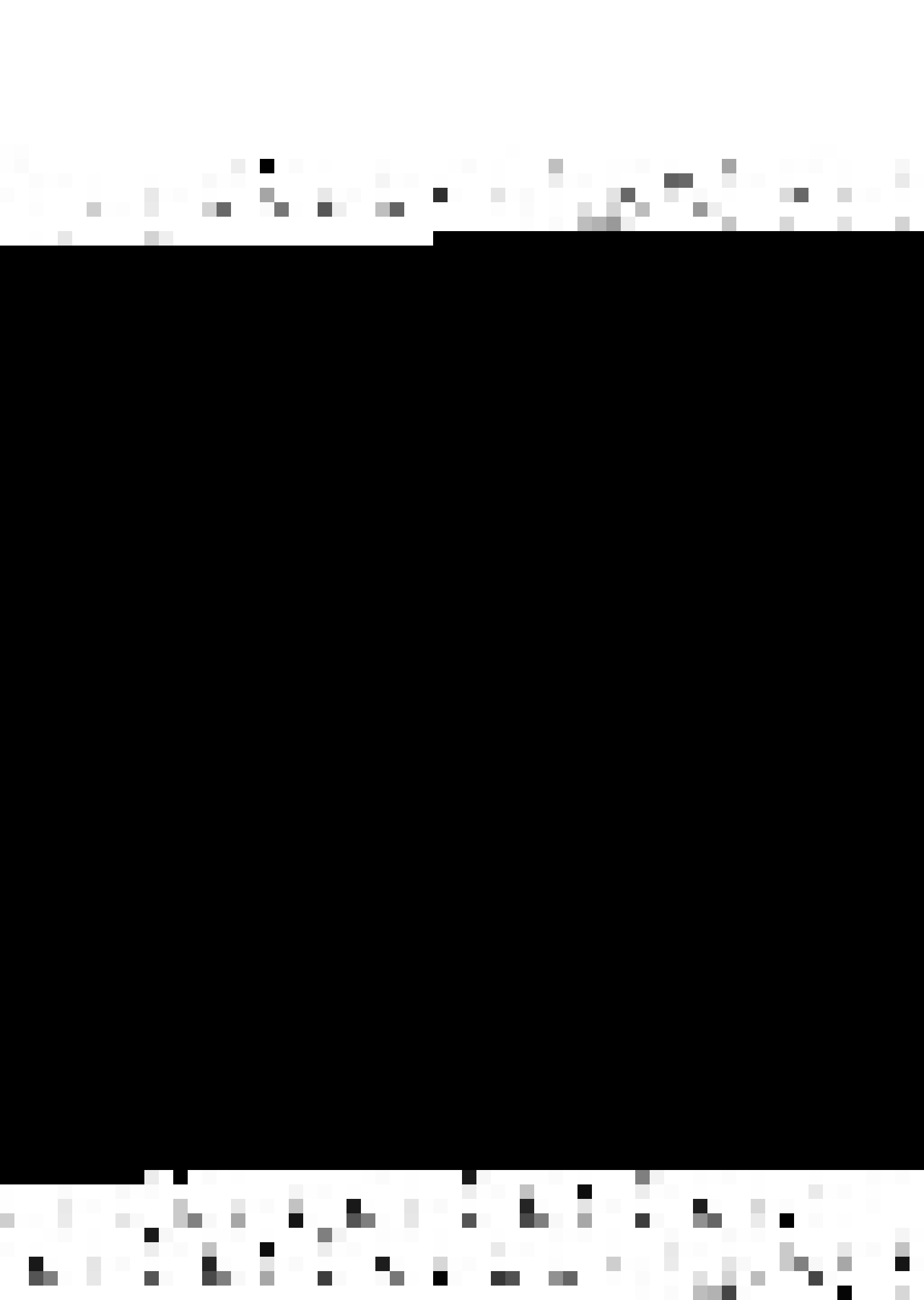
3.1 Subsonic Wind Tunnel

The shedding frequency measurements were made in a specially built low-speed wind tunnel. It was of open-type with a rectangular cross-section of 20 cm. height and continuously variable width (H) upto 13 cms. made of transparent perspex sheet. Air was sucked by a blower (Wolf, portable, maximum capacity 51.5 cu.ft/min) having a universal motor, so that air speed in the test section was continuously variable upto around 2.2 meter/sec (at maximum tunnel wall's separation) by the help of a variac.

Fairings were attached at the entrance of the tunnel to make the flow uniform. Velocity measurements, at the test section, made by hot wire anemometer showed a uniform velocity except near the walls. No honeycomb etc. was used but still the maximum turbulence level was found to be approximately as low as 0.02%.

3.2 Models.

Circular tubes were used to generate the vortex street. Tubes of .166 cm and .3 cm diameter were made of



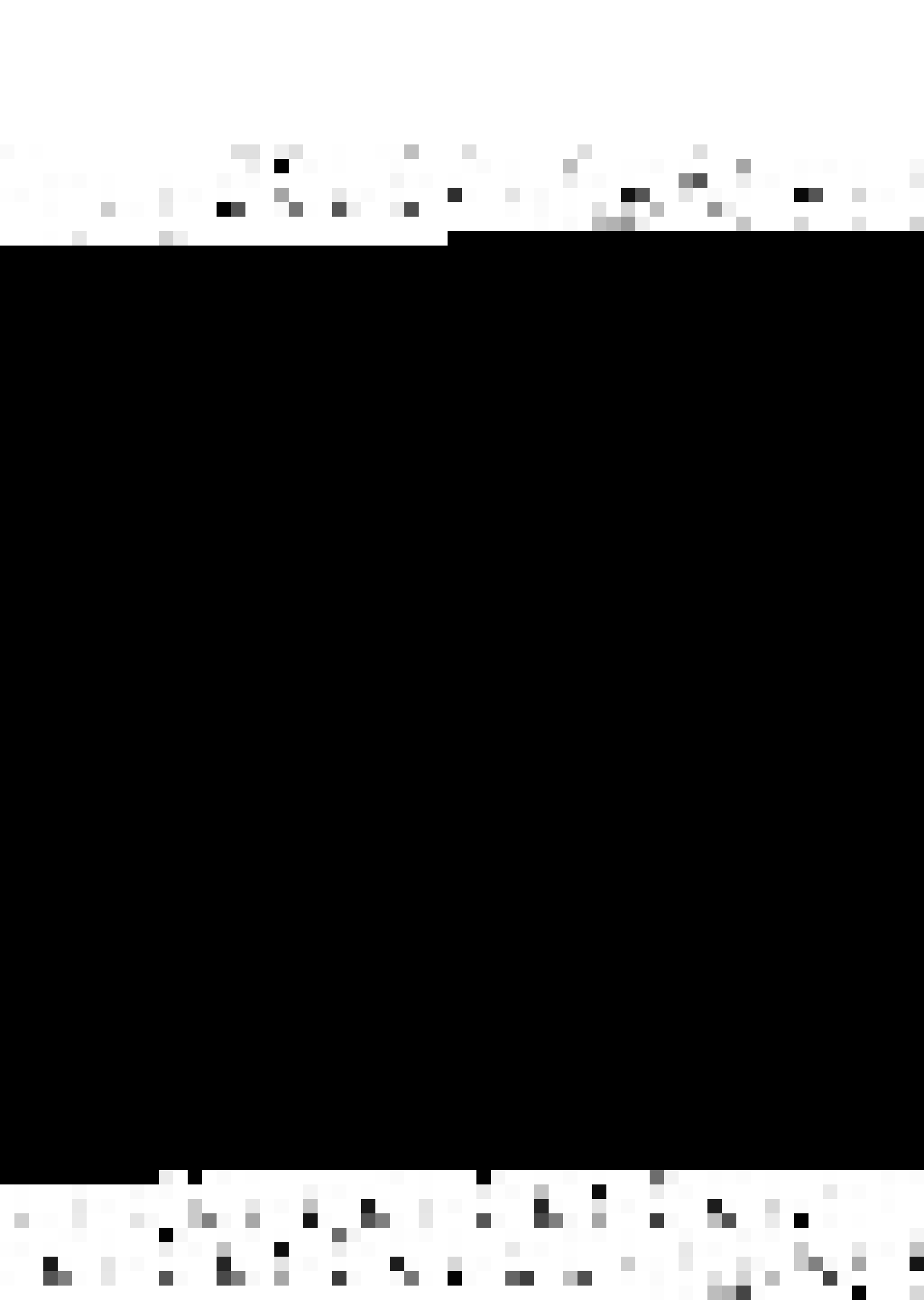
stainless steel having polished, smooth surface, while tubes of .59, .8 and 1.0 cm dia. were made of glass having uniform diameter.

The tubes spanned the complete height of the tunnel having sliding fit at the top and bottom of the tunnel. They could be positioned at any distance from 35 cm to 40 cm , from the tunnel entrance. It was ensured that tubes had sufficient rigidity and do not start vibrating by the oscillating force generated by the vortex street. Results were checked by filling the tubes by sand, no difference in shedding frequency was noted.

3.3 Measurement of Velocity

3.3.1 Defining the Velocity

It was decided to choose the characteristic value for velocity (V) for a given experiment, to be the velocity which would exist at the same location as that of the centre of the cylinder under flow conditions identical with those of the experiment but in absence of the cylinder. The basis being that it is the velocity near the cylinder which is more effective in causing vortices and secondly to use the same definition of velocity as used by most of the investigators. It was decided to make the blockage correction later in presenting the results.



3.3.2 Micromanometer and Pressure Probes

A micromanometer (Model MM-3 Flow Corporation) was used to measure the pressures accurate upto 0001" of water. A pitot tube, which could be aligned in a plane perpendicular to the cylinder axis but in line with it, was used to measure the stagnation pressure. A tap on the tunnel's top wall was used to measure the static pressure.

3.3.3 Measurement

By the help of the above pressure measurements and temperature by a thermometer (0.1° least count), velocity was calculated. It was then used to calibrate the hot wire. It must be pointed out that velocity measurements by pitot tube had to be done only once at the start of a particular set of readings (when the walls were at their maximum separation). For other wall separation, same velocity was obtained by balancing the null circuit of hot wire amplifier (for same D.C. current) by changing the intake of the blower by the help of variac.

3.4 Vortex Sensing Transducer and Amplifier

3.4.1 Hot Wire Probe:

A hot wire probe was used to detect the vortices and for turbulence measurement. It was also used to make



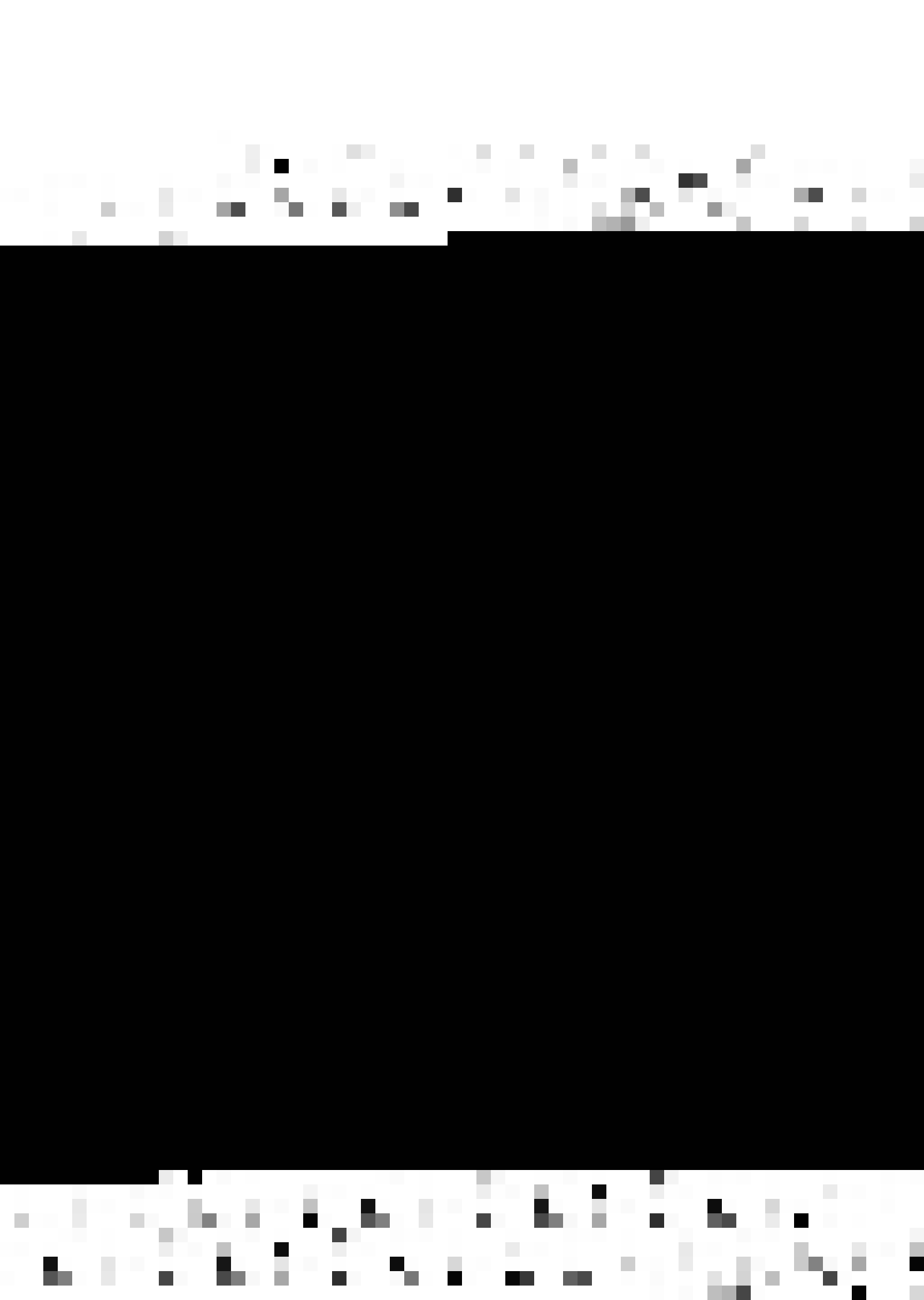
the velocity same at the position of cylinder at various wall separation as described in 3.3.3. 2 needles were attached at right angle to a 0.3 cm stainless tube by the help of shellac, across which Wollaston (10% Rh, Pt) wire of .00497" diameter was soldered (resistance 448 ohms/ft). The wire was heated by means of D.C. current from hot wire anemometer amplifier (3.4.2), connected by wires going through the tube and being attached to the needles. The needles were electrically insulated from the tube. The arrangement then acted as a hot wire probe.

3.4.2 Hot Wire Anemometer Amplifier.

A constant current type of compensated hot wire (Flow Corporation model HWB3) amplifier was used to heat the hot wire probe and to provide the amplified output, for turbulence and eddy shedding frequency measurement. It had correct frequency response range from 2 to 100,000 c.p.s. It could match any hot wire probe with a time constant between 0.23 millisecc to 30 millisecc.

3.4.3 Low Pass Filter

As the amplifier (3.4.2) used had an input noise figure of 0.25 microvolt (transformer input) and as we also know that rapid input fluctuating signal produce less and less input signal, hence it becomes meaningless to measure



signals which have large frequency but input less than 0.25 microvolt. Hence to reduce this extraneous noise a 7 kilo-cycle plug in low pass filter (Flow Corporation) was used at the output of the amplifier. It should be noted that the frequency of generated vortices were well below this limit (50 to 200 c.p.s.)

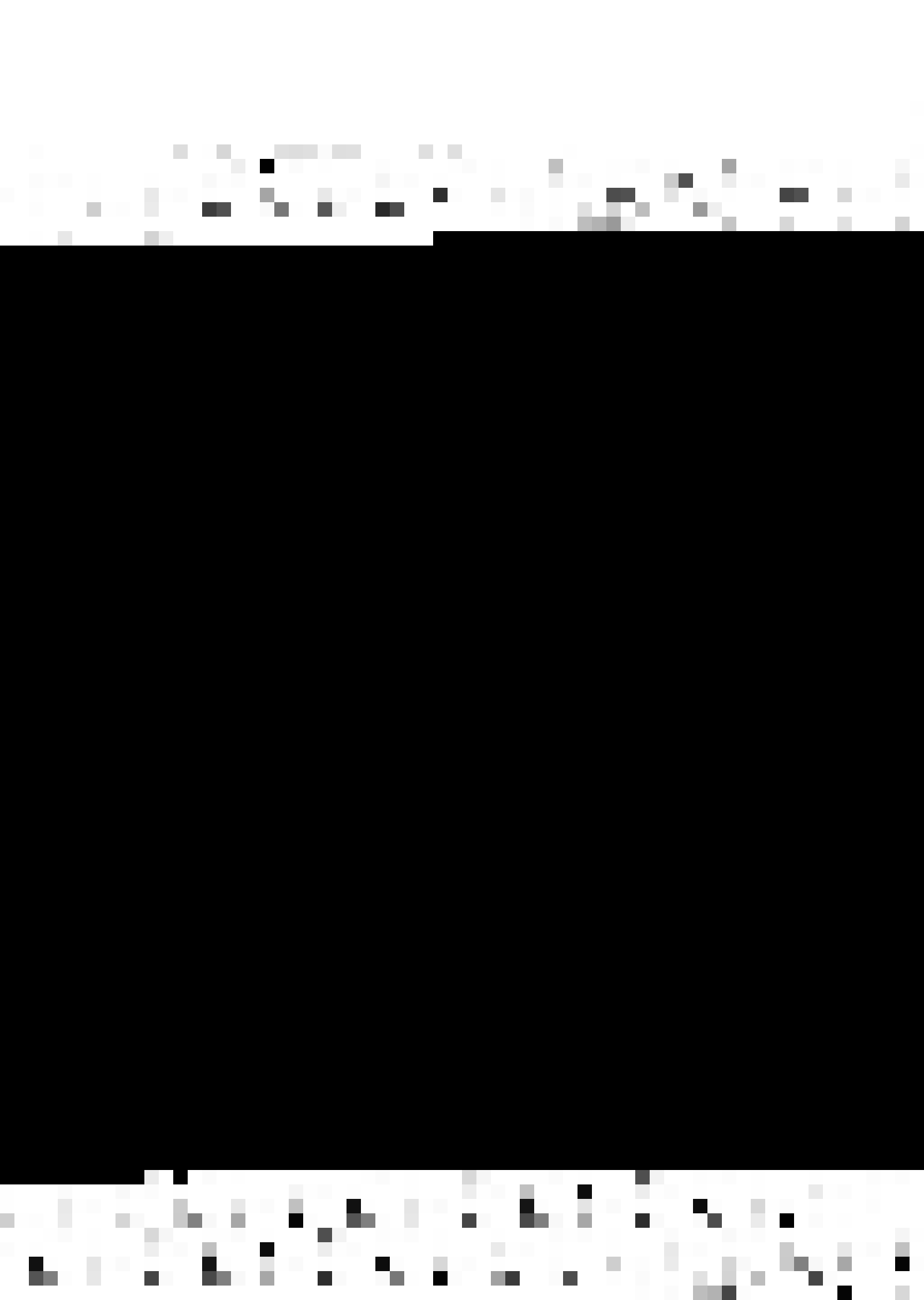
3.5 Measurement of Turbulence

As it is known from literature that turbulence level of the flow affects the shedding frequency, it was decided to measure percentage turbulence level (r.m.s. value of fluctuating signal/average signal) for each blockage in a set of readings. The true r.m.s. meter of 'DISA 55A06 random signal indicator and correlator' was made use of, in absence of anyother true r.m.s. meter. Formulas given in the manual of the Flow Corporation hot wire anemometer were used to calculate the percentage turbulence level (only in the direction of flow). Fortunately, it was found that percentage turbulence level did not ~~change~~ with wall separation. A small variation of $\pm 5\%$ was observed from the mean value of .020.

3.6 Measurement of Shedding Frequency.

3.6.1 Positioning the Hot-Wire Probe

The output signal from the hot-wire amplifier



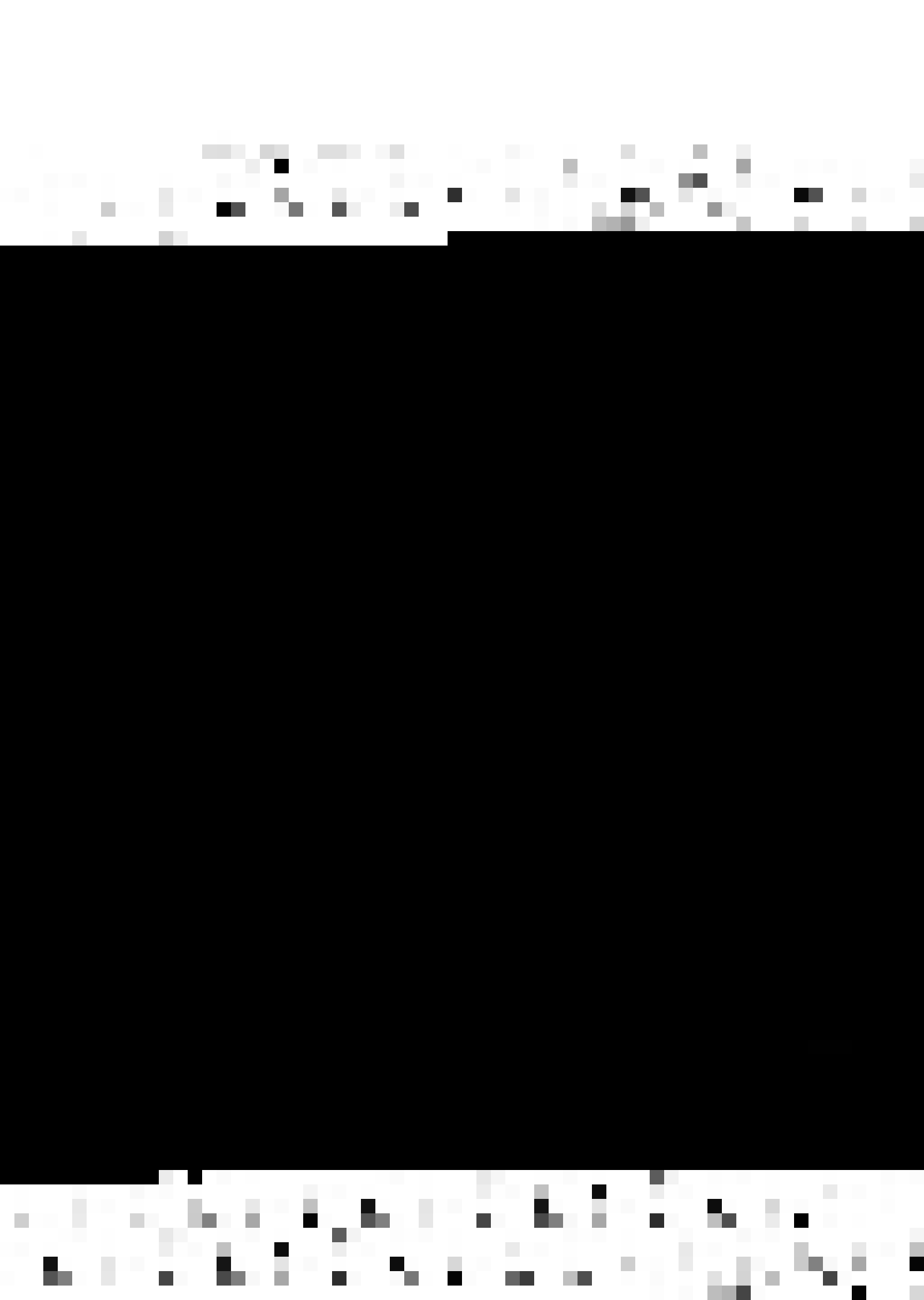
was monitored on a Tektronix 502-A oscilloscope. The hot wire probe was mounted on a uni-slide and could be traversed horizontally. It was moved by help of vernier and so positioned that best possible periodic trace was available on C R.T. screen.

3.6.2 Filtering the Input Signal - Wave Analyzer

To find the dominant eddy shedding frequency, after positioning the hot wire probe, the signal was fed to a Wave-Analyzer. (Model 1900-A General Radio having a frequency range 20 to 54,000 c.p.s.) The frequency dial (with vernier attachment) was hand tuned, for maximum input as seen on the Analyzer meter. A 3 cycle bandwidth with slow meter response was used.

3.6.3 Measurement of Shedding Frequency - Frequency Counter

The filtered input signal by the Wave Analyzer was fed to a frequency counter for accurate frequency counting (Model 7370, Beckmann Universal Eput and Timer, least count .1 c.p.s.). A kind of averaging the frequency was used here by electronically increasing the count period to 10 seconds. However the frequency readings shown on the counter were fairly constant and there was no ambiguity as to the shedding frequency.



Each time in a set for various wall spacing, the cylinder was taken out and velocity at the cylinder position was made same by changing the r.p.m. of the blower. For studying the effect of convergence and divergence, both the vertical walls of the tunnel were put at the desired angle and the tunnel width was measured at the position of the cylinder.

3.7 Leading Specifications of the Instruments Used

(A) Hot Wire Anemometer

Model HWB3 Flow Corporation, U.S.A.

constant current type.

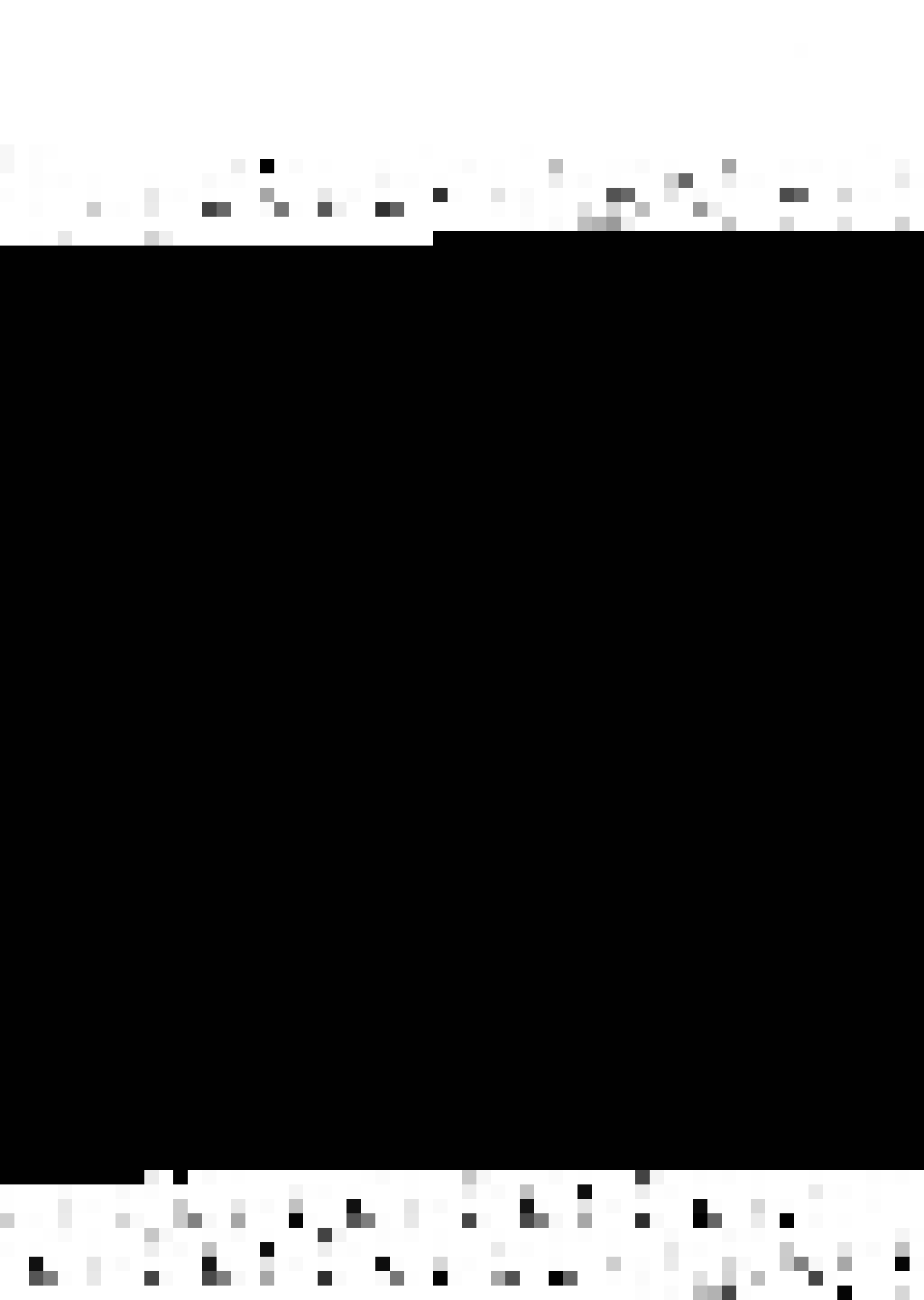
Frequency Range

Correct for 2-100,000 c.p.s., continuously variable R-C compensation to match any hot wire with a time constant between .23 millise. to 30 millise.

Heating Current Supply

Front-panel metered and controlled 0 to 300 m.A.

Heating current measurement	• (least count) $\pm .25$ m.A
Maximum gain at 100,000	: 2×10^6
Input noise figure	• 0.25 micro volt (transformer input)
Output voltage	• 20 volts maximum undistorted with 1, 4, 16, 64, 256, 1024 step attenuators



Output Impedance 200 ohms.

(B) Hot Wire Probe

Locally made.

Wire material Wollaston (10% Rh , Pt)
 Wire dia. .00497 inches.
 Resistance 448 ohms/ft.
 Maximum wire current 180 milli ampere

(C) R M.S. Meter

Model 55A06 DISA Random Signal Indicator and
 Correlator, Denmark.

Frequency response 3 c/s - 200,000 c.p.s.
 Crest factor 5 . 1
 Input Impedance 1 Mego Ohm in parallel
 with 50 p.F.
 Noise level less than 50 micro volt
 r.m.s
 Meter response low or high damped
 Input voltage range .2 mV to 100 volts.

(D) Wave Analyzer.

Model 1900-A General Radio, U.S A.

Frequency response 20 to 54,000 c.p.s.
 Voltage input : 30 micro volt to 300 Volt
 (10 ranges)

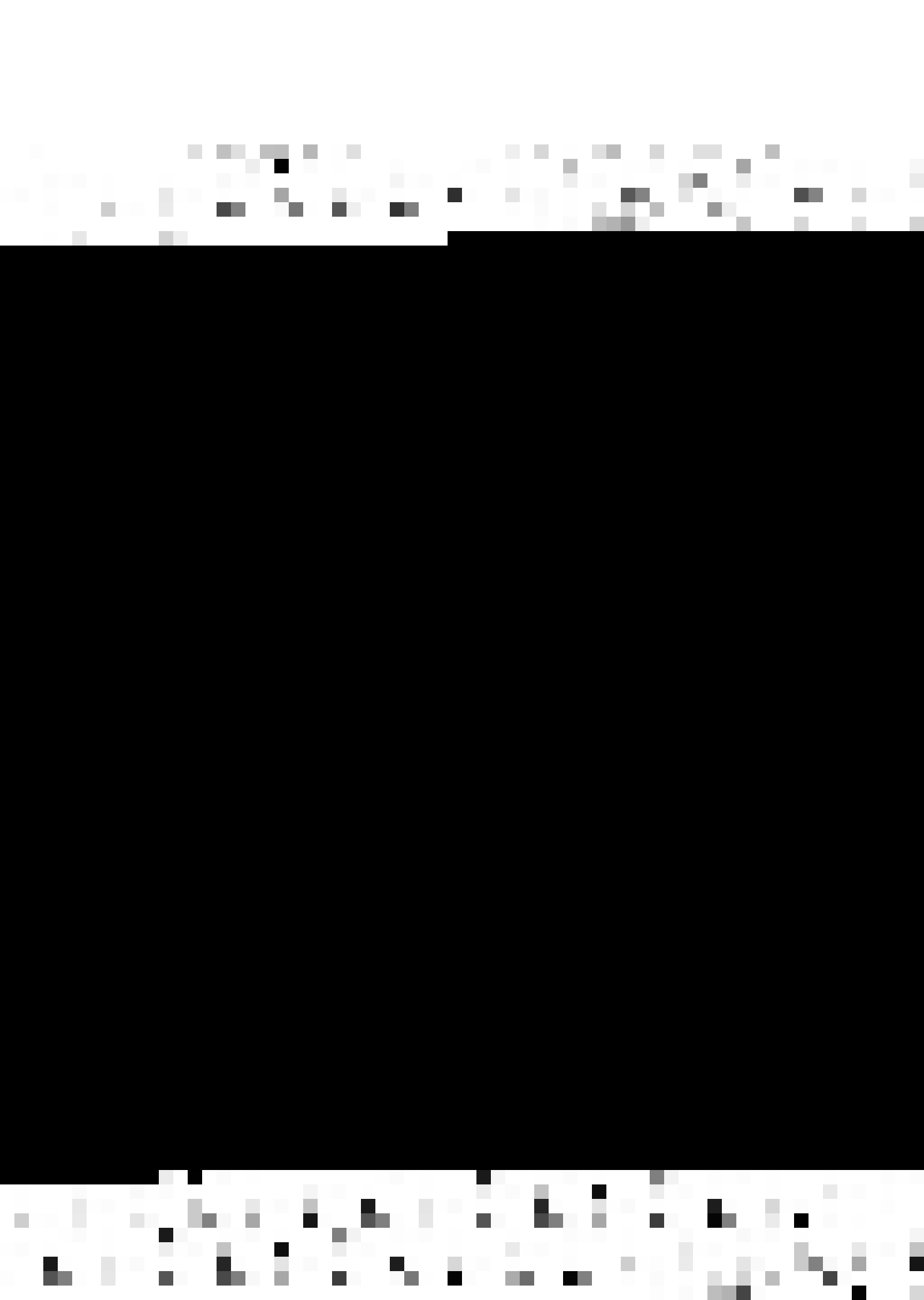


Input Impedance	1 mega ohms in all ranges
Band width	.3, 10, or 50 c.p.s.
3 Cycle band	30 d.B. down at ± 6 c.p.s. from Center Frequency
	60 d.B. down at ± 15 c.p.s. from center frequency
	80 d.B. down at ± 25 c.p.s. from center frequency.
Output	Filtered input component at least 1 volt across 600 ohm load
Internal Noise	5% of full scale for 3 and 10 cycle band
	10% of full scale for 50 cycle band

(E) Frequency Counter

Model 7370 Universal Eput and Timer, Beckmann, U.S.A.

Frequency response	.10 c.p.s. to 175 M. c.s.
Counting period	1 microsec. to 10 sec. with manual extension beyond 10 sec.
Count accuracy	± 1 count \pm crystal frequency
Input range	$\pm .3$ volt peak to peak, 500 volt maximum D.C. to 3 M.c.s.
Input Impedance	.1 Mego ohm in parallel with 40 micro-micro farad.
Count display	display time continously variable from .05 to 5 sec.



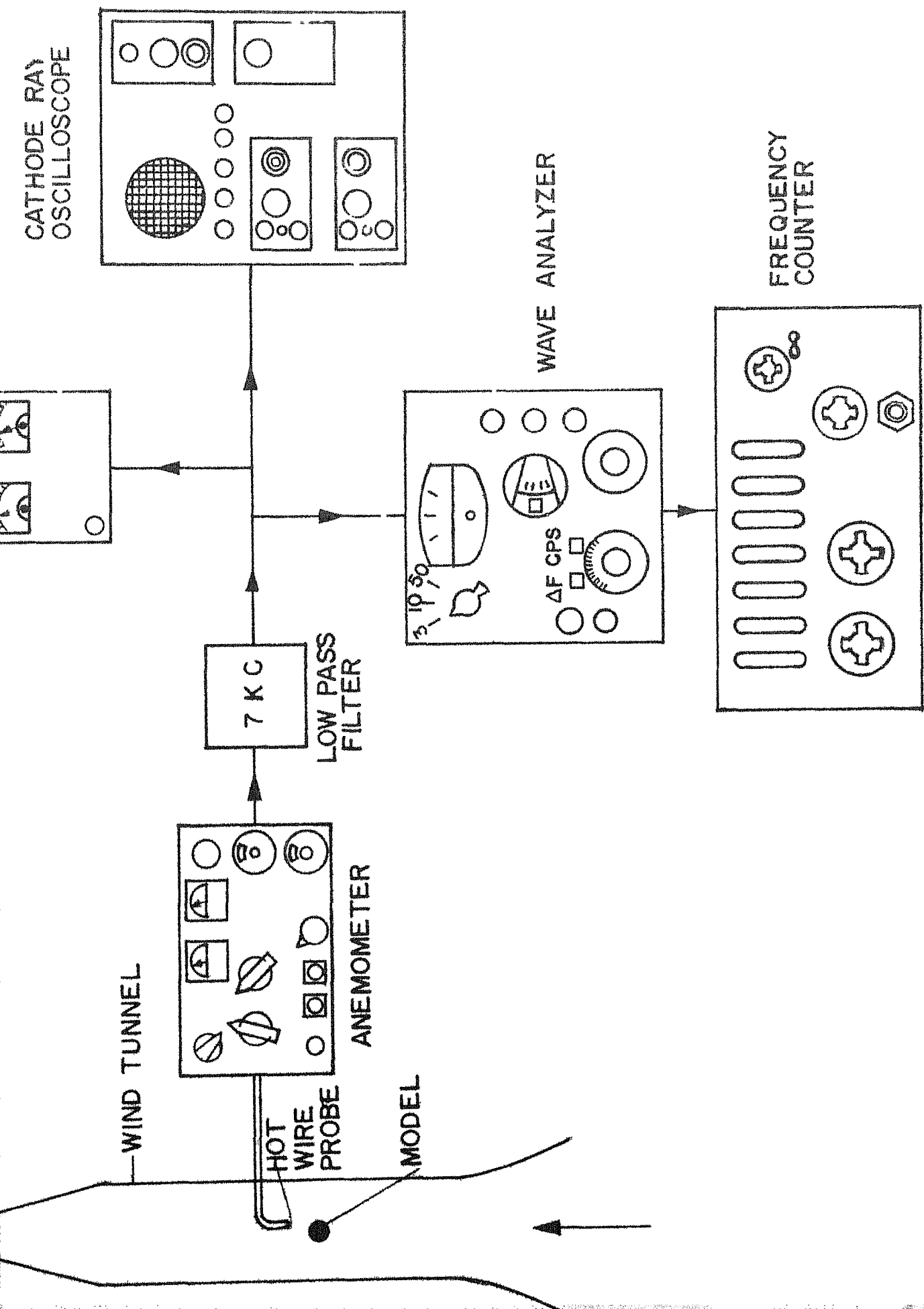
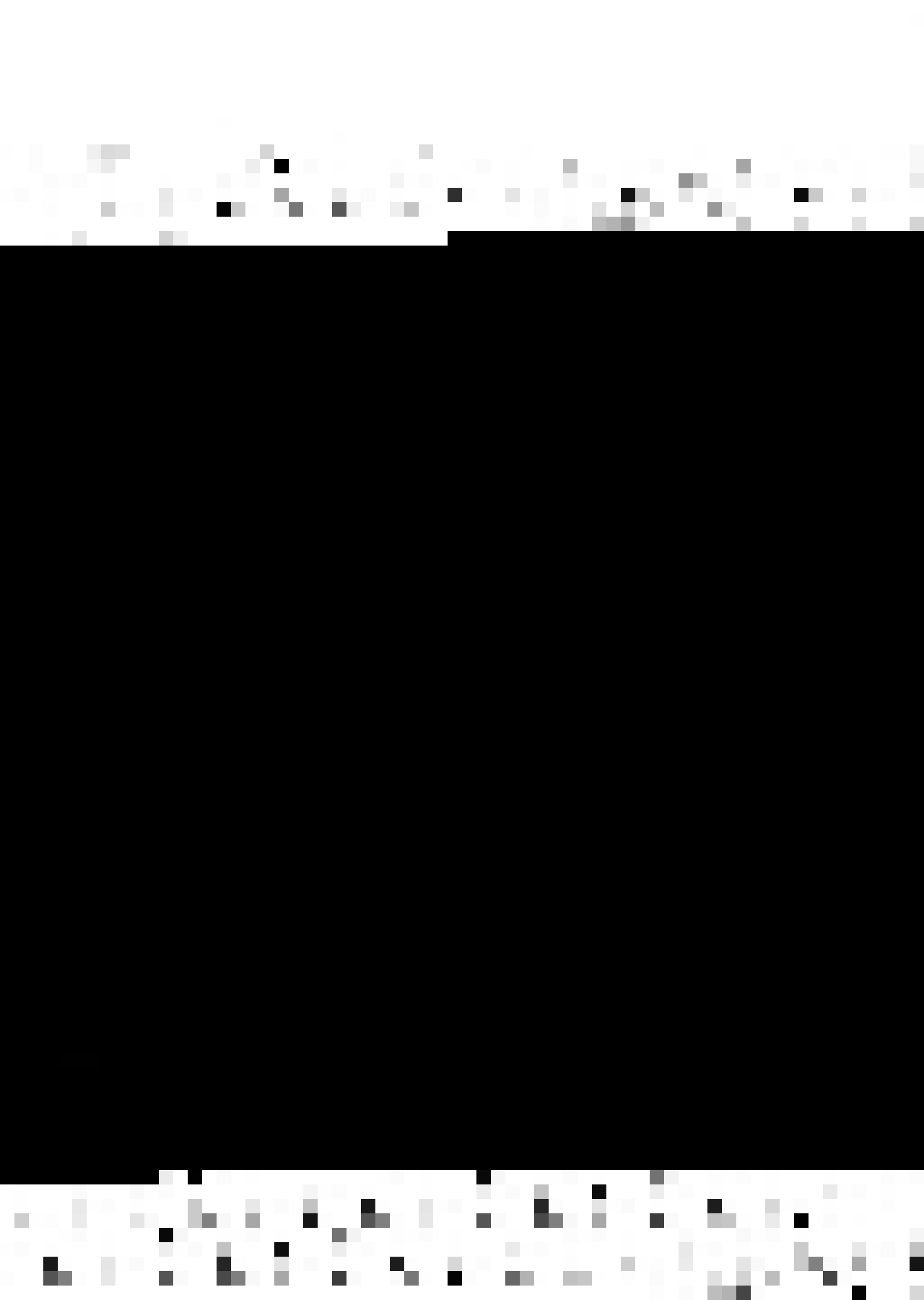


FIG. 1 LINE SKETCH OF EXPERIMENTAL SET-UP



CHAPTER-IV

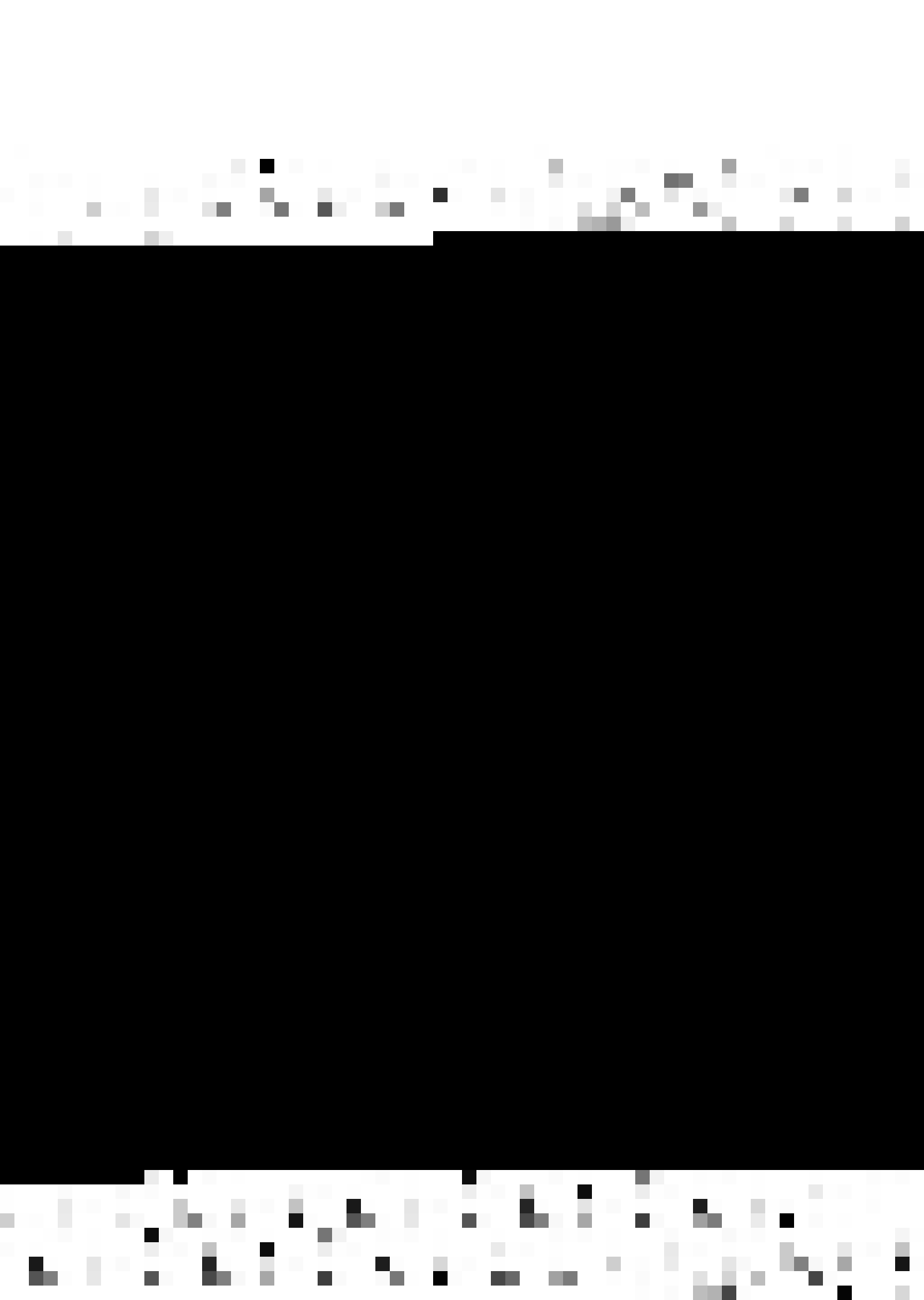
RESULTS AND DISCUSSIONS

4.1 General

The experiments are carried out to see the effect of the tunnel walls, on the vortex shedding frequency. Four different cases are studied

- (1) The vertical walls are kept parallel to each other and the distance between them is changed.
- (2) One of wall is kept at maximum distance from the model while the other wall is brought closer to the model. (One Wall Effect)
- (3) The vertical walls are kept so as to form a convergent section and the distance between them is changed.
- (4) Same as (3) but the walls now form a divergent section.

In each set of the various cases, the model and the velocity at the model position, but in absence of it, was kept the same while the wall separation was changed. This ensured the elimination of Reynolds number effect in a particular set of readings.



The graphs are plotted with H/d (inverse of conventional definition of blockage) as abscissa and shedding frequency or Strouhal number as ordinate.

4.2 Parallel Wall Effect (Both Walls)

4.2.1 Graphical Plots

Fig. 2 shows the effect of blockages at Reynolds numbers of 144, 161, 258, 436, the models being rigid circular tubes of uniform cross-section. Both the .166 and .3 cm. diameter tubes were made of stainless-steel.

Fig. 3 shows the same effect at greater Reynolds numbers - 902, 1230 and 1530. The tubes were made of glass with diameters .59, 0.80 and 1.00 cm. respectively.

In Fig. 4 existing blockage correction theories are applied (Modi's and Tsuchiya's). The plot is given as percentage error from no wall effect value (Roshko's value at the particular velocity was chosen to represent it) of the measured or the corrected values versus H/d ratio.

4.2.2 Discussion

Fig. 2 shows that walls begin to effect the shedding frequency when their separation (H) is as large as 40 to 44 diameters (d) (that is, when the blockage is greater than 2 to 2.5%). The rise becoming very



sharp for blockages greater than 10%. For H/d greater than 44, the curves reach Roshko's (29) infinite wall value.

Fig. 3 shows the same trend. All the readings at the Reynolds numbers 902, 1230, 1530 lie on the same curve. It is thus significant that in this Reynolds number range (which extends upto around 2000), we can predict the no wall effect value from the measured experimental value for any blockage. It is to be noted that Roshko predicts a constant value of Strouhal number (.210) at these Reynolds number values for infinite wall separation. The present curve tend to the infinite wall value of Roshko as H/d becomes large.

Fig. 4 shows the inadequacy of existing blockage correction theories. The curves should have been horizontal lines if the theories were able to predict the vortex frequency correctly. Only Modi's (19) analytical equation and Tsuchiya (7) equation assuming complete physical blockage were used. The expression given by Allen and Vincenti (25), Glauret (22) etc. involve experimental measurement of drag coefficient, the study of which was not made during present experimentations. However Modi (19) found that these methods are also inadequate, specially at higher blockages. The curve



which has to be noted is that of Tsuchiya's. The corrected value of Strouhal number according to his equation is much below the experimental points. This means that if we would have defined the Strouhal number on the basis of velocity between the model and the walls--the gap velocity (which seems to be valid, as it is the velocity near the model which greatly effects the shedding frequency), then the Strouhal number becomes much less than the experimental values. This would suggest that the wall confinement tends to reduce the rate of change of shedding frequency with velocity. This statement is however open to question because the characteristic velocity on which the Strouhal number should be based is itself unknown.

4.3 One Wall Effect

4.3.1 Graphical Plot:

Fig. 5 shows the effect of only one wall. The other wall being kept at a maximum constant distance of 6.5 cms. Readings were taken similarly as in finding the two wall effect for Reynolds numbers of 902, 1230 and 1530.



4.3.2 Discussion

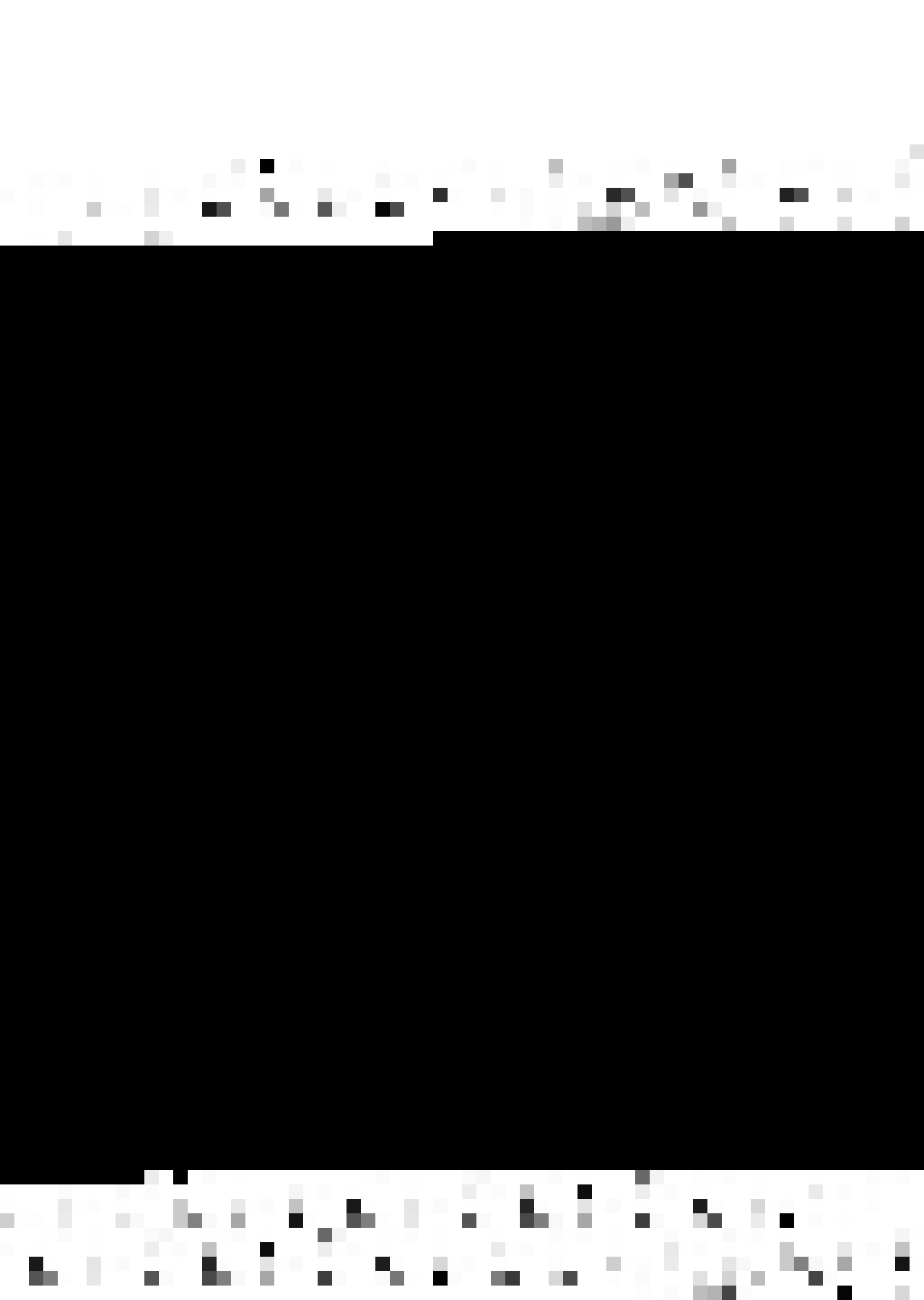
From the plot it is clear that the effect of only one wall in increasing the shedding frequency with greater blockages is not so large as in two wall effect. The maximum increase is 50% at $w/d = 1.3$. However as in 2 wall effect all the points lie on same curve in the Reynolds number range (902 - 1530). As already reported, Caldwell, et. al. (6) found 500% increase in shedding frequency in their study of one wall effect on flexible cylinders, implying that aero-elasticity plays a very important role in vortex formation mechanism.

4.4 Effect of Converging Walls

4.4.1 Graphical Plots

Figures 6 to 9 show the effect of converging walls on the shedding frequency with various blockages at Reynolds numbers of 311, 902, 1230 and 1530. At each Reynolds number the effect of increasing convergence ($\alpha = .9^\circ, 1.8^\circ, 2.7^\circ$ and 3.6° , where 2α is the angle between the 2 convergent vertical walls) is also shown.

The characteristic velocity 'V' to define the Strouhal number and Reynolds number was chosen as in the case of parallel wall effect case, that is, at the



cylinder position but in absence of it. In a particular set of reading it was kept constant.

4.4.2 Discussion.

From the plots, three different regimes can be seen

- (a) Walls very far from each other ($H/d > 40$).
- (b) Walls separated by a distance of 10-15 to 40 cylinder diameter.
- (c) Walls very close to each other ($H/d < 12$)

When the walls are very far ($H > 40 d$) the shedding frequency tends asymptotically to the parallel infinite wall value. (Fig. 6) This value is attained at greater wall separation as the convergence is increased.

When the walls are at a moderate distance from each other ($H = 10-15$ to $40 d$) the convergent walls stabilize the shedding frequency, that is, the vortex formation rate becomes independent of blockages. (The S value, however, being higher than the infinite wall value).

When the walls are brought still closer ($H < 12 d$) the shedding frequency again begins to rise (Figs. 7, 8, 9). The rise begins earlier and is sharper as the Reynolds number is increased.



The effect of greater convergence, in general, is to increase the shedding frequency more than that at smaller convergence, the blockage in both cases being the same.

4.5 Effect of Diverging Walls

4.5.1 Graphical Plots.

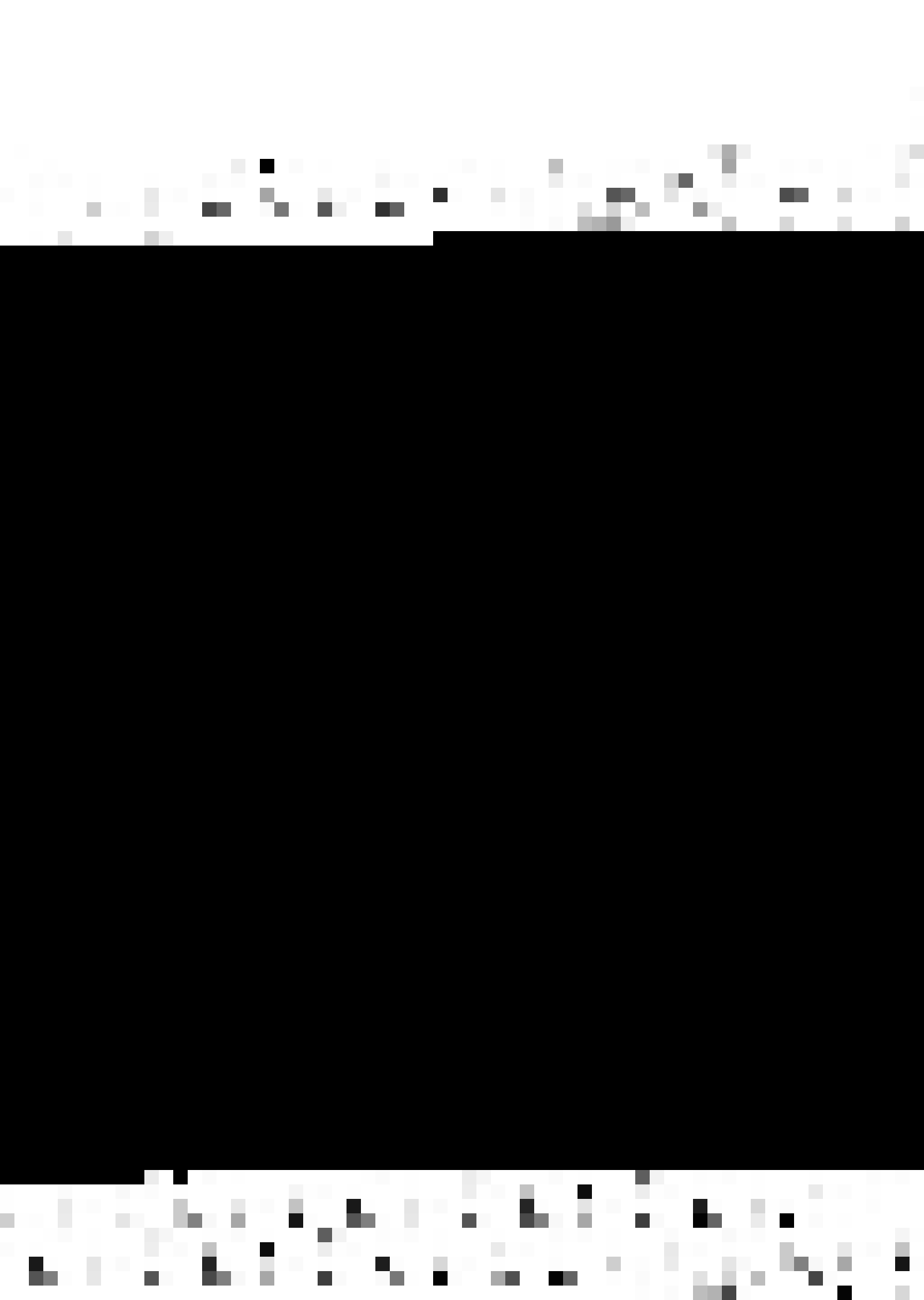
Figures 10 to 13 show the effect of Diverging Walls on the shedding frequency at Reynolds numbers of 311, 902, 1230, 1530. The effect of increasing convergence in each set of Reynolds number is also shown.

4.5.2 Discussion

Besides the 3 regimes of walls separation, as in the case of converging walls, the Reynolds number effect is also prominent as seen from the plots.

For large wall separation ($H > 40 d$) the curves tend asymptotically to the parallel infinite wall value.

In the intermediate range $H = 10$ to 40 diameters and at Reynolds number of 311, the effect of even slight divergence ($\alpha = .9^\circ$) is to decrease the shedding frequency. This decreasing effect becomes more pronounced

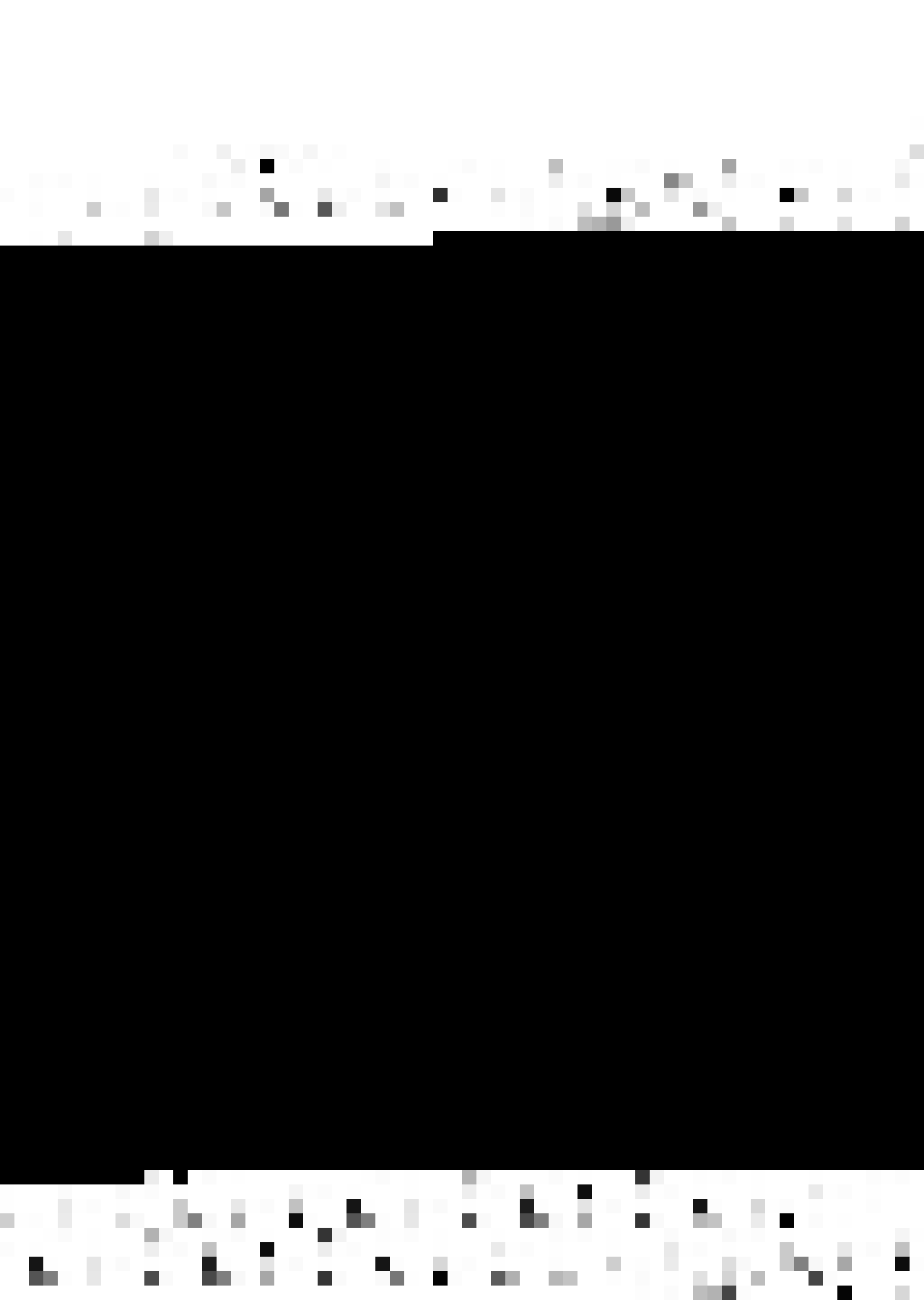


for greater divergence. However, as the Reynolds number is increased (Figs. 11 - 13) the effect of small divergences in reducing the shedding frequencies becomes small. In figures 11 to 13 it can be seen that at $\alpha = 0.9^\circ$ the plot of $S - H/d$ is almost horizontal, it begins to rise for $R = 1230$ and still more for $R = 1530$. However the rise is not at all as steep as in the case of parallel wall effect. For larger divergences we still see the pronounced decreasing effect.

From the Figs. we also see that a critical position is reached, above ($H \approx 6$ to $10 d$) at which if the walls are still brought closer the shedding frequency again begins to rise. The rise being quite steep for smaller divergences. Hence if in some application we want to reduce the shedding frequency by putting diverging walls around the vortex generator, then there exists an optimum wall separation distance, below which the walls are not useful. In tall structure - usually nowadays a cylindrical shell with multiple openings called 'shroud' is put around the structure for some length at the top, to reduce these vortex generated vibrations, From this study it seems that instead of

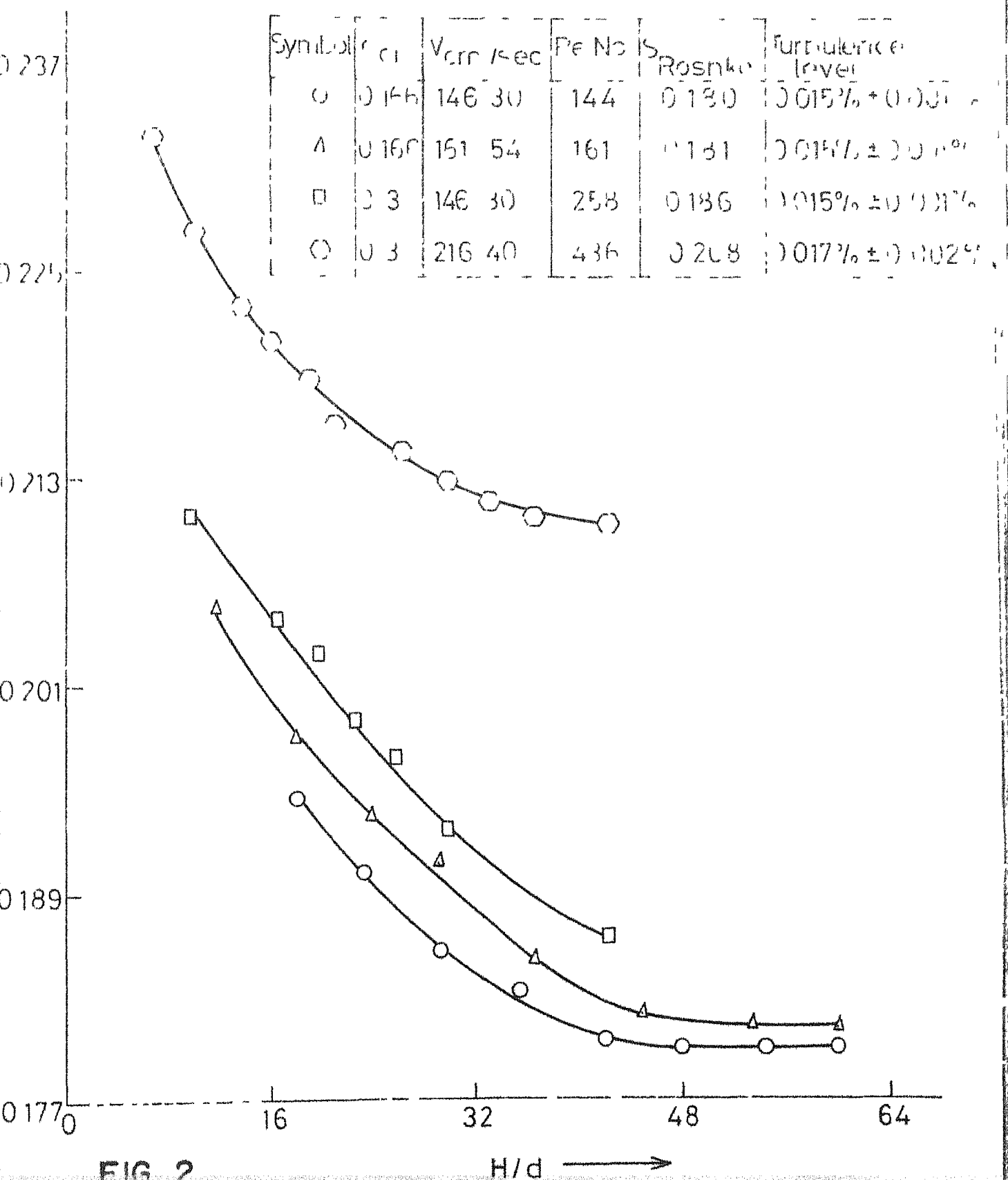


a cylindrical shell, two diverging plates placed about the structure, whose direction should be automatically aligned along the wind direction, can act as a better vortex inhibitors.



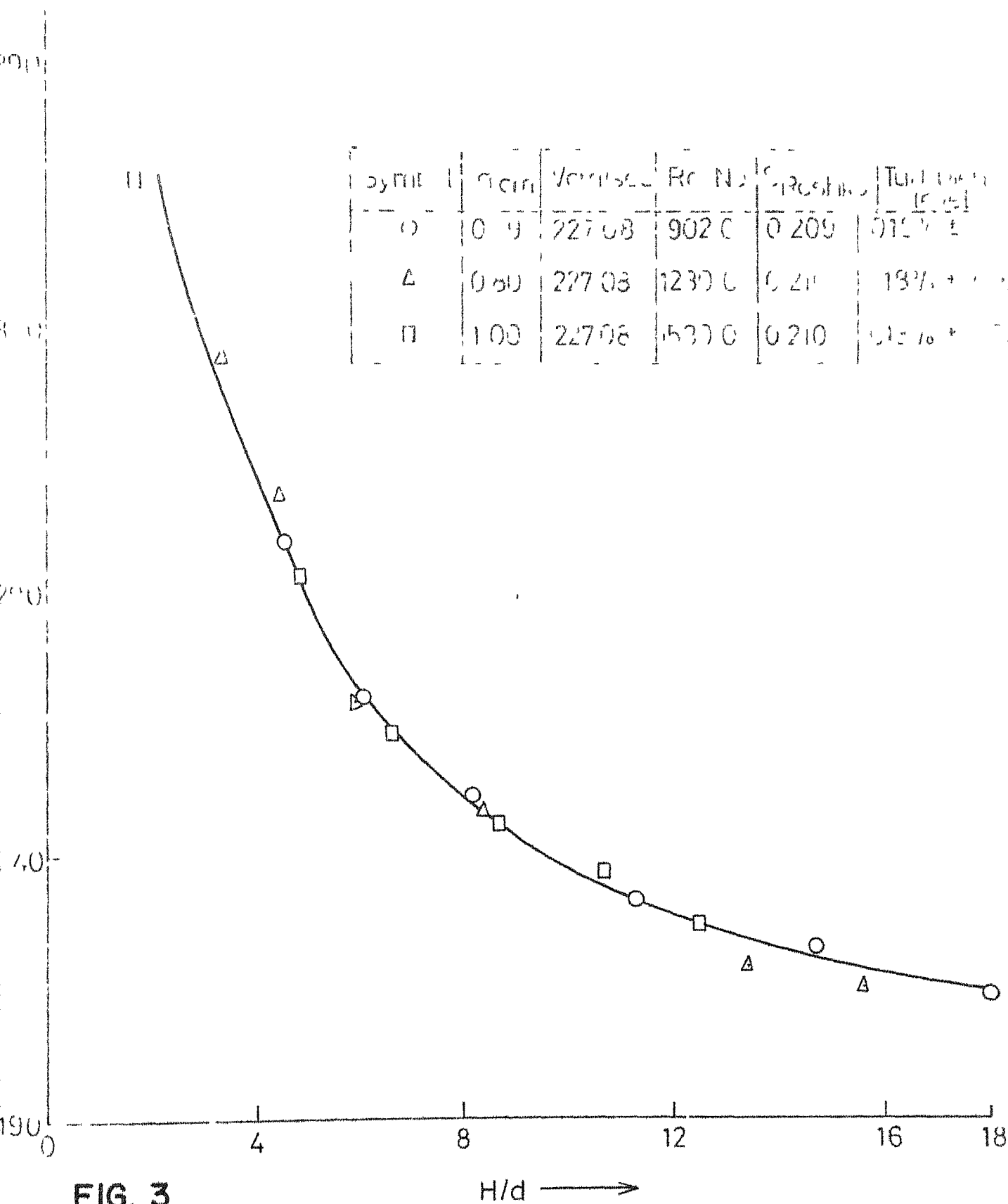


Effect of Parallel Walls

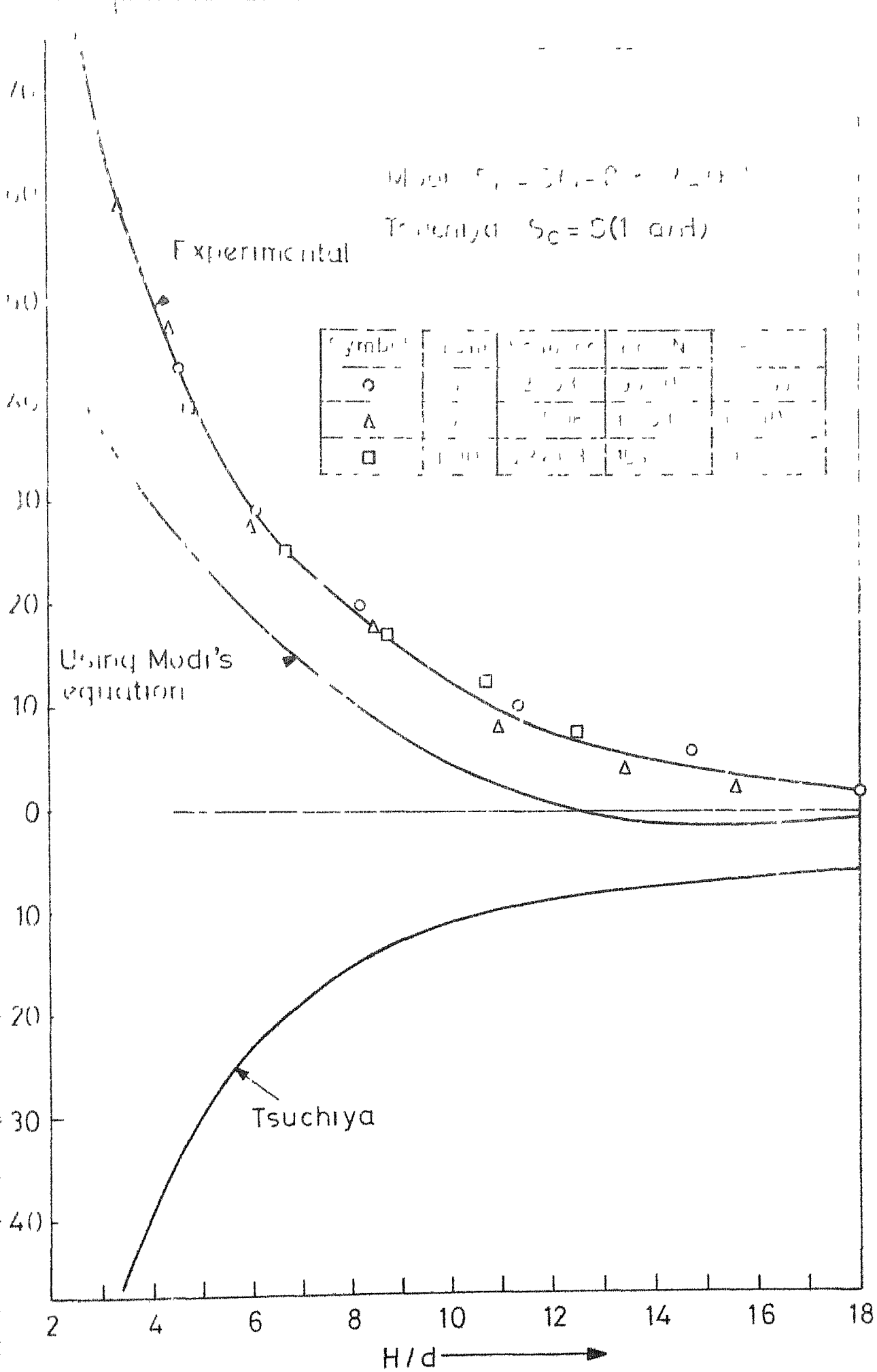




1900









Effect of Line Width

Symbol	Len	V_{eff}/V_0	Re No	$\epsilon_{FOS}(\mu)$	Turbulent layer	Turbulent layer
	0.59	27.03	9220	0.009	0.13% $\pm 0.02\%$	2%
	1.33	17.08	12300	0.210	0.13% $\pm 0.02\%$	1.1%
	1.90	22.00	15300	0.210	0.13% $\pm 0.02\%$	0.2%

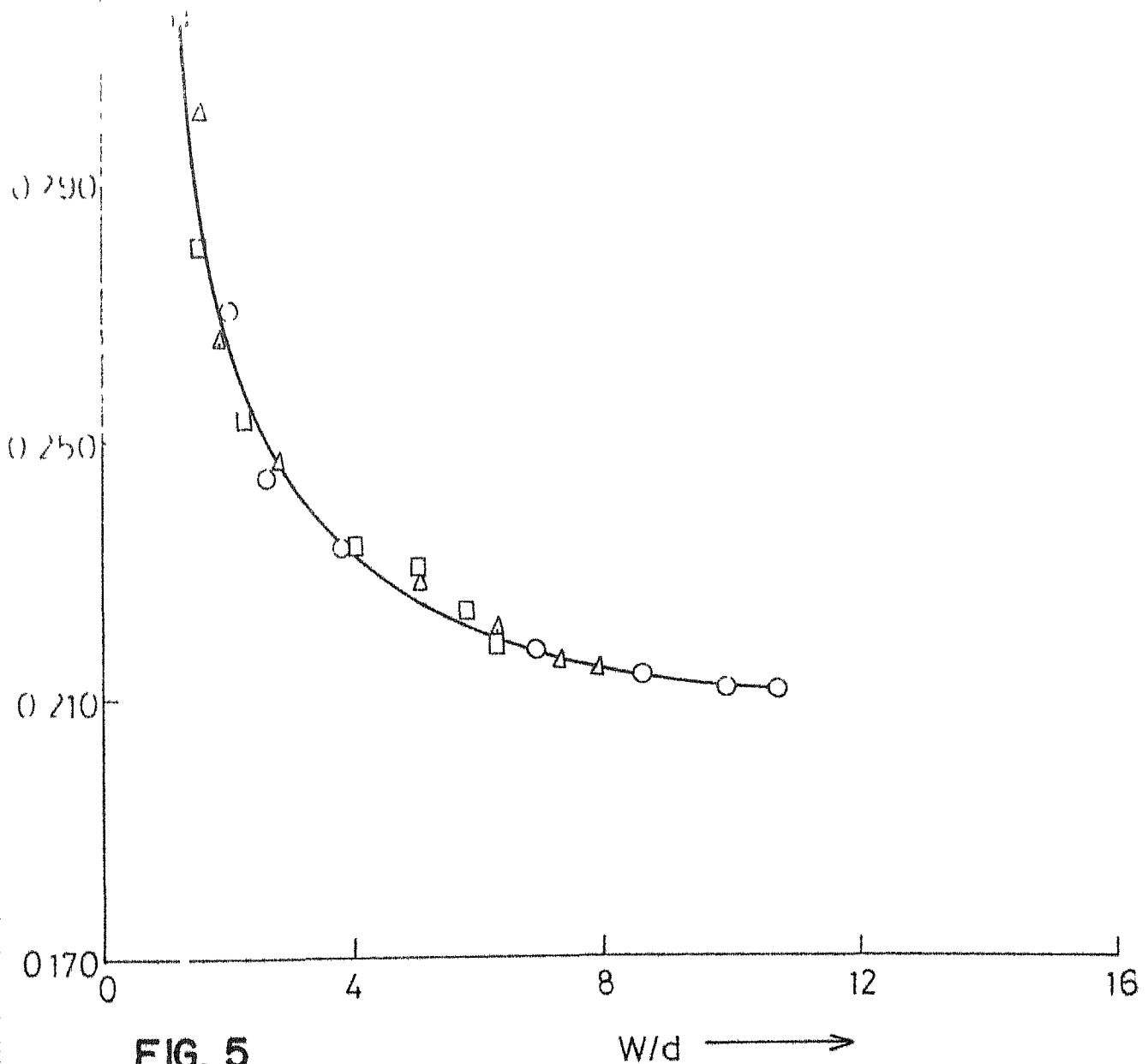
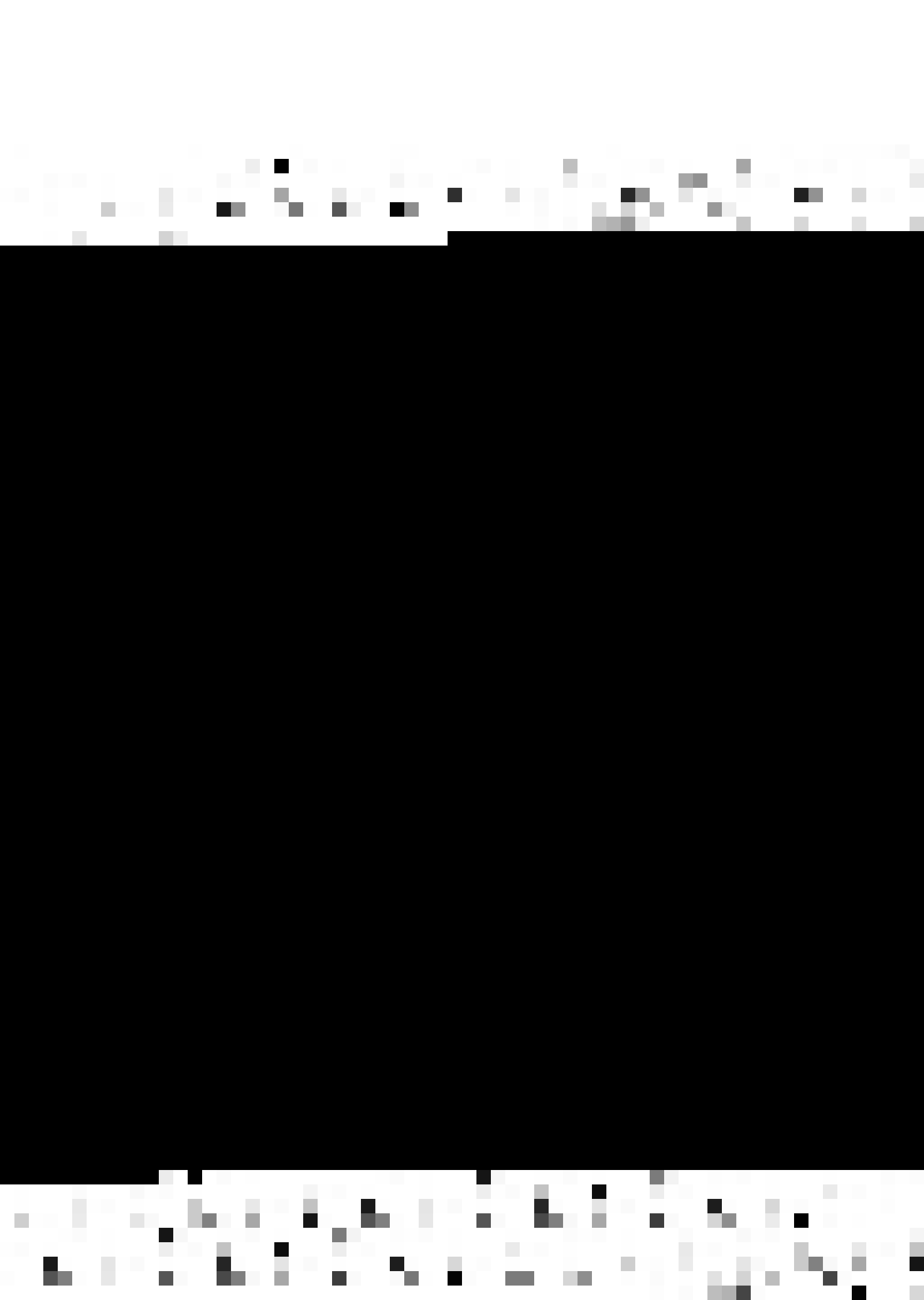
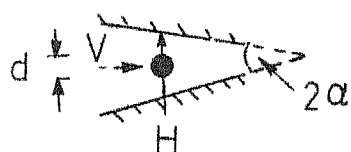


FIG. 5



Effect of Walls in Converging Tunnel



Cylinder dia = 0.3 cm

Velocity = 154.3 cm/sec

Re No = 311

Turbulence level = 0.015 %

* Parallel wall value (exp) for $H/d = 420$

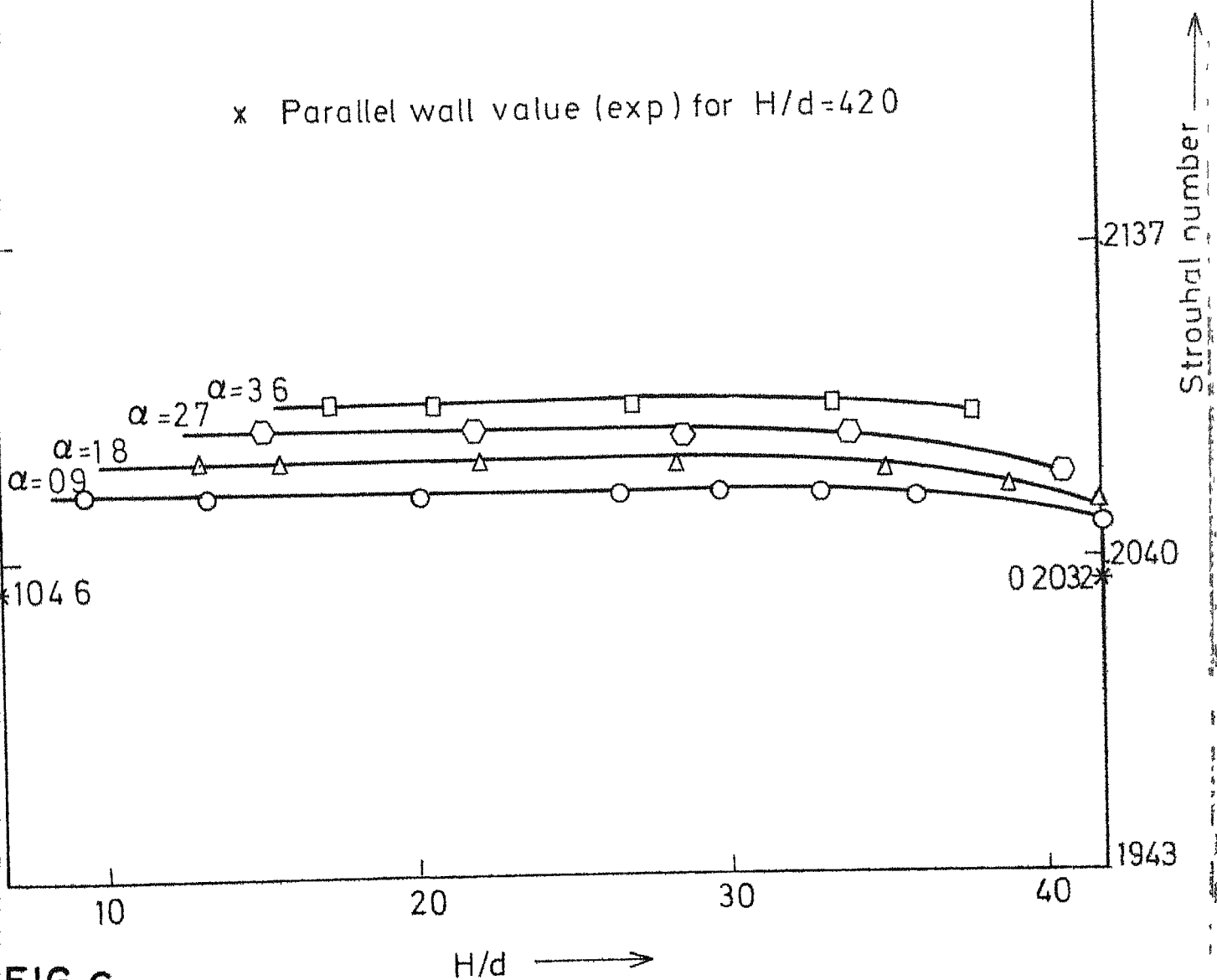
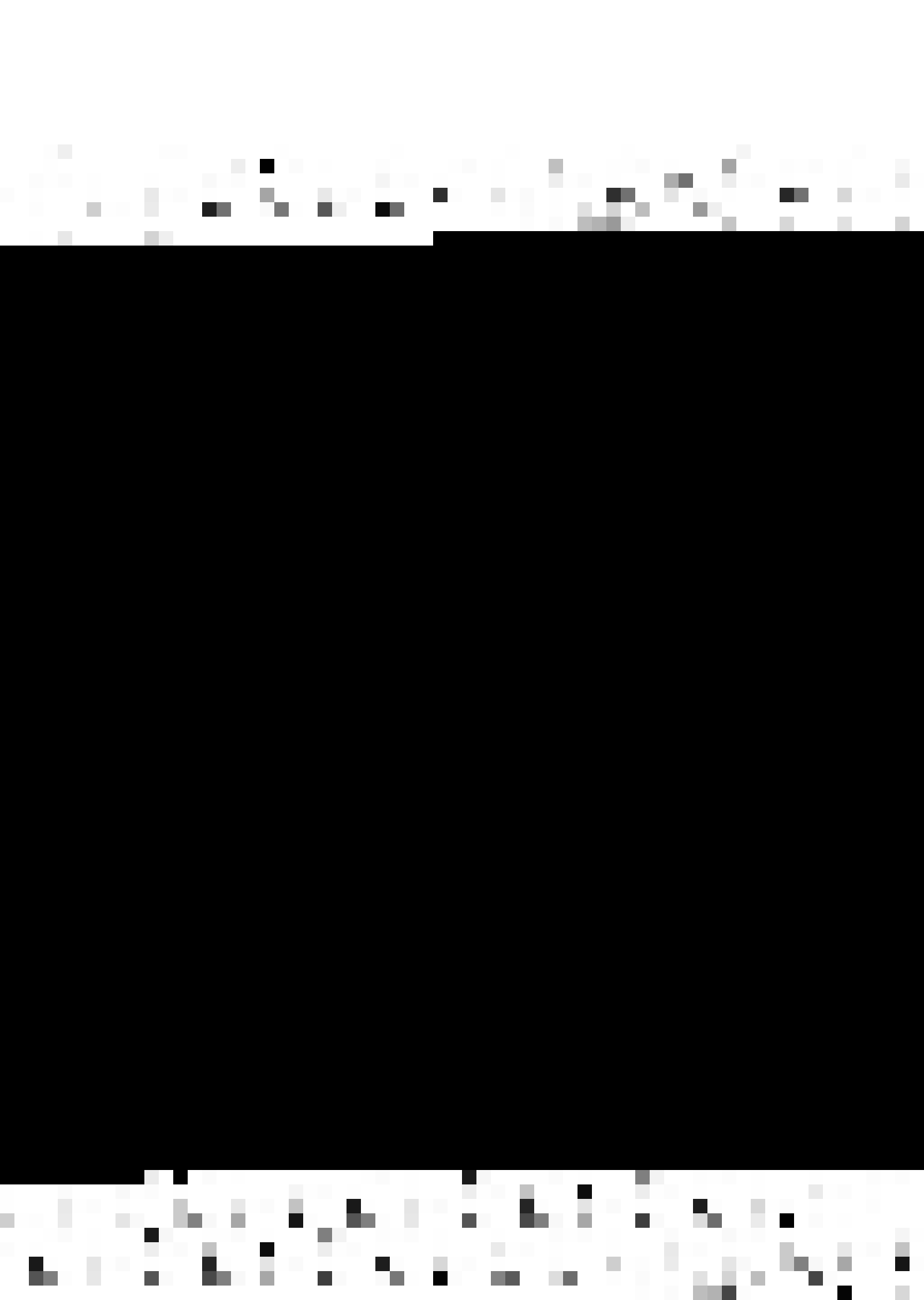


FIG. 6



Effect of Walls in Converging Tunnel



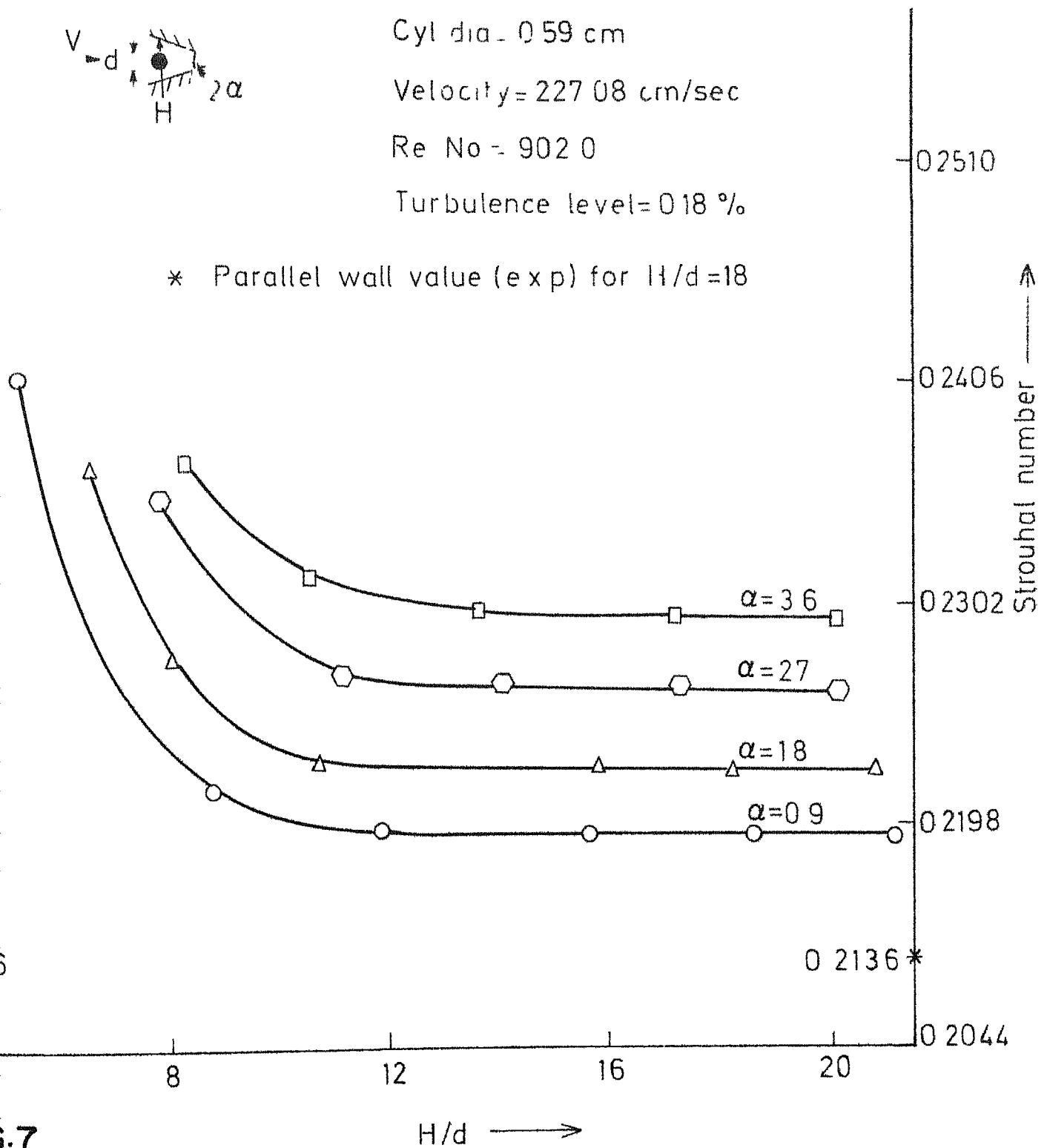
Cyl dia. = 0.59 cm

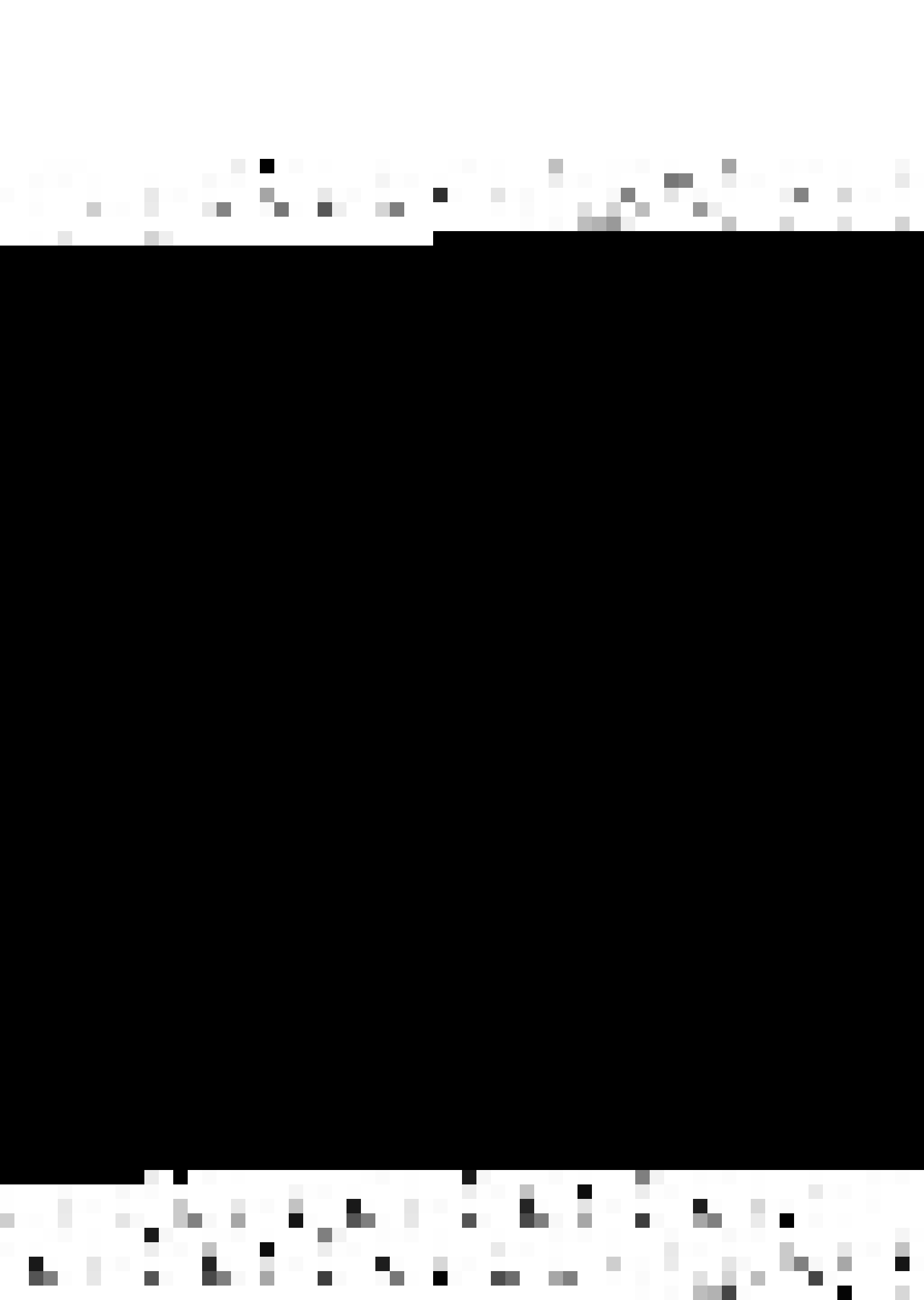
Velocity = 227.08 cm/sec

Re No = 902.0

Turbulence level = 0.18 %

* Parallel wall value (exp) for $H/d = 18$





Effect of walls in converging tunnel.

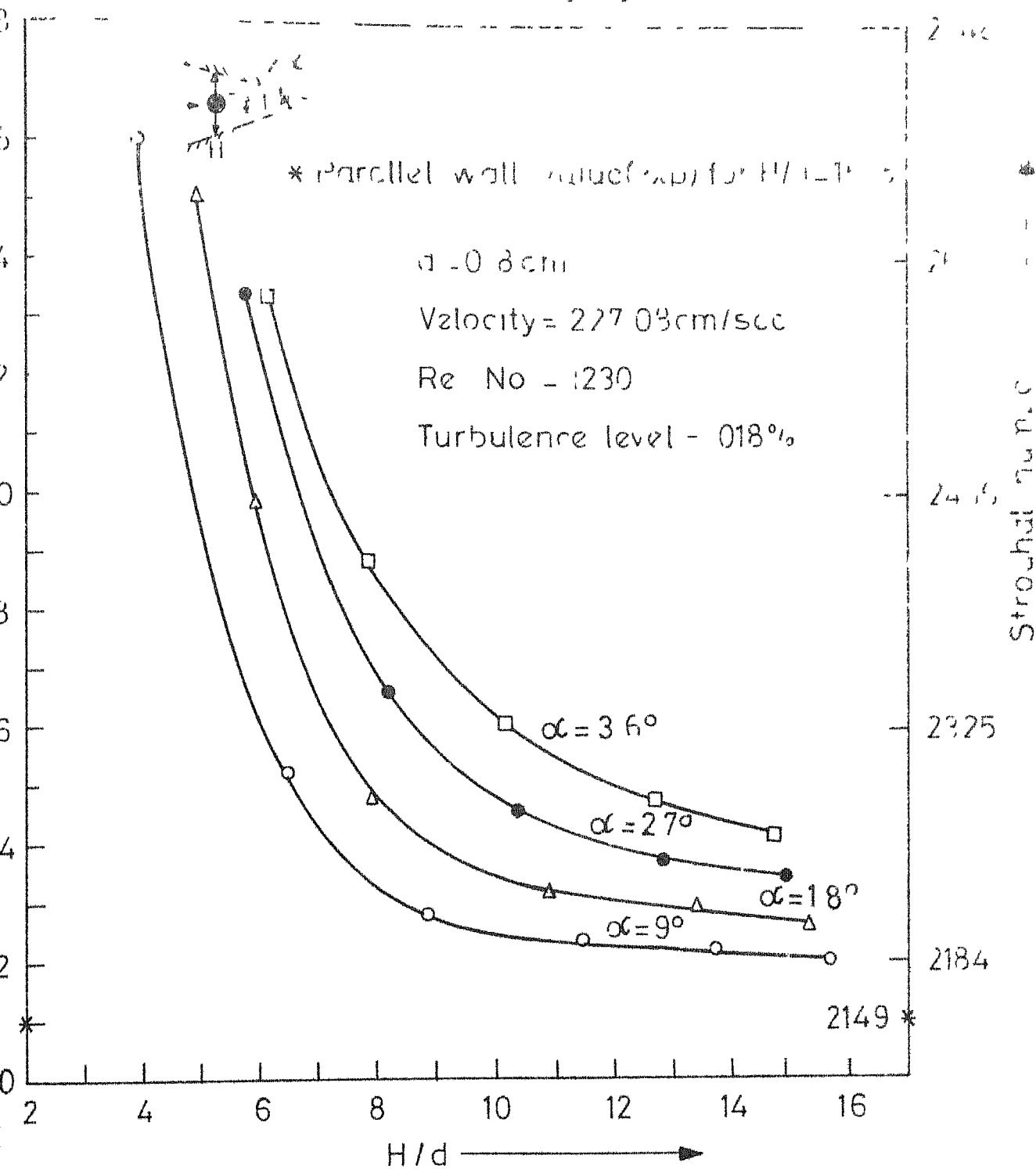
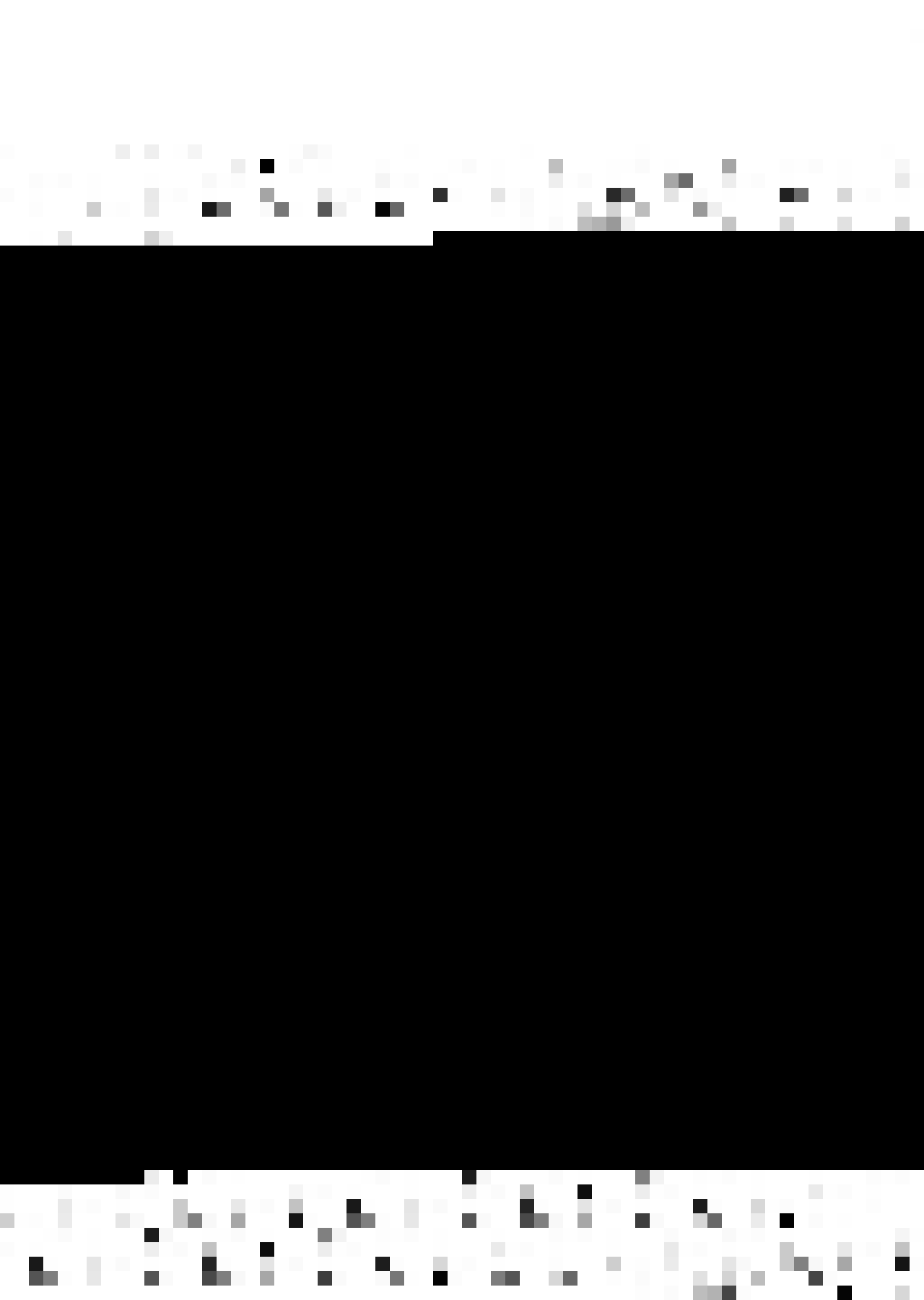


Fig 8



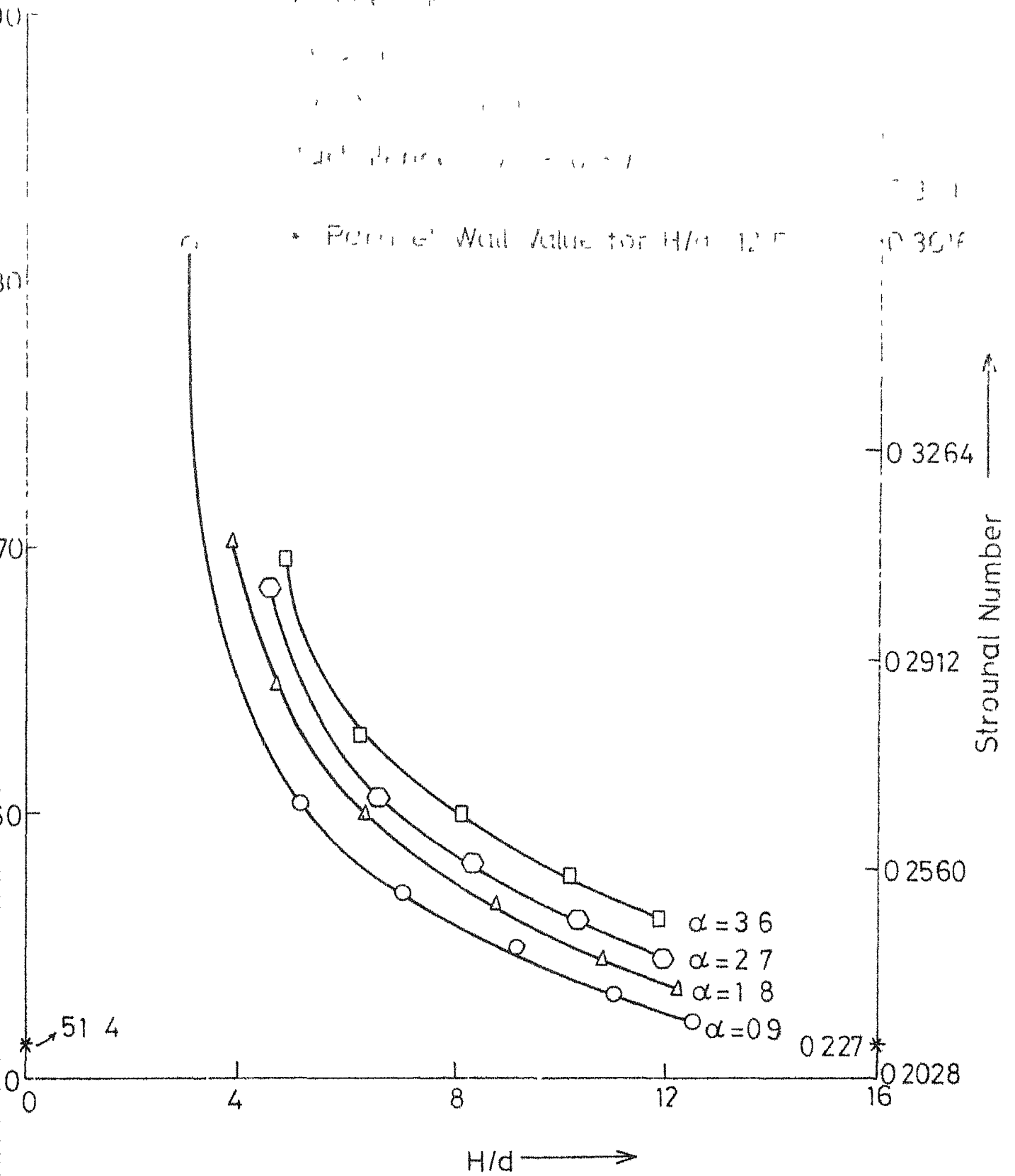
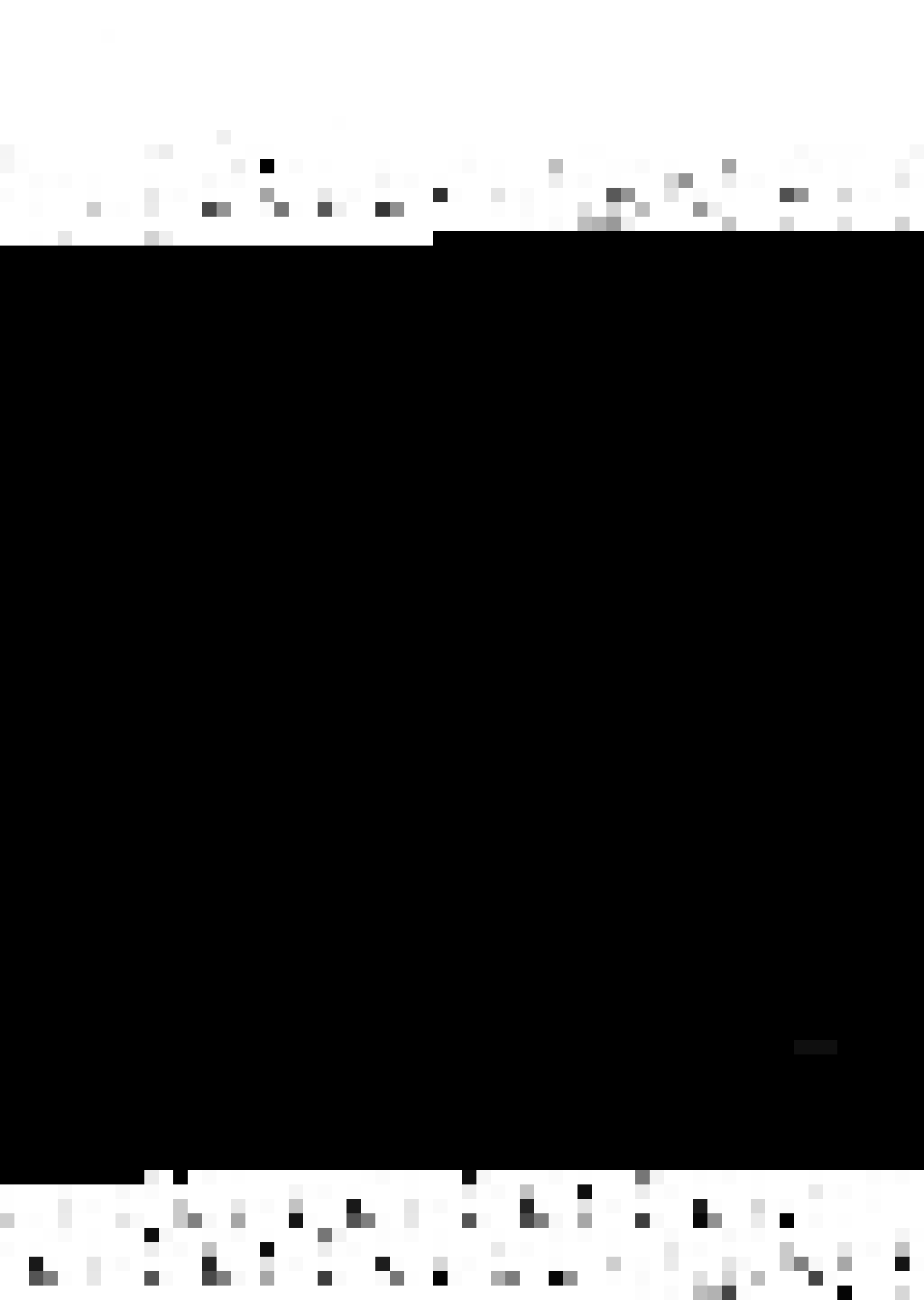


Fig. 9



Effect of width of diverging tunnel.

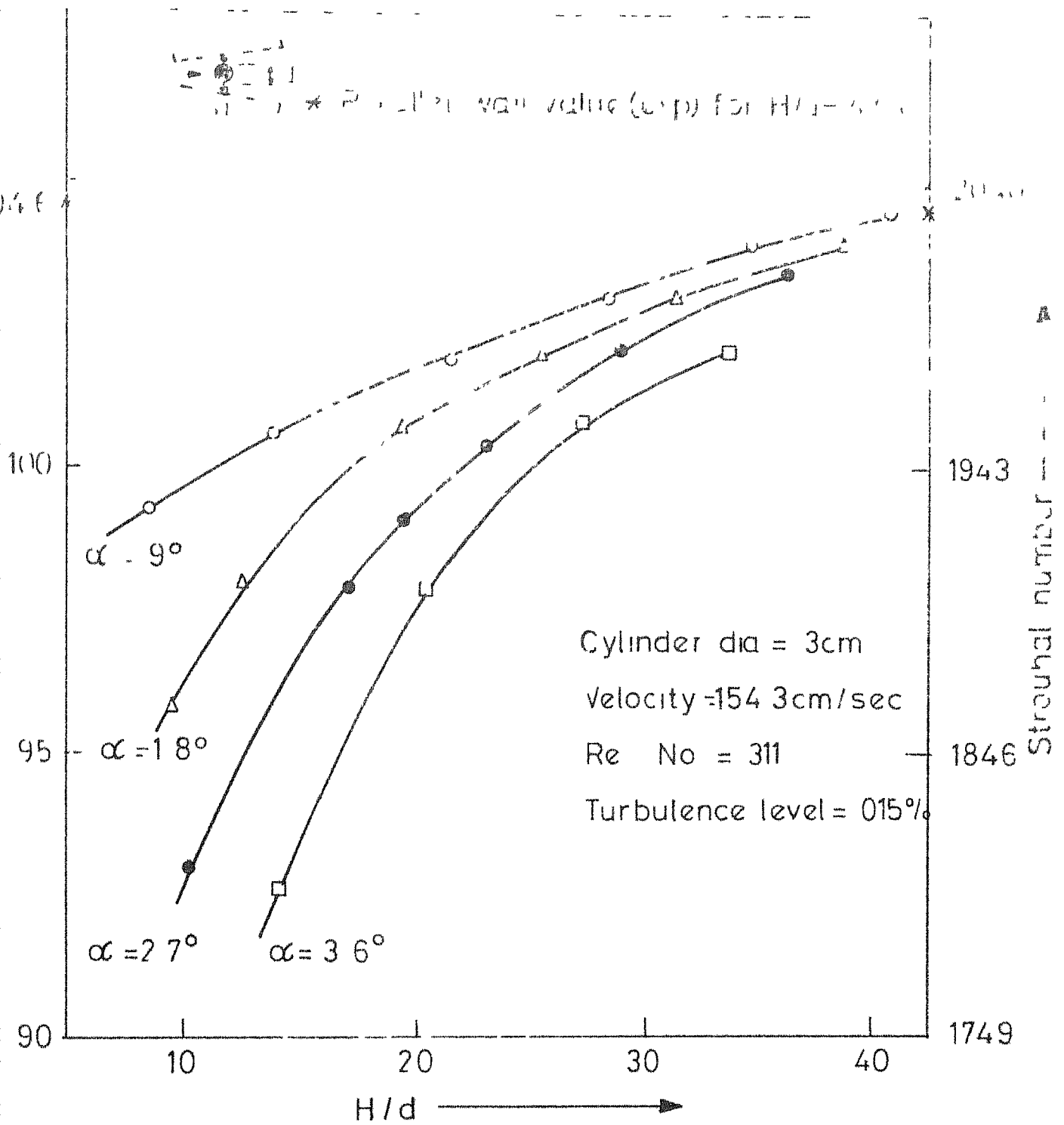


Fig 10



Effect of Walls in Diverging Tunnel



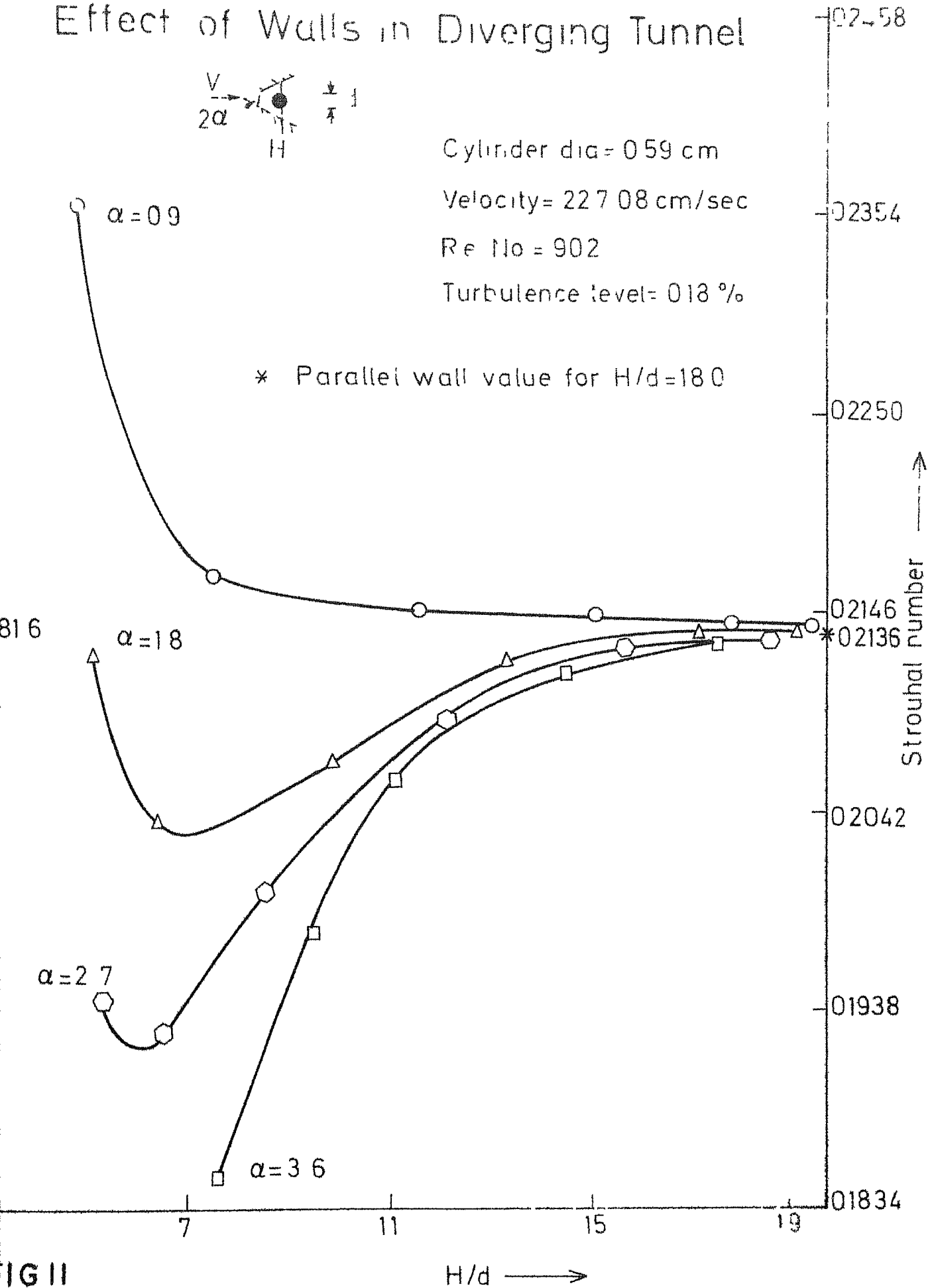
Cylinder dia = 0.59 cm

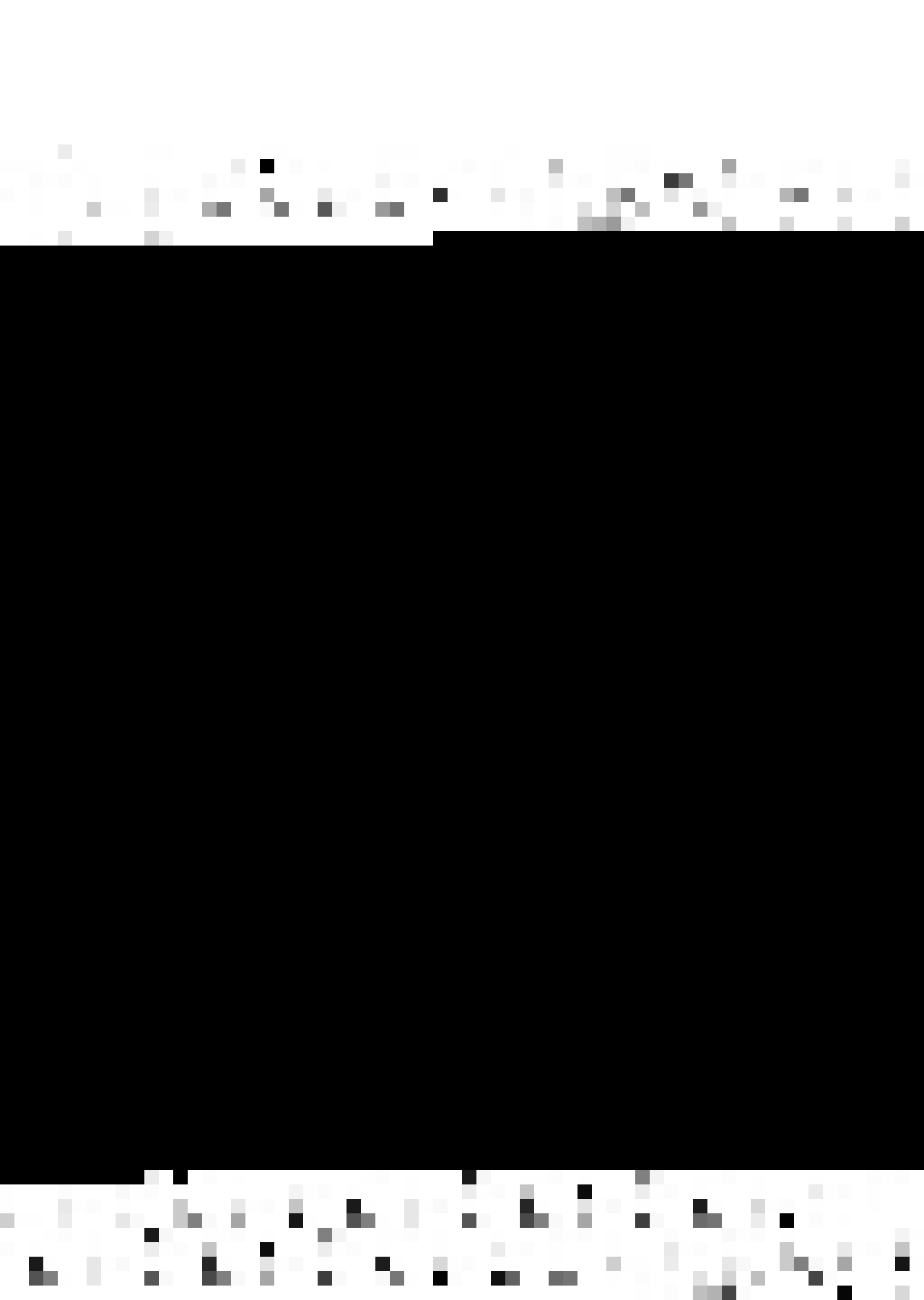
Velocity = 227.08 cm/sec

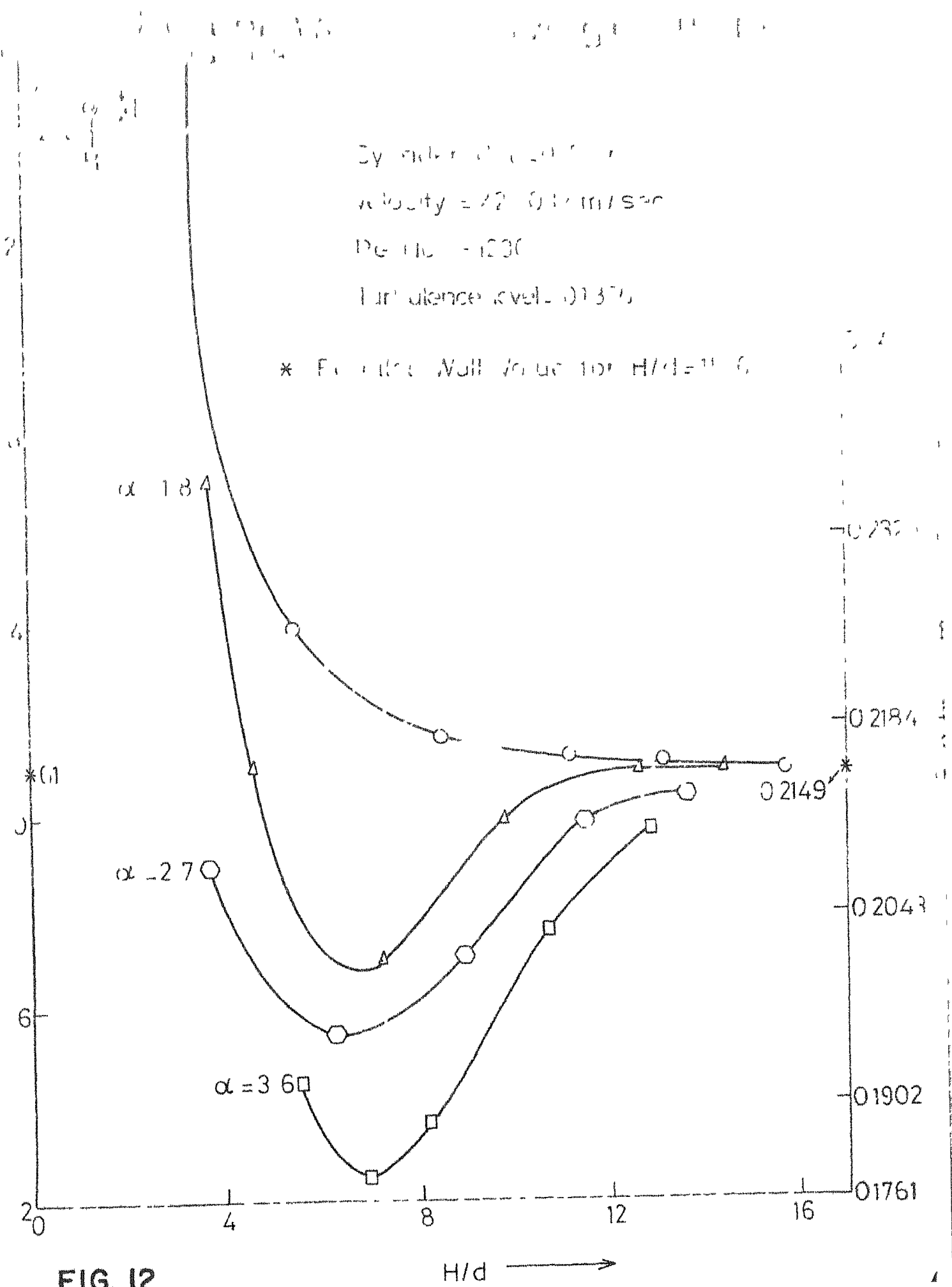
Re No = 902

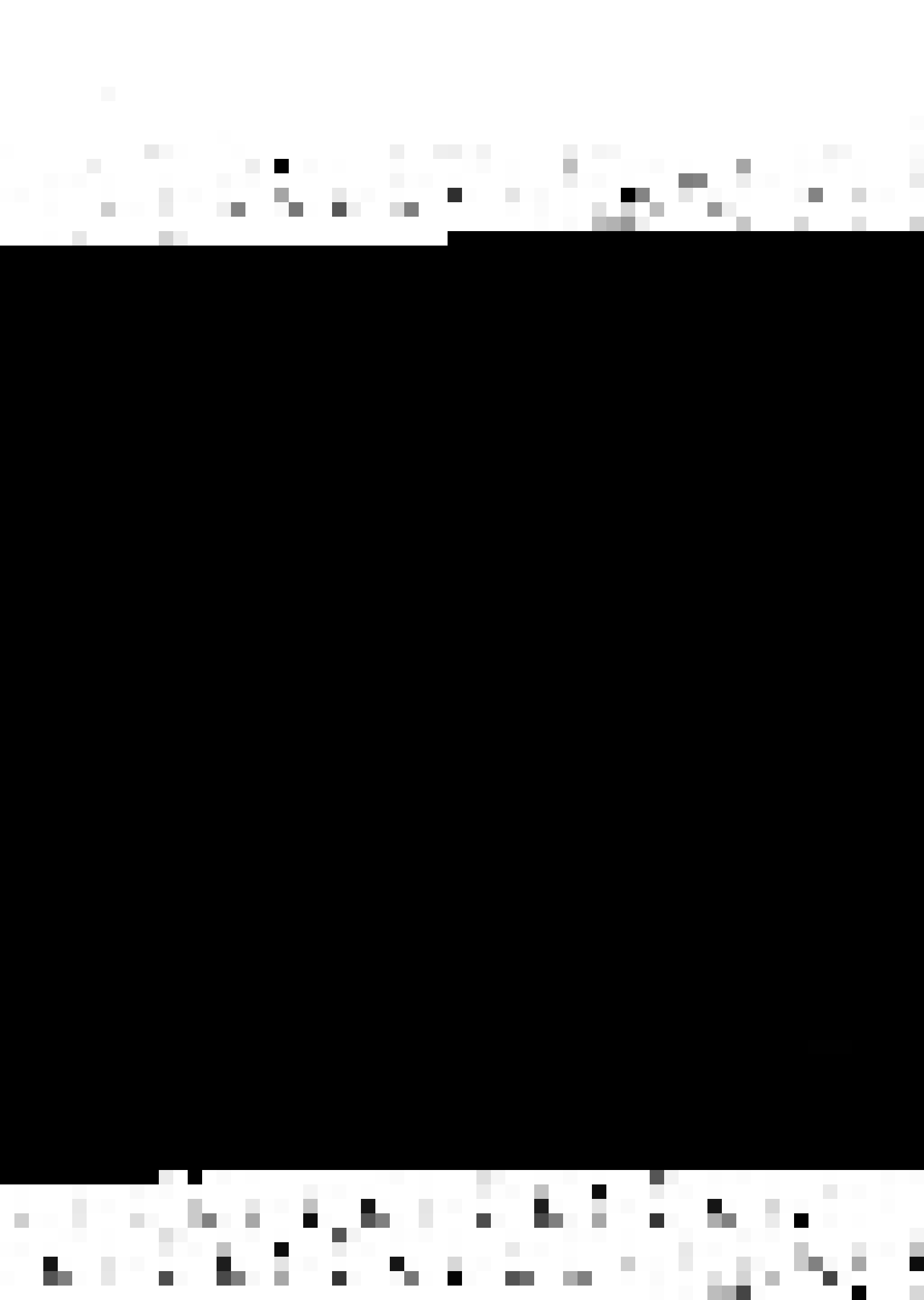
Turbulence level = 0.18 %

* Parallel wall value for $H/d = 180$









For No. 10

Properties of steel

α Factor: W_{ed} / h_{ed} for $H/d = 10$

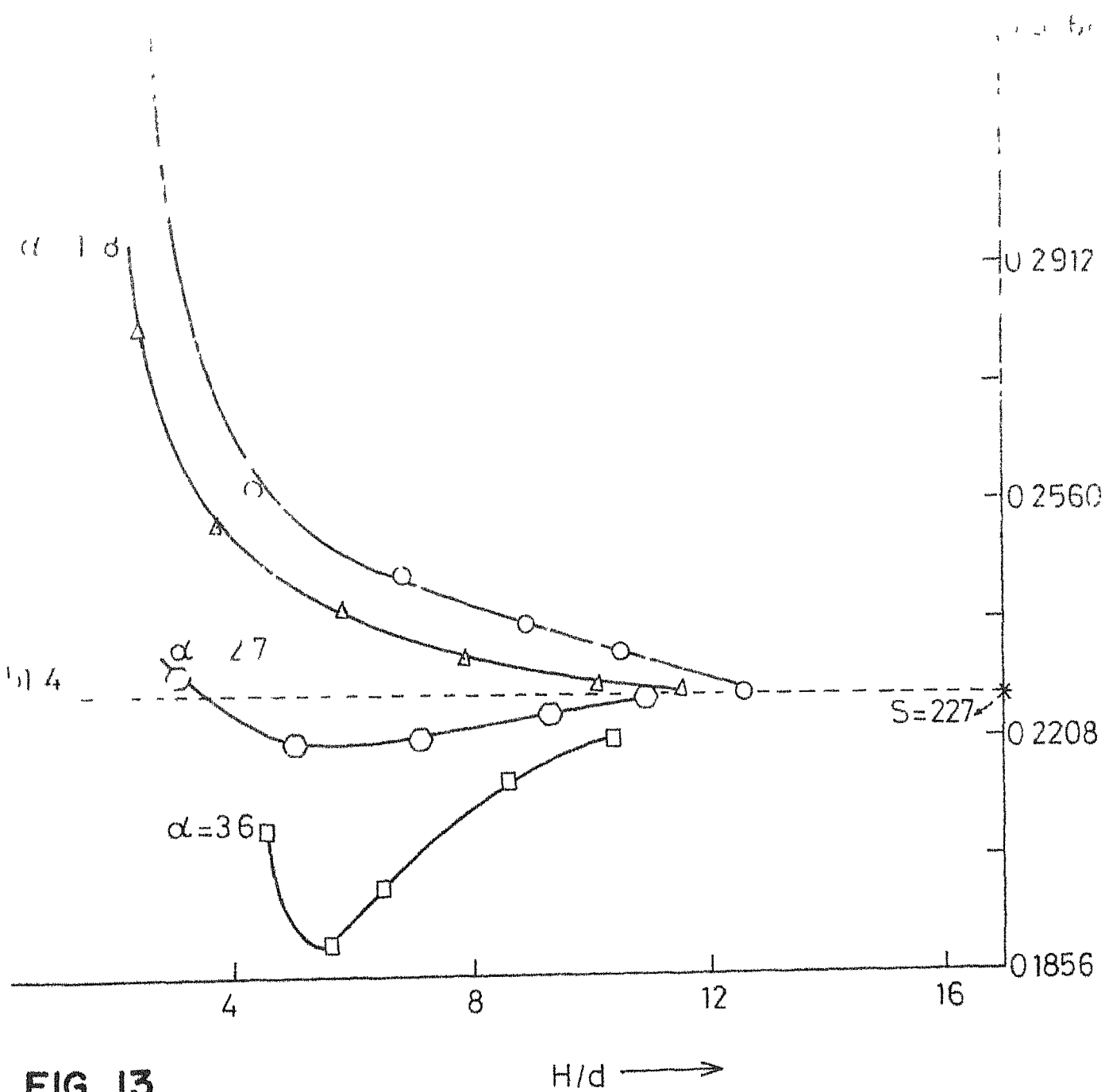
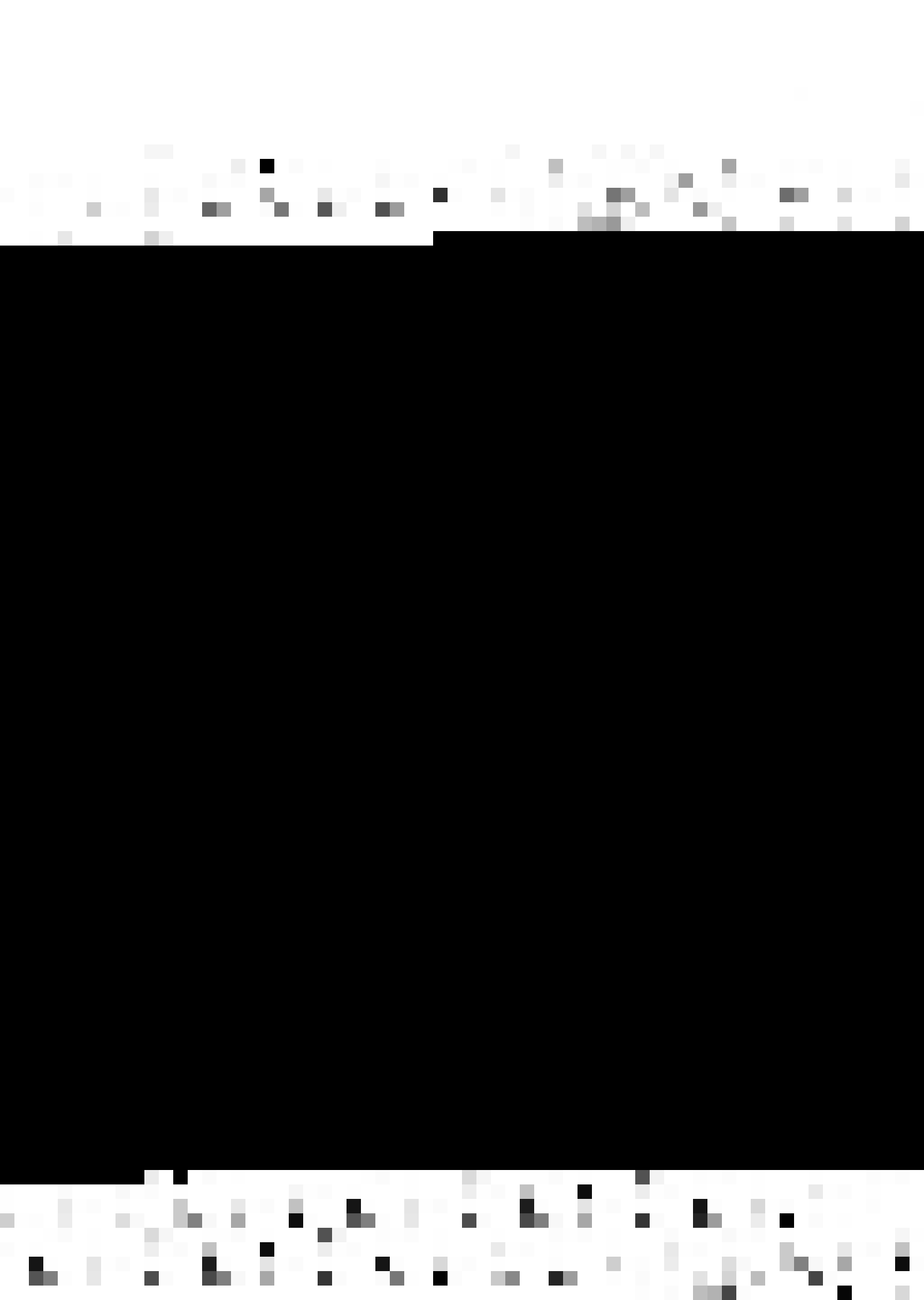


FIG. 13

$H/d \rightarrow$



CHAPTER-V

CONCLUSIONS AND SCOPE FOR FURTHER WORK

5.1 Conclusions

Parallel Wall Effect (2 Walls)

(1) Strouhal number increases with blockage. It starts deviating from Roshko's value for blockages greater than 2 to 2.5%. The rise becomes very steep for blockages greater than 10%.

(2) In the range $R = 902 - 1530$ (subcritical range), where Roshko's value is almost constant, the experimental readings for various blockages are independent of the Reynolds number.

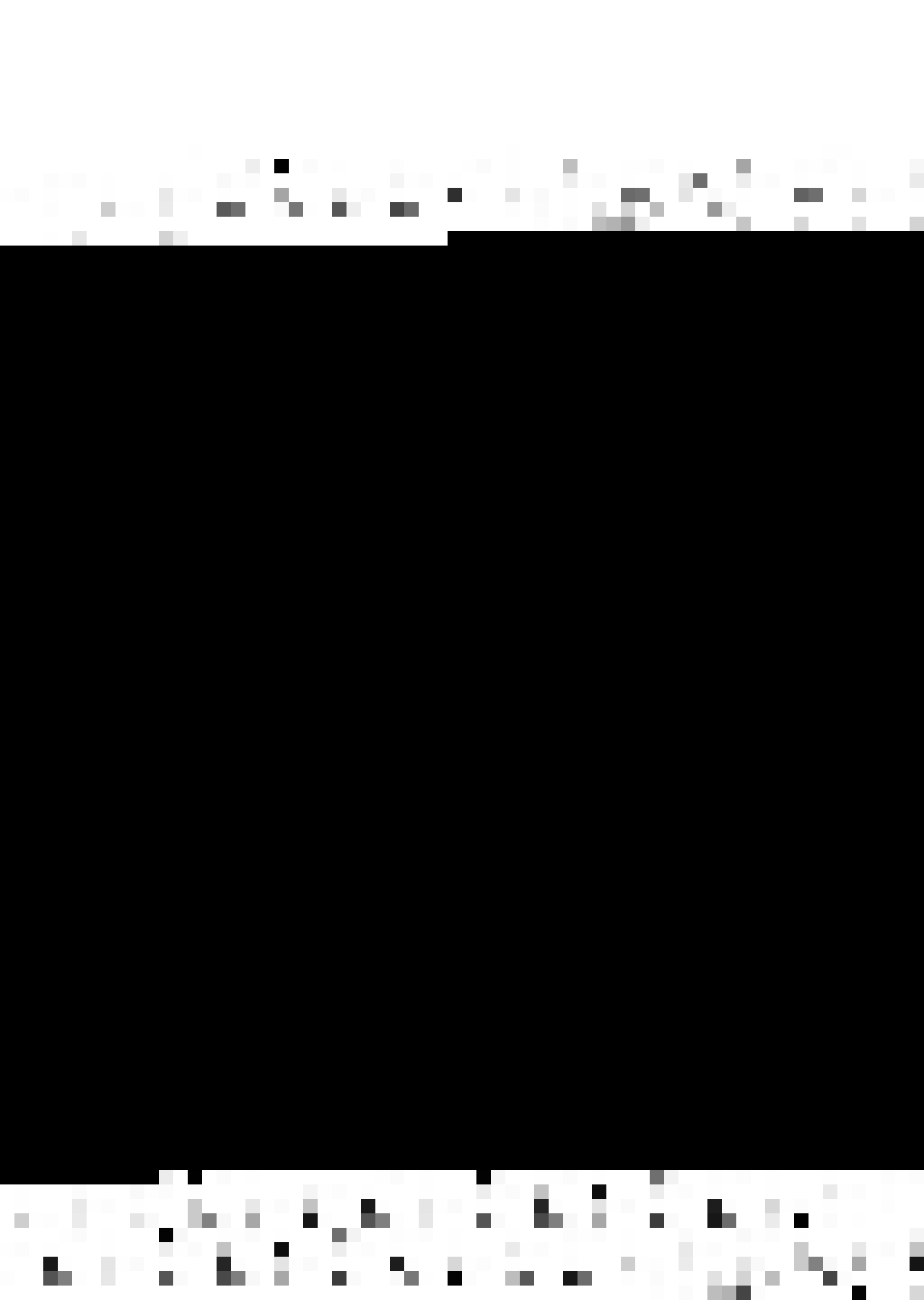
(3) Existing theories to correct the Strouhal number taken at high blockages are inadequate.

One Wall Effect

Strouhal number increases with increasing blockage but the rise is not as sharp as in the 2 wall case.

Convergent Walls Effect.

(1) The effect of convergence is in general to increase the shedding frequency in comparison to the



parallel wall value at the same value of blockage. Greater convergence effect the shedding frequency more.

(2) When the walls are very far ($H > 40 d$) the shedding frequency tends asymptotically to the parallel infinite wall value.

(3) When the walls are at a moderate distance from each other ($H = 10-15$ to $40 d$) the convergent walls stabilize the shedding frequency at a particular value.

(4) When the walls are brought very close to each other the shedding frequency again begins to rise.

Divergent Walls Effect

(1) For large wall separation ($H > 40 d$) the curve tend asymptotically to the parallel infinite wall value.

(2) In the intermediate range $H = 10$ to 40 diameters and at small Reynolds number (300) even slight divergence reduce the shedding frequency. At larger Reynolds number ($900 - 1500$) the decreasing effect is not so large at smaller divergencies. Greater divergence reduce the shedding frequency more.

(3) There exists a critical wall separation ($H = 6$ to $10 d$) below which the shedding frequency again begins to rise.

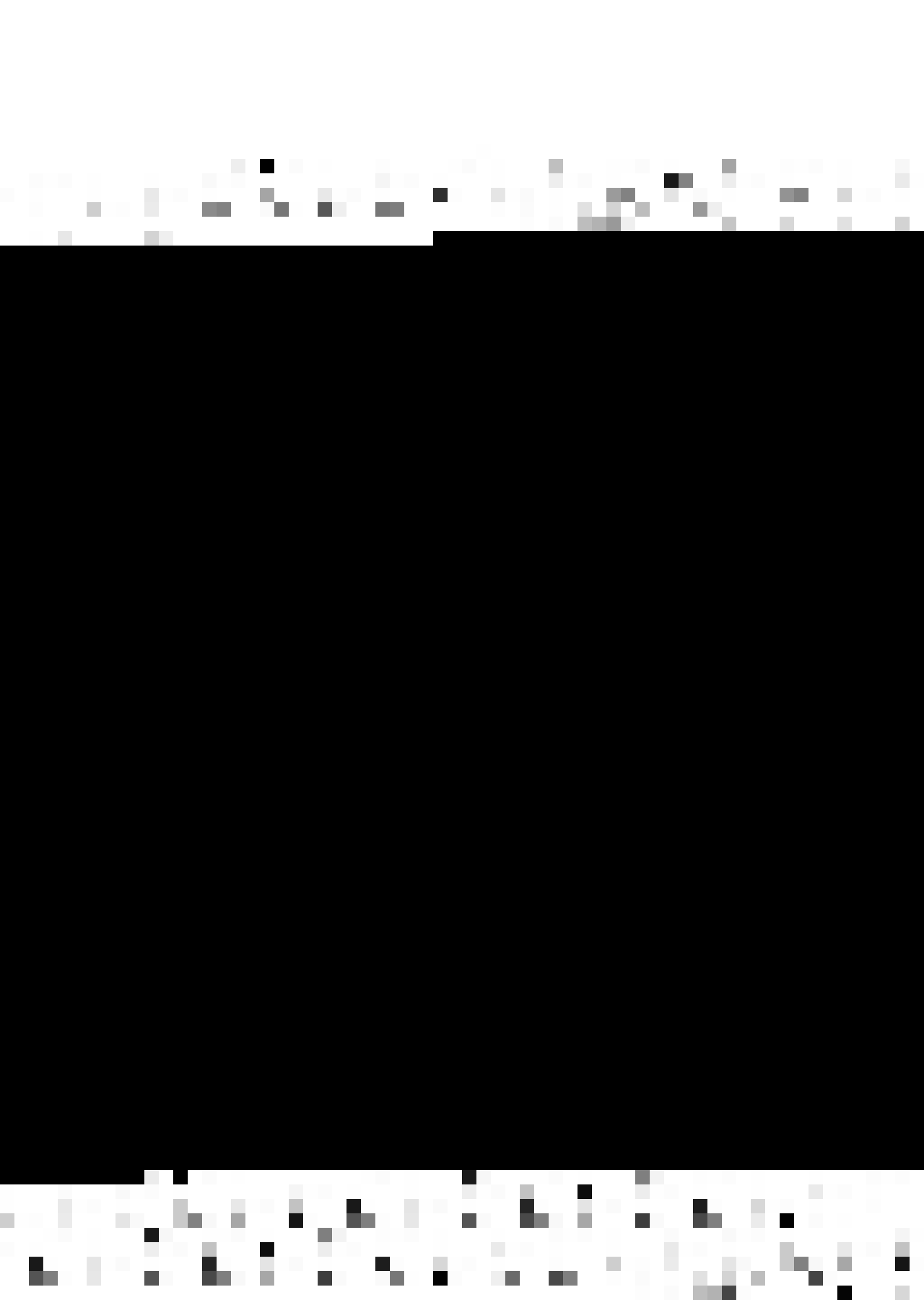


5.2 Scope for Future Work

In the present study of vortex shedding on rigid circular tubes the effect of only one wall was not so large (maximum 50% increase) in comparison to the reported (6) effect on elastic cylinder (500% increase). This indicates that investigations has to be made on vortex shedding of elastic bodies under confined flows. Also the actual structures are never absolutely rigid.

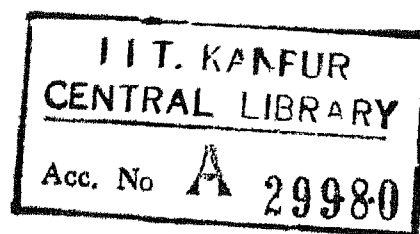
The flow confinement effects can be further studied on models other than having circular cross-section, for example, elliptical and ogival models, flat plates, triangular prisms etc.

For forming any analytical model of the confined flow effect, other parameters of the vortex street like vortex strength, distance between 2 row of vortices (h) and the longitudinal distance between 2 vortices (a) would also have to be measured experimentally.



REFERENCES

1. Thom Procc. of Royal Society, sec.A, V 141,
p651-669, 1933.
2. Shair, F.H., Grove, A.S.; Peterson, E.E., Acrivos, A.
'The effect of confining walls on the
stability of the steady wake behind a cir-
cular cylinder' J.F M -V17, p546-550, 1963.
3. Page, A 'On the 2-D. flow past a body of symme-
trical cross-section mounted in a channel
of finite breadth', British ARC, R & M
1223, Feb. 1929.
4. Tomochika, S. Aero. Res. Inst., Univ. of Tokyo,
report No. 48, p213, 1929-8
report No. 58, p101, 1930-3.
5. Rosenhead, L. & Schawabe, M. 'An experimental
investigation of the flow behind circular
cylinders in a channel of different
widths', Procc. Royal Soc. A, 129,
p115-135, 1930.
6. Wilson, J.F. & Caldwell, H.M. 'Force and stability
measurement on models of submerged pipes'
J. Engg. for Industry, p1290-1298, Nov. 1971.
7. Tsuchiya, K., Ogata, S. & Ueta, M. 'Karman
vortex flow meter', Bull. of J S.M.E.
v13, No. 58, 1970.
8. Vortex-Flow-Meter Ultra-Sonics, VII, n3,
p104, May 1973.

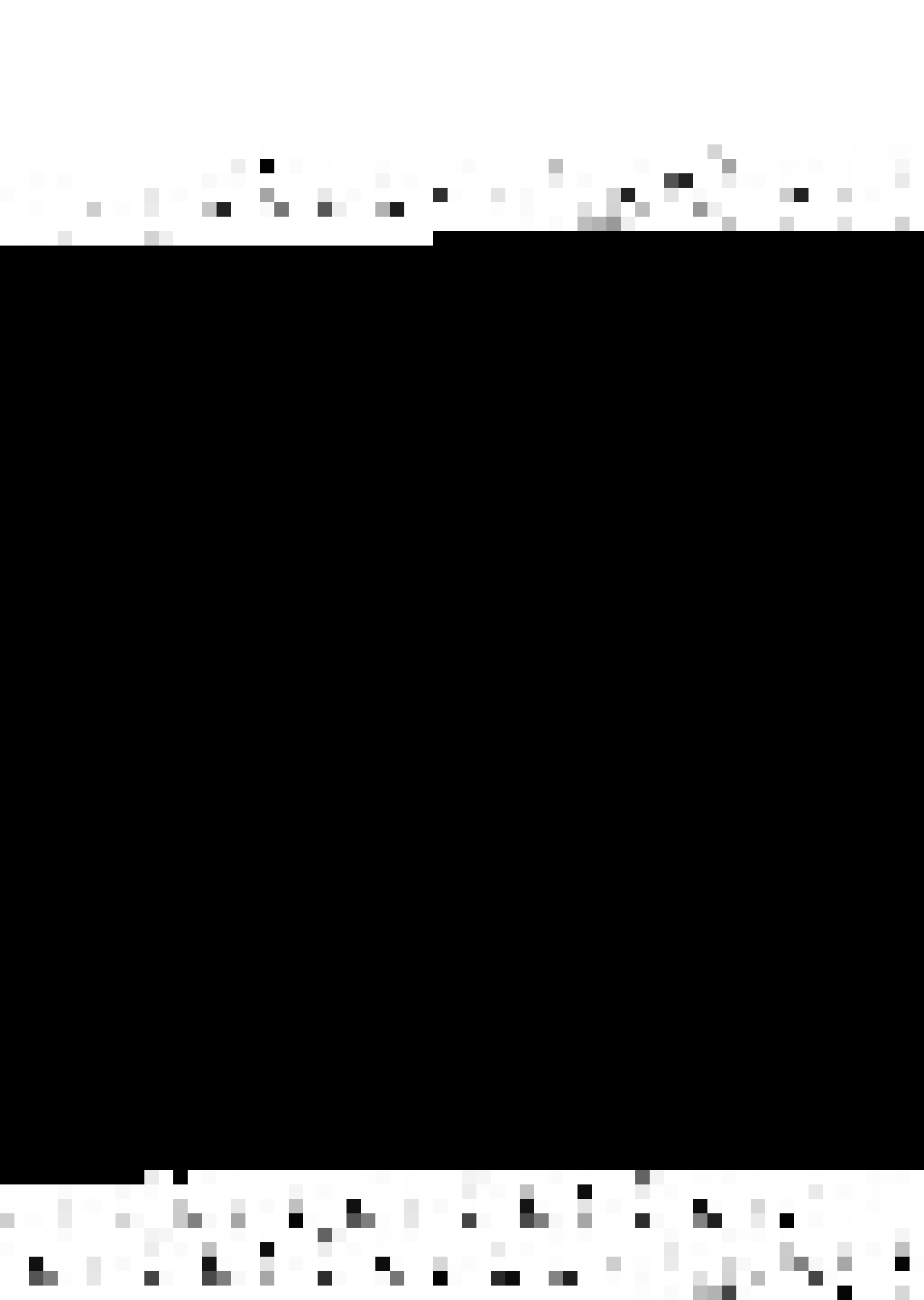




9. Ramamurthy, A.S. & Ng, C P. 'Effect of blockage on steady force coefficients', J. Engg. Mech., Procc. of A.S C.E , v99, EM4, Aug.1973.
10. Twigge - Molecey, C F M & Baines, D.W . 'Aerodynamic forces on a triangular cylinder', J. of Engg. Mechanics, Procc. of A S C E., v99, EM4, Aug. 1973.
11. Chen, Y.S. 'Effect of confining wall on the periodic wake of 90° wedges', Deptt. of Engg. Mech. & Hydraulics, Univ. of Iowa, Iowa City, 1967.
12. Toebe, G.H. & Ramamurthy, A.S. 'Lift and Strouhal frequency for bluff shapes in constricted passages', Conference on flow induced vibration in nuclear-reactors, Argonne National Lab., Argonne, Ill., p225-247, 1970.
13. Tozkas, A.. 'Effect of confining walls on the periodic wake of cylinder and plates', M. Sc. thesis, Univ. of Iowa, Iowa City, Iowa, 1965.
14. Abernathy, F.H. 'Flow over inclined plates', Ph.D. thesis, Harvard Univ., Cambridge, Mass., 1958.
15. Champagne, P.H.. 'Vortex shedding from inclined plates in a restricted channel', Int. report, Deptt. of Civil Engg., Univ. of Bristol, June 1971.
16. Shaw, T.L. 'Wake dynamics of 2-D. structures in confined flows', Procc. 14th. Congress of I.A.H.R. v2, B6-1 to B6-8, 1971.
17. Shaw, T.L. 'Effect of side walls on flow past bluff bodies', J. of Hyd. Div., Procc. of A.S.C.E., v97, HY1, p65-79, Jan. 1971.



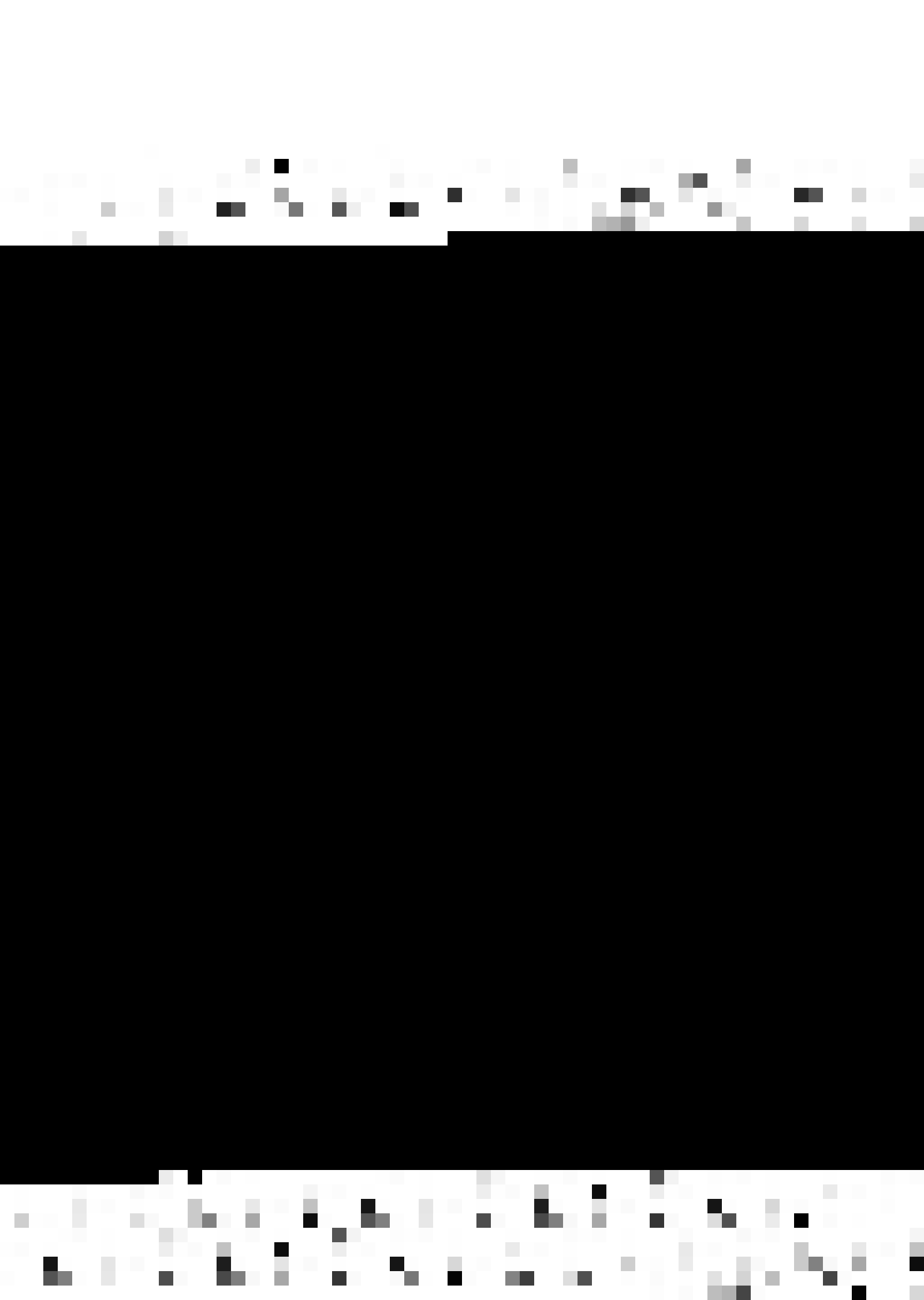
18. Toebes, G.H. 'The frequency of oscillatory forces acting on bluff cylinders in constricted passages', Procc. 14th Congress of I.A.H.R., Paris, v2, B7-1 to B7-10, 1971.
19. Modi, V.J. & El-Sherbiny, S. 'Effect of wall confinement on aerodynamics of stationary circular cylinder', Procc. Inst. Conf. on wind effects on Buildings & Structures, Tokyo, Japan, pII-19-1 to II-19-12, 1971.
20. Modi, V.J. & Saad El-Sherbiny 'On the wall confinement effects in industrial aerodynamics studies', Int. Symp. on vibration problems in industry, Keswick, England, April 1973.
21. El-Sherbiny, S. 'Effect of wall confinement on the Aerodynamics of bluff bodies', Ph.D. thesis, Univ. of British Columbia, Sep. 1972.
22. Glauret, H. 'The characteristics of Karman Vortex Street in a channel of finite breadth',
 (a) Procc. Royal Society sec. A, v120, p34, 1928.
 (b) British ARC, R & M867, March 1923.
 (c) British ARC, R&M1151, Nov. 1923.
23. Rosenhead, L.: 'The Karman Street of vortices in a channel of finite breadth', Phil. Trans. of Royal Society sec. A, 228, p275-329, 1929.
24. Roshko, A. 'Experiments on flow past a circular cylinder at very high Reynolds number', J.F.M., v10, part 3, p345-356, 1961.
25. Allen & Vincenti: 'Wall interference in a 2-D. flow wind tunnel, with consideration of the effect of compressibility', Natl. Adv. Comm. Aero., Wash., Rep. No. 782.
26. Maskel, E.C. 'A theory of blockage effects on bluff bodies and stalled wings in closed wind tunnel', British ARC, R&M 3400, 1965.



27. Tritton, D.J. 'A note on vortex street behind circular cylinder at low Reynolds number', J F.M , v45, No. 1, p203-208, Jan. 1971.
28. Schaeffer, J W. & Salomon, Eskinazi ' An analysis of vortex street generated in a viscous fluid', J.F.M. v6, No. 2, p241, Aug. 1959.
29. Roshko, A.. 'On the development of turbulent wakes from vortex streets', N.A C A. T.N.1191, 1954.
30. Chen, Y.N. 'Properties of Von Karman Vortex Street', Sulzer Technical Review, Research number, p68-80, 1972.
31. Surry, D. 'Some effects of free stream turbulence on vortex shedding at subcritical Reynolds number', papers presented at European Mechanics Colloquium No. 17, Cambridge 1-3 July 1970.
32. Petty, D.G. 'Vortex shedding from circular cylinder in turbulent flow', *ibid.*
33. Chiu, Wen Shyong 'Vortex shedding by yawed cylinders', Bull. Md. 209, Wash. State Univ., College of Engg. research div., Pullman, Wash..
34. Steinman, D.S. 'Problem of Aerodynamic and Hydrodynamic stability', Procc. of 3rd. Hyd. Conf., Univ. of Iowa studies in Engg., Bull. 31, 1946.
35. Hartog, Den. 'Recent technical manifestation of Von Karman Vortex wake', Procc. of Natural Academy of Sciences, v40, no. 3, p155-157, 1954.
36. Griffen, O.M., Skop, R.A. & Koopman, G.H. 'The vortex excited resonant vibrations of circular cylinder', J. Sound & Vibration, v31, No. 2, Nov. 1973.



37. Gerrard, G.H. 'Measurement of fluctuating pressure on the surface of a circular cylinder', A R C , 19, 844, Jan. 1958.
38. Humphreys, J.S. 'On a circular cylinder in a steady wind', Ph. D. thesis, Harvard, Aug. 1959.
39. Keefe, R.T. 'An investigation of the fluctuating forces acting on a stationary cylinder in a subsonic stream and of the associated sound field', U T.I.A report No. 76, Sep. 1961.
40. Glauret, H. 'Wind tunnel interference on wing, Bodies and Air Screws', British ARC, R.& M. 1956, Sep. 1933.
41. Lock, H. 'The interference of a wind tunnel on a symmetrical body', British, A.R C., R.&M. 1275, 1929.
42. Vickery, B.J. 'Fluctuating lift and drag on a long cylinder of square cross-section in a smooth and in a turbulent stream', J.F.M., v25, p481-494, July 1966.
43. Roshko, A. 'On the drag and shedding frequency of 2-D. bluff bodies', N.A C A., Tech. Note 3169, 1954.
44. Mujumdar, A.S. & Douglas, W.J.M. 'Vortex shedding from slender cylinders of various cross-section', J. of Fluid Engg., p474, Sep. 1973.
45. Lin, C.-C. 'Effect of channel walls on base pressure and flow about blunt bodies', M.Sc. thesis, Univ. of Iowa, Iowa City, 1966.



BIBLIOGRAPHY

1. Marris, A.W. 'A review of vortex streets, periodic wakes and induced vibration phenomena', J. Basic Engg., v86, p185-196, June 1964.
2. Morkovin, M.V. 'Flow around circular cylinder - A kaleidoscope of changing fluid phenomena', Symposium on fully separated flows, Am.Soc. Mech. Engrs., p102-118, 1964.
3. Wille, R. 'Karman Vortex Street', Advances in Applied Mechanics, Vol. VI, Academic Press p273-287, 1960.
4. Rosenhead, L. 'Vortex system in wakes', Advances in Applied Mechanics, Vol. III, Academic Press, p685, 1953.
5. Mair, W.A. & Maull, D.J. 'Bluff bodies and vortex shedding-a report on Euromec 17', European Mechanics Colloquium, Cambridge, July 1970. (J. Fluid Mechanics v45, No. 2, p209-224, 1971)
6. Wille, R. 'On unsteady flows and transient motion', Progress in Aeronautical Sciences, v7, Pergamon, 1966.
7. Lienhard, J.H. 'Synopsis of lift, drag and vortex frequency data for rigid circular cylinder', Bull. No. 300, Wash. State Univ., College of Engg. Research Div.
8. Kryzwoblocki, M.Z. 'Vortex street in incompressible media', Applied Mechanics Review, v6, No.9, p393, Sep. 1953.
9. Macovsky, M.S. 'Vortex induced vibration studies', David Taylor Model Basin Report 1190, July 1958.



10. Roshko, A. 'A review of concepts in separated flow',
Procc. Canadian Cong. Appl. Mech., Vol. 3,
p81-115, 1967.
11. Parkinson, G.V. & Modi, V.J. 'Recent research on
wind effects on bluff 2-dimensional bodies',
Int. Res. Seminar', wind effects on Buildings
and Structures, N.R.C Ottawa, Vol. 1, p485-
513, Sep. 1967.
12. Ross, D. 'Vortex shedding sounds of propellers',
Bolf, Breank and Newman Inc., Cambridge,
Mass., Report 1115, March 1964.
13. Parkinson, G.V. 'Aeroelastic galloping in one degree
of freedom', Procc. First Int. Conf. on wind
effects on Buildings and Structures, Natl.
Phys. Lab. Teddington, Vol. 2, p581-609, 1965.
14. Chen, Y.N. 'Fluctuating lift forces of the Karman
Vortex Street on single circular cylinders
and in tube bundles', part I, II, III, J.Engg.
for Industary, p603-628, May 1972.
15. Bearman, P.W. 'On Vortex Street wakes', N.P.L
Teddington, Engg. Aero. Rep. No. 1149, 1966.
16. Shaw, T.L. & Chaplin, J.R. 'Dynamic waves in Civil
Engineering'.
17. Kuchemann, D. 'Report on the I.U.T.A M.Sym. on
Conc. Vortex Motion', J. Fluid Mechanics,
v21, p1-20, 1965.
18. Berger, E. & Willie, R. 'Annual review of fluid
mechanics', periodic flow phenomena, Palo
Alto, Annual Review Inc., v4, p313, 1972.
19. Scruton, S. 'On the wind excited oscillations of
stack, tower & masts', Procc. Symp. on wind
effects on Buildings & Structures, N.P.L.
Teddington, p798-832, 1965.
20. Goldstein, S. 'Modern Development in Fluid Dynamics',
v2, p552, 1938.



APPENDIX-A

WALL CORRECTION THEORIES

1

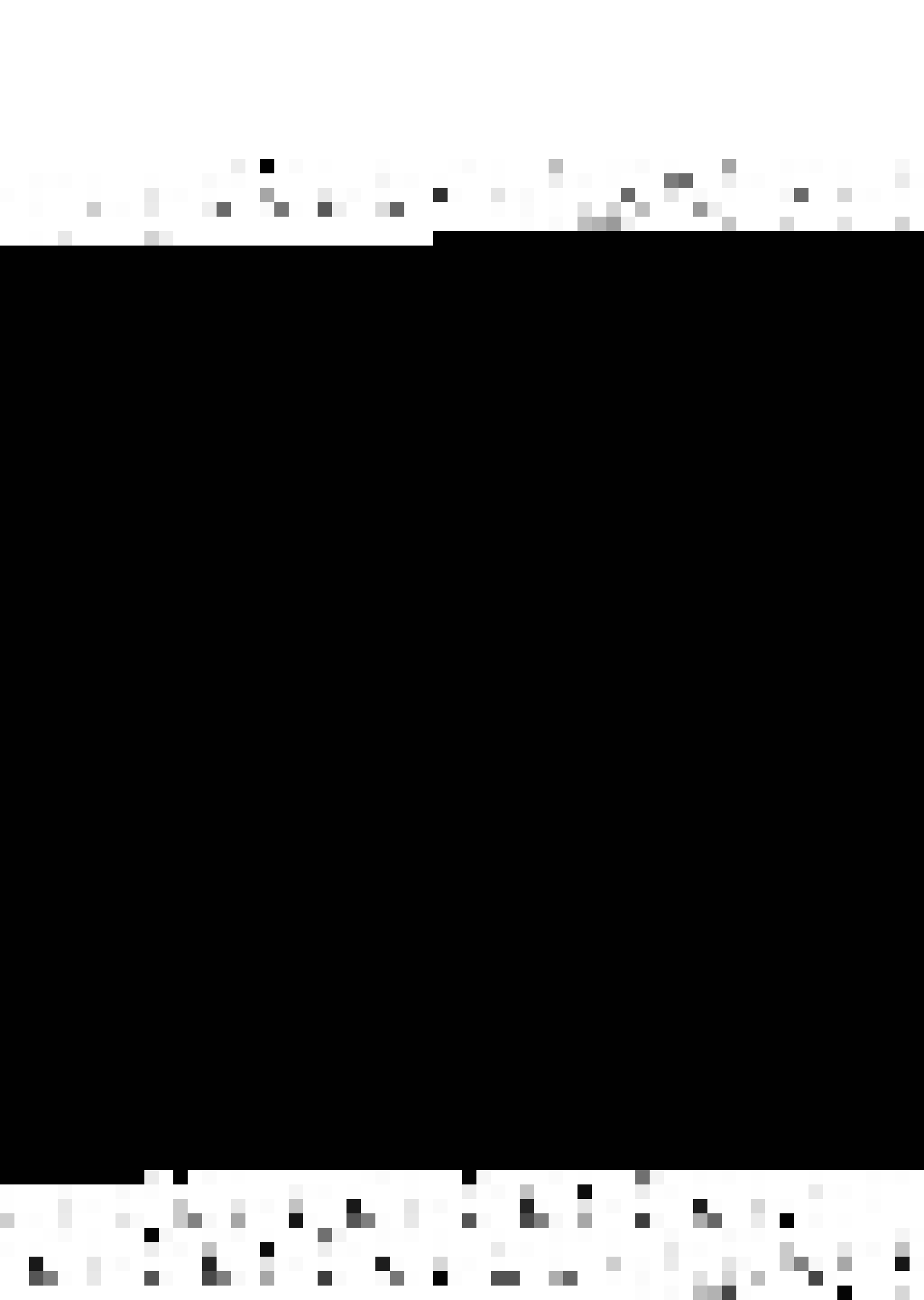
No satisfactory theory is available which can predict correctly the blockage effects. Some models have been proposed using certain assumptions, but are found to be particularly inadequate at higher blockage ratios. Recently, modification of these methods through inclusion of higher order terms and curve fitting of the experimental data, has been tried to improve their applicability.

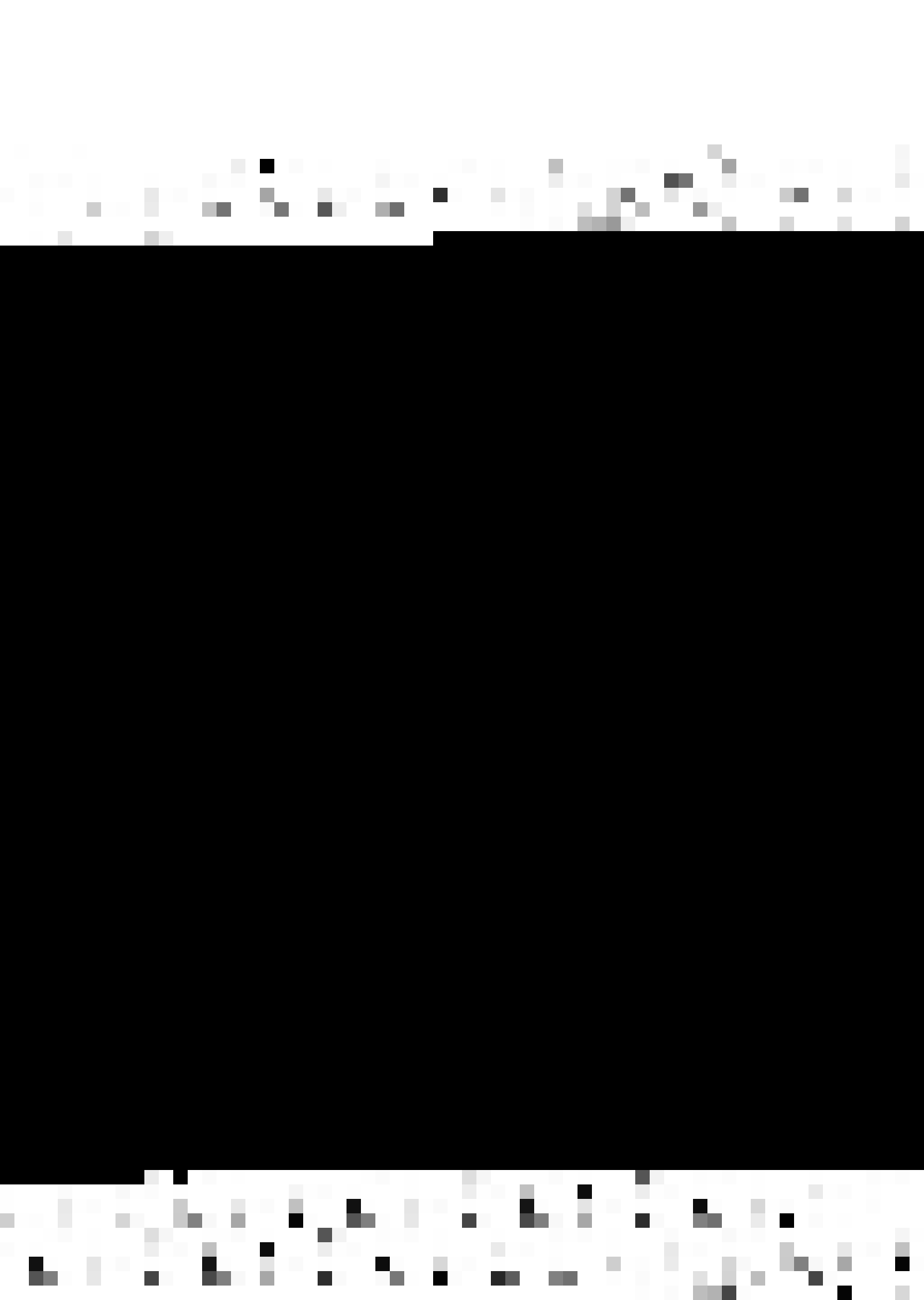
1. Glauert's Correction Method 1928

Glauert (22) obtained estimates for translational velocity of vortex street (u) wake parameters (h , a), vortex strength (k) and drag coefficient (C_d) in a channel of finite breadth.

He used the method of images to represent the boundary conditions on the walls of channel and velocity field of this series of images to the constraint experienced by the vortex street. He also assumed that

- (1) The increase of the suction in the dead water region behind the body, due to the constraint of the channel walls, is equal to the drop





(2) Allen and Vincenti Correction Method 1944

Allen and Vincenti (25) used image doublets to represent the interference between wall and cylinder (third term in formulae) and image sources to represent interference between wall and wake (second term in formulae) to obtain corrected velocity and drag coefficient.

$$\frac{V_c}{V} = 1 + \frac{1}{4} C_d \left(\frac{d}{H}\right) + .82 \left(\frac{d}{H}\right)^2$$

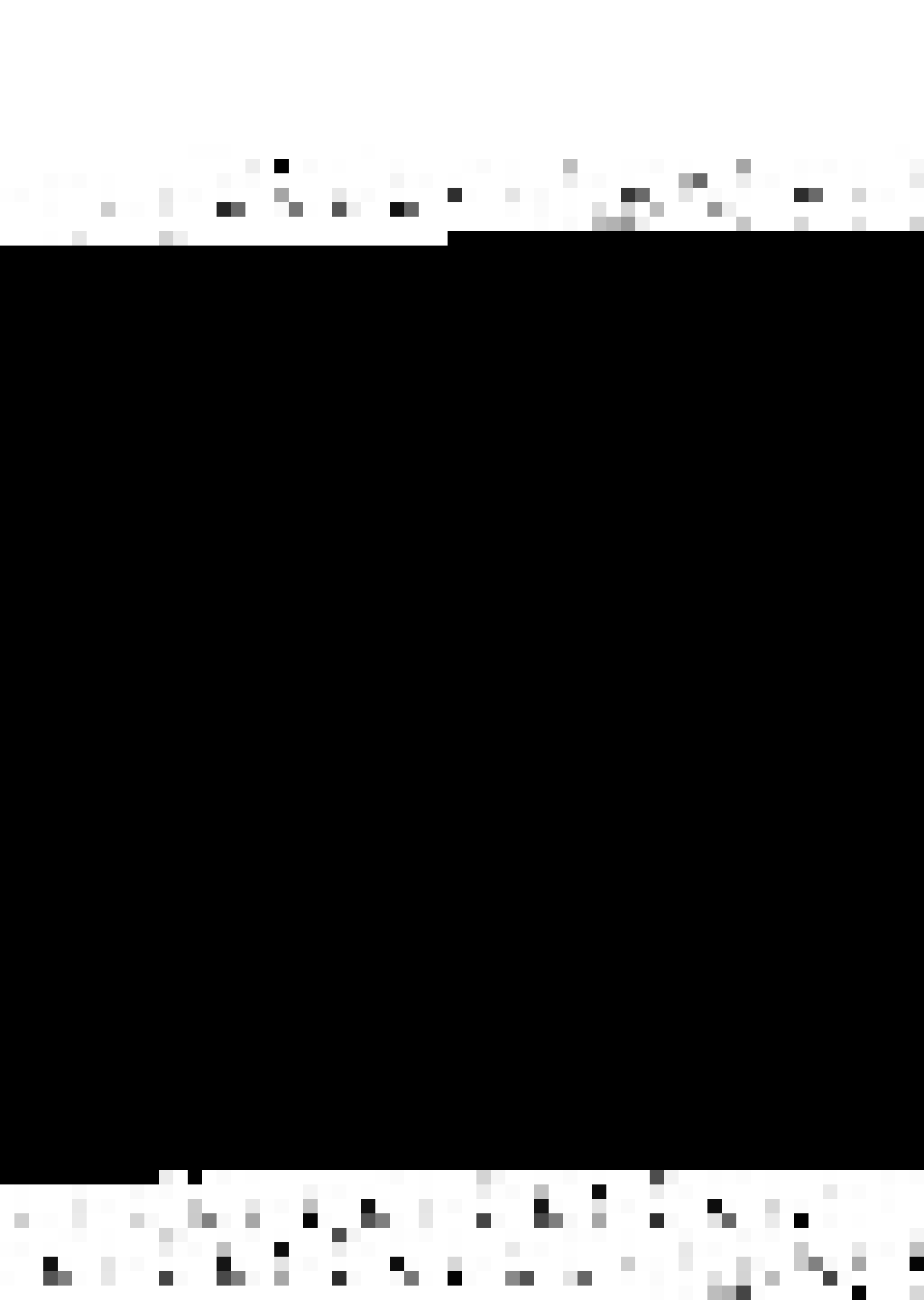
$$\frac{C_{d_c}}{C_d} = 1 - \frac{1}{2} C_d \left(\frac{d}{H}\right) - 2.5 \left(\frac{d}{H}\right)^2$$

Corrections for Reynold number and Strouhal number are the same as for the velocity. However such an analysis do not take into account possible interference effects on the separation mechanism and the structure of the wake close behind the body.

Roshko (24) found that maximum correction for velocity and drag coefficient were 4 and 10% respectively using the above formulae. (blockage 13.6%, Reynolds number $10^5 - 10^7$).

(3) Maskel's Method of Correction 1963

Maskel (26) developed a theory for blockage correction based upon momentum balance between the



undisturbed flow upstream of the body and that of downstream where the effective wake reaches its maximum width.

He derived

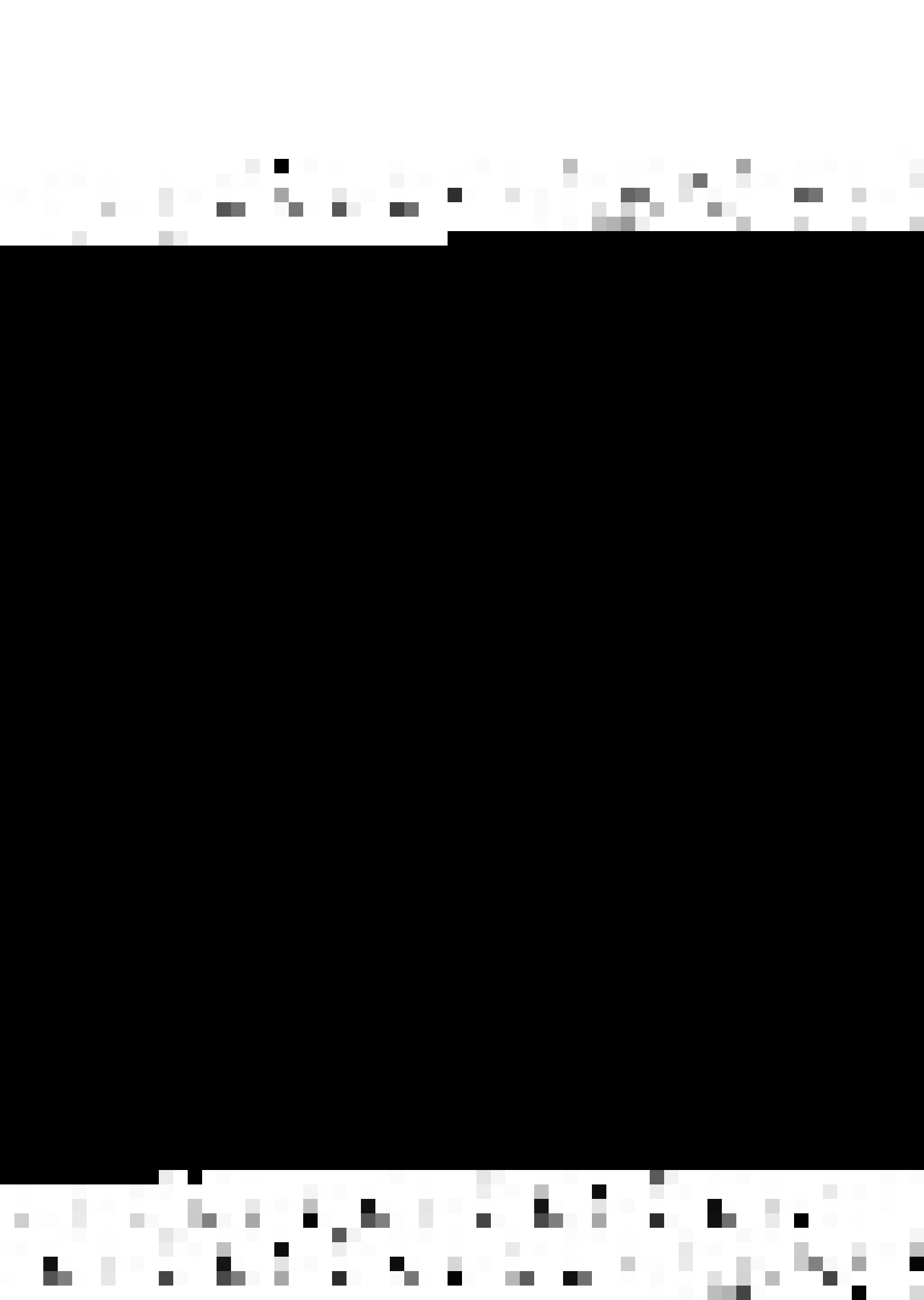
$$\frac{1 - C_{pb}}{1 - C_{pb_c}} = \frac{C_d}{C_{d_c}} = \frac{B_p^2}{B_{p_c}^2} = 1 + \frac{C_d}{B_{p_c}^2 - 1} \left(\frac{A_m}{A_t} \right) + O \left(\frac{A_m}{A_t} \right)^2$$

$$\frac{S}{S_c} = \frac{B_{p_c}}{B_p} \left[1 + \frac{C_d - C_{d_c}}{(B_p^2 - 1)(B_{p_c}^2 - 1)} \left(\frac{A_m}{A_t} \right) \right]$$

Where terms of order $\left(\frac{A_m}{A_t} \right)^2$ were considered negligibly small. However the experimental results for circular cylinders indicate some difference from Maskell's assumptions, the main discrepancy being the variation of the ratio C_d / B_p^2 with the constraint. Also the pressure over the base was found not to be uniform especially at higher blockage ratios.

Vickery (42), during his experiments found that the bracketed term in expression of Strouhal number correction was approximately equal to one and he used the simply relation $S/S_c = B_{p_c} / B_p$ for its correction.

Modi, et. al (20) found that the theory is able to account only for bluntness of around 5 - 10%.



(4) Mod1 and Sherbiny Correction Formulae 1971

Based on Maskell's correction formula, Mod1 and Sherbiny (19,20) used curve fitting of the experimental results in a polynomial of the form.

$$C_d = C_{d_c} \left[1 + \sum_{n=1}^n A_n \left(\frac{A_m}{A_t} C_d \right)^n \right] \quad A_n - \text{constant}$$

The same approach was applied to correct the fluctuating lift coefficient ($C_{L'}$) and the Strouhal number.

Reynolds number 10 to 12×10^4 , blockage 3 to 35.5% , circular cylinder . A straight line fit was found to be the best for the three measured parameters. The correction relations are

$$C_{d_c} = C_d \left[1 - 1.495 \left(\frac{A_m}{A_t} \right) \right] \quad \text{average } C_{d_c} = 1.058$$

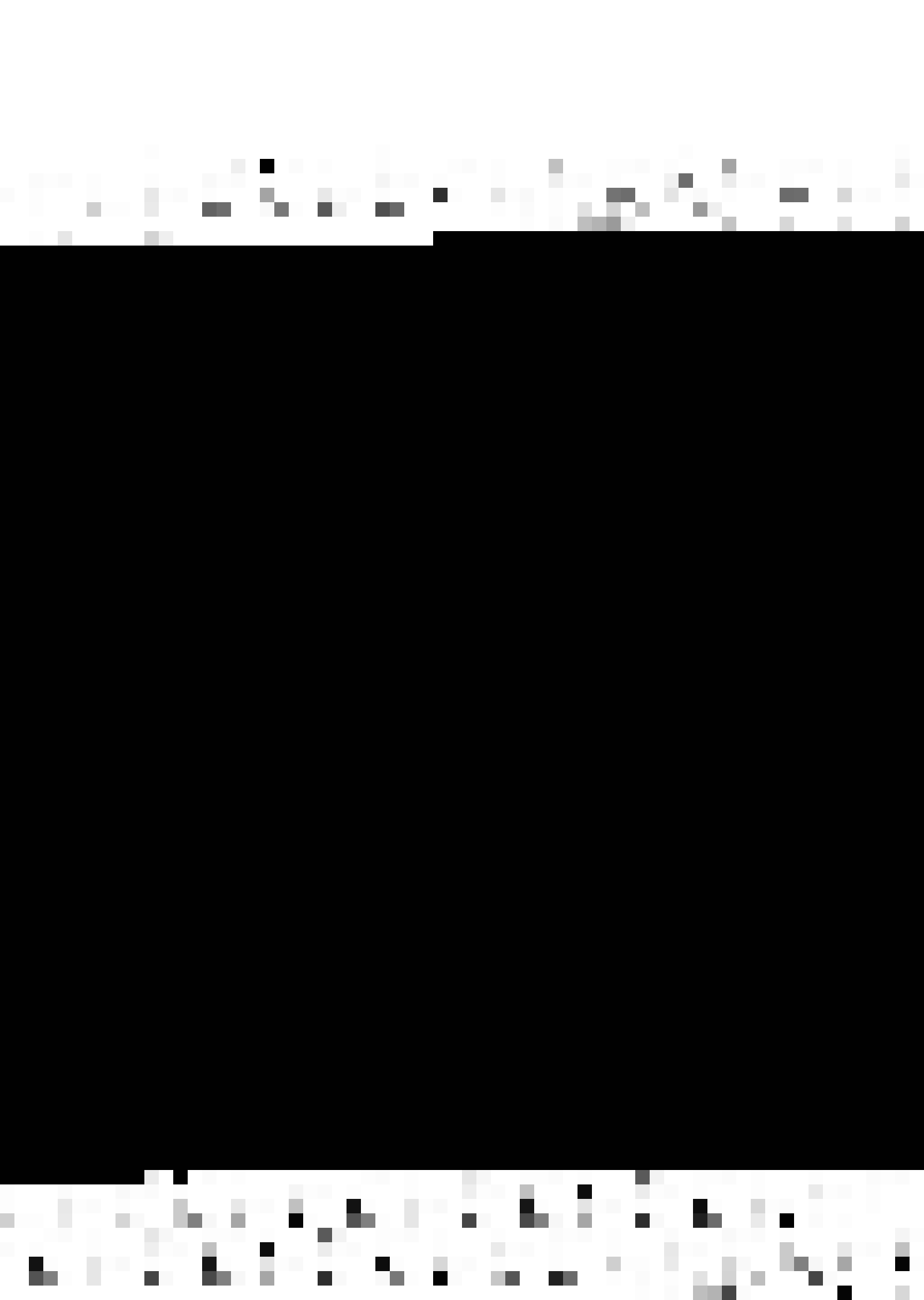
$$C_{L'_c} = C_{L'} \left[1 - 1.95 \left(\frac{A_m}{A_t} \right) \right] \quad \text{average } C_{L'_c} = 0.672$$

$$S_{d_c} = S_d \left[1 - 0.552 \left(\frac{A_m}{A_t} \right) \right] \quad \text{average } S_{d_c} = 0.191$$

Similar expression were also tried by them for correcting drag coefficient of flat plate at various angle of attack (20).

(5) Roshko's Universal Strouhal Number Approach 1954

Roshko (43) proposed that if in Strouhal number calculations, 'h' (maximum distance between two row of



vortices) instead of cylinder dia. and separation velocity (V_s) instead of free stream velocity (V) was taken, then a universal Strouhal number (S^*) could be achieved, which was independent of blockage ratio, Reynolds number and shape or size of the body.

$$S^* = \frac{f h^*}{V_s} \quad \begin{aligned} V_s &= \text{separation velocity} \\ &= V_o (1 + C_{p_s})^{\frac{1}{2}} \end{aligned}$$

C_{p_s} = pressure coefficient at point of separation

hence

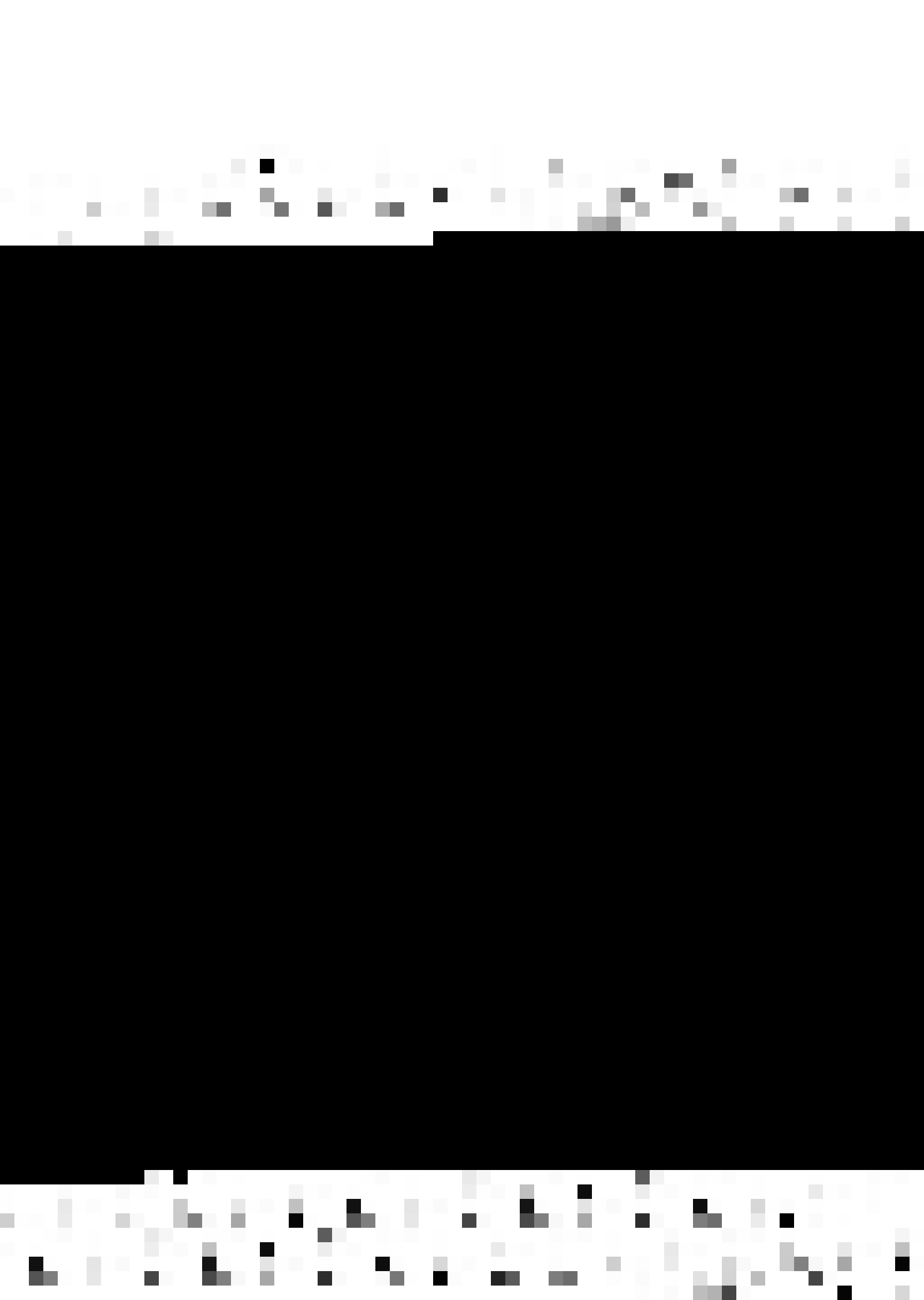
$$\frac{f_c}{f} = \frac{h^* V_{s_c}}{h_c^* V_s}$$

A number of researchers do confirm this point. Modi, et. al. (20) found that S^* for the cylinders was quite close to that for plates, for a wide range of blockage ratio's. (3 to 35.5%) and angle of attack. He attributed the small deviations to differences in the accuracy of experimental measurements of h^* .

(6) Tsuchiya, Ogata, Veta Method

Tsuchiya, et. al. (7) 1970, said that if Strouhal number is defined on the basis of velocity near the cylinder and not on far upstream then a constant Strouhal number could be achieved independent of blockage, i.e.

$$S_1 = \frac{f d}{V_1} \quad \text{where} \quad V_1 = \frac{V}{m}$$



where m is a geometrical factor which takes in account pure geometrical blockage. For circular cylinder (d) in circular tunnel (D)

$$m = 1 - \frac{2}{\pi} \left[\frac{d}{D} \sqrt{1 - (d/D)^2} + \sin^{-1} \frac{d}{D} \right]$$

and for circular cylinder (d) in rectangular tunnel (H).

$$m = \left(1 - \frac{d}{H}\right)$$

In their experiment they found that S_1 had a constant value of .184 for blockages less than 30%. But, as they also admit, it is experimentally found (44) that this simple approach is no longer valid for higher blockage.



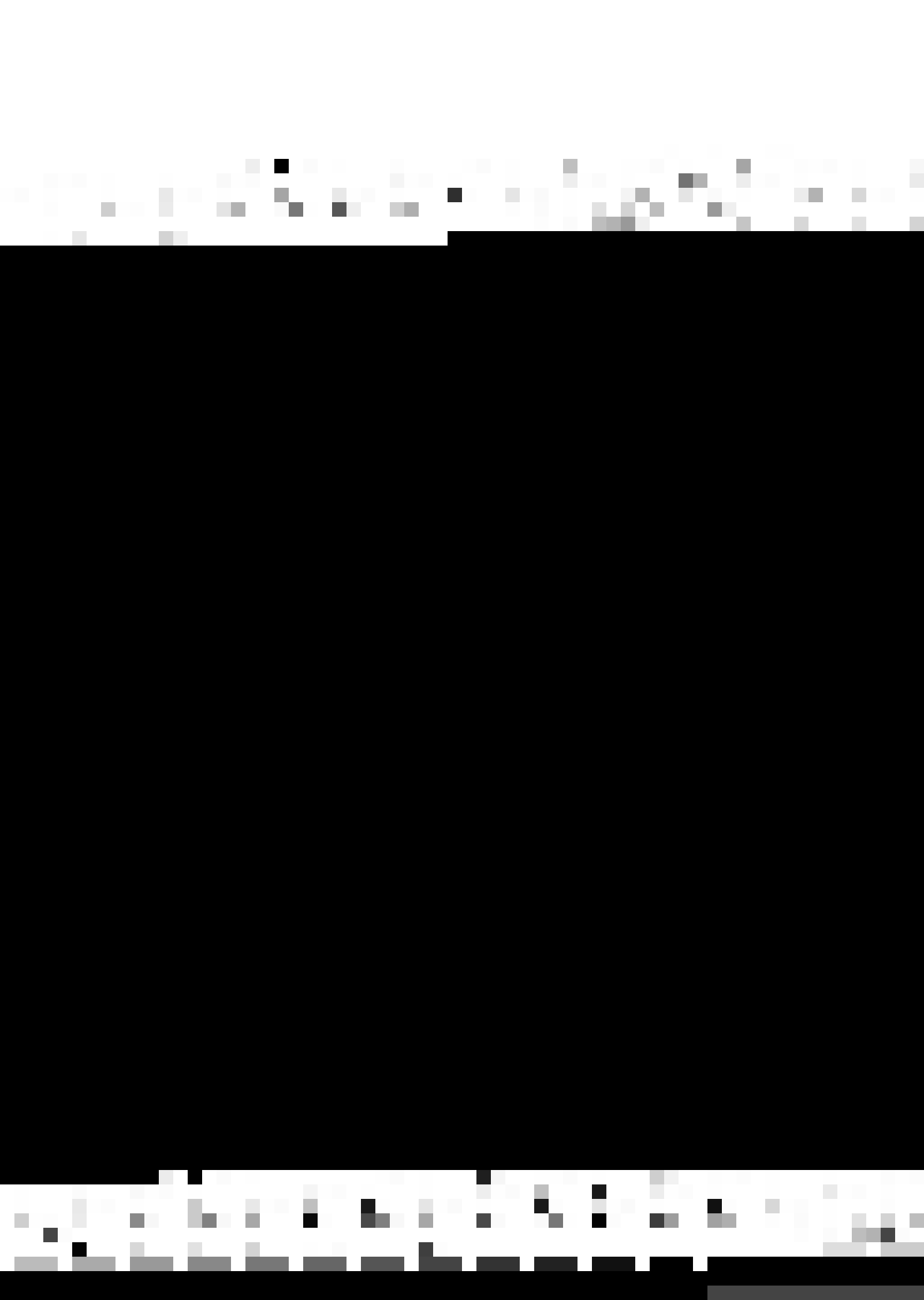
where m is a geometrical factor which takes an account pure geometrical blockage. For circular cylinder (d) in circular tunnel (D)

$$m = 1 - \frac{2}{\pi} \left[\frac{d}{D} \sqrt{1 - (d/D)^2} + \sin^{-1} \frac{d}{D} \right]$$

and for circular cylinder (d) in rectangular tunnel (H),

$$m = \left(1 - \frac{d}{H}\right)$$

In their experiment they found that S_1 had a constant value of .184 for blockages less than 30%. But, as they also admit, it is experimentally found (44) that this simple approach is no longer valid for higher blockage.



ME - 1974 - M - AGA - VOR

